Department of Mechanical and Aerospace Engineering
Doctorate of Mechatronics
XXVI Cycle (2011-2014)

Settore Scientifico-Disciplinare
ING-IND/14

April 2014

Ph.D. Thesis

Robotic Biomedical Device for Recovering Cardiovascular Efficiency in Paraplegic Patients

Author
Hamidreza HAJIMIRZAALIAN
matr. 179493

Tutor
Prof. Carlo FERRARESI

Co- Tutor
Prof. Daniela MAFFIODO

Coordinator
Prof. Giancarlo GENTA

PREFACE

This thesis is submitted to the Politecnico di Torino University (Polito) in partial fulfilment of the requirement for the Doctoral degree in Mechatronics. The work has mainly been performed at Polito, Mechanical and Aerospace Engineering department (DIMEAS), Turin, Italy, with Professor Carlo Ferraresi as main supervisor and Professor Daniela Maffiodo as Co-supervisor from the DIMEAS. The research project was supported by grants from the Italian Ministry of university and Research (MIUR) through the PRIN'08 project. The thesis was publically defended at 14th April 2014 in the lecture hall of the DIMEAS, Turin, Italy.

ABSTRACT

This thesis is studying on the Design and development of a biomechanical robotize IPC device to accomplish a therapeutic methodology for recovery of cardio-circulatory functions, which may be seriously impaired in paraplegic patients. This impairment is caused by the reduction of venous return, due to the missing muscular contraction in zones without innervations.

Intermittent Pneumatic Compression (IPC) is a well-known technique, which can be used for several therapeutic treatments like sports recovery, lymphoedema drainage, and deep vein thrombosis prevention. An IPC device produces a definite massaging action on the limb by inflating and deflating a given number of bladders according to particular time laws.

The designed IPC device in this thesis is proposed for the lower limb to recover the venous return and preventing the Deep Vein Thrombosis (DVT) in the patients. The experimental tests on the volunteer persons showed the significant improvements on the important parameters of the cardiovascular, like the stroke volume (SV), the cardiac output (CO), and the end diastolic volume of left ventricle (LVEDV).

To understand the dynamic behaviour of the IPC device and to optimize its performances, the device is characterized based on the mechanical and physiological aspects and its mathematical model is simulated in Simulink-Matlab. The validation of the mathematical model is done by comparing results with the experimental one.

In addition, to apply the desired pressure pattern on the limb, two control strategies based on the PID algorithm and regulating inflating time are implemented on the model. The results of the controlled model, shows about 60% improving in performances of the

device as concerns the bladder pressure control. In this case the experimental test has been done and it verified the control results of the simulation.

Keywords*: cardiovascular efficiency, IPC device, mathematical modelling, controls strategies.*

ACKNOWLEDGMENT

The acknowledgment is the most important and fun part of this thesis, since this is where I have the opportunity to thank all wonderful people, who have contributed to make this thesis possible.

This thesis has been seen through to completion with the support and encouragement of numbers people including my well-wishers, my friends and colleagues. At the end of my study I would like to thank all those people who made an unforgettable experience for me.

First of all, I would like to thank to Professor Carlo Ferraresi my PhD supervisor for believing in me, introducing me to a very interesting research area and providing me with work that has been important for my development and progress as a researcher. Thank him for always being kind and caring, seeing solutions instead of problems and for his ability to share his excitement and visions about science. Without his supervision and constant help this dissertation would not have been possible.

I also would like to express my sincere gratitude and appreciation to Professor Daniela Maffiodo, my Co-supervisor for helping and supporting me during these past three years and sharing her great knowledge and experience with me. The great of thanks for all the help in doing the experimental tests.

I want to thank to my colleagues during this research, Encarna, Michela, Miguel and Michele. Thank them for creating a wonderful atmosphere and many enjoyable moments at the laboratory. I will never forget them.

Many thanks also to all persons in the laboratory and department of the Mechanical and Aerospace engineering of Politecnico di Torino for all help and being always positive and friendly.

I had unbelievable and full of happiness times in Turin during these years. I found many friends who made unforgettable memories for me. I thank them and I wish see them soon.

Finally, my greatest thanks go to my beloved family, my father, mother, sister and brothers. I could not have been done it without their continuous support and sincere encouragement. I owe everything to them.

Dedicated to:

My family who are the most valuable asset in my life

TABLE OF CONTENTS

LIST OF FIGURES

LIST OF TABLES

1. INTRODUCTION

In immobilized people, e.g. paraplegic subjects, due to absence of leg muscle contraction, venous return to the heart is reduced and this may induce a reduction of cardiac output. As a matter of fact, according to the well-known Starling's law, "the output of the heart is equal to and determined by the amount of blood flowing into the heart, and may be increased or diminished within very wide limits according to the inflow". In other words, the cardiac output is directly influenced by the venous return, which is determined primarily by the mechanical properties of the systemic circulation.

Therefore it is reasonable to suppose that, the application to legs of a mechanical stimulation operated by actuators, in replacing striate muscle pump on limbs veins, may recover in these patients venous return to the heart, thus restoring sufficient performance of the cardiovascular system.

Since 1930s, it was evaluated that intermittent pneumatic compression (IPC) has a positive effect on lower extremity blood flow of the calf and foot [1, 2]. IPC devices were therefore used to prevent deep vein thrombosis (DVT) [3-7], Critical Limb Ischemia (CLI) [8-10], congestive heart failure [11] and it was recommended for lymphedema treatment [12] and sport recovery [13, 14]. Studies have shown that IPC application on legs changes central venous pressure, pulmonary artery pressure, and pulse pressure [15] and IPC application on foot increases popliteal artery blood flow [16]. Moreover various researches have suggested that this mechanical method effectively reduces the incidence of the diseases without any side effects, increasing volume flow and velocities in deep veins [10, 11, and 17].

Although the various forms of mechanical intermittent compression of limbs have a 70-year history of published clinical effectiveness, a complete knowledge of the cause and effect process is not yet fully reached.

Despite there are many researchers investigating on IPC effects, the lack of a general methodology to study and develop an IPC device with physical and dynamical characteristics suitable for the intended application, is evident. In particular, the dynamic behaviour of the device in response of the control command is practically ignored.

This research proposes and realizes a new prototype of IPC device to act on the lower limb to specialty recover the venous return in the immobilized and paraplegic patients. In addition, a methodology based on the realization of a mathematical model to represent the dynamic behaviour of the device and its interaction with human is proposed.

To optimize the performances of the model, two control strategies based on the PID algorithm and regulating inflating time are implemented on the model. Moreover, the results of the experimental test to verify the simulation results are presented.

1.1 Thesis outlook

The thesis is organized into 7 chapters followed by the three included papers. After this short introduction, the aims are stated. The physiology of the cardio circulatory system and the related diseases and the ways to prevent and treatment of its diseases are described in Chapters 3. Chapter 4 provides a literature review of using IPC device to effect and improve the cardiovascular function as well as describe briefly the commercial IPC devices in the market and finally introduces the design IPC device in this research. The experimental results of the IPC device on the volunteer people to show the effect of the IPC device on cardio circulatory function are shown also in this chapter. The obtained mathematical model of the device and its validation are presented in the chapter 5. In chapter 6, two control strategies to control the device are described and the experimental results of the PID controller are depicted. Finally in chapter 7 the conclusion of the thesis is provided. The future work, other scientific contributions by the author and references are presented in the last part of the thesis. Also the three published Papers based on the thesis in full format are presented in the index part.

2. AIMS

The general aim of this thesis is to develop and realize a biomechanical robotized IPC device to accomplish a therapeutic methodology for the recovery of cardio circulatory functions, seriously impaired in paraplegic patients. The aim originates from the knowledge of cardio circulatory system malfunctioning in patients with spinal injury. This impairment is caused by the reduction of venous return, due to the missing muscular contraction in zones without innervations. Such impaired patients have therefore, in comparison to healthy subjects, a higher death risk due to cardiovascular pathologies and particularly the coronary disease.

The device mechanically interact with the patient and is equipped with own auctioning and control systems, to produce a massaging-pumping action on the striated muscles of the lower limb according to control laws.

The specific aims of the research can be listed into 3 parts which in the below are described.

- Design and realization of a new IPC device. The device must be different from the previous samples in the performances on the patients.
- Propose a methodology based on the realization of a mathematical model able to represent the dynamic behaviour of the device and its interaction with the human.
- Control of the device to exert a desired pressure pattern on the limb. This causes to increase the efficiency of the device for improving the cardiovascular parameters.

3. PHYSIOLOGY OF THE CARDIOVASCULAR SYSTEM

This chapter contains an overview of the anatomy and the function of the cardiovascular system and provides brief descriptions of some of the most common cardiovascular diseases, and some ways to prevent and treatment of them. The cardiovascular system consists of the heart, blood vessels and blood, and is responsible for the transportation of gases, nutrients, hormones and blood cells throughout the body. Additional functions of the cardiovascular system are to regulate body temperature and acid-base balance.

3.1 Cardio circulatory system

The main function of the cardio-circulatory system is to transport useful substances in the metabolism of the cells and remove the waste substances through the body. The cardio-circulatory can be divided into two parts, systemic circulation and pulmonary circulation. Through the systemic circulation, the oxygenated blood from the heart is come to the organs by the arterial and the deoxygenated blood is returned to the heart by the veins. In addition, the pulmonary circulation transports the deoxygenated blood from heart to lungs and brings back to the heart the fresh oxygenated blood. In the figure 3.1, the cardio-circulatory of the body is depicted. The energy of the blood circulation through the veins comes from the heart.

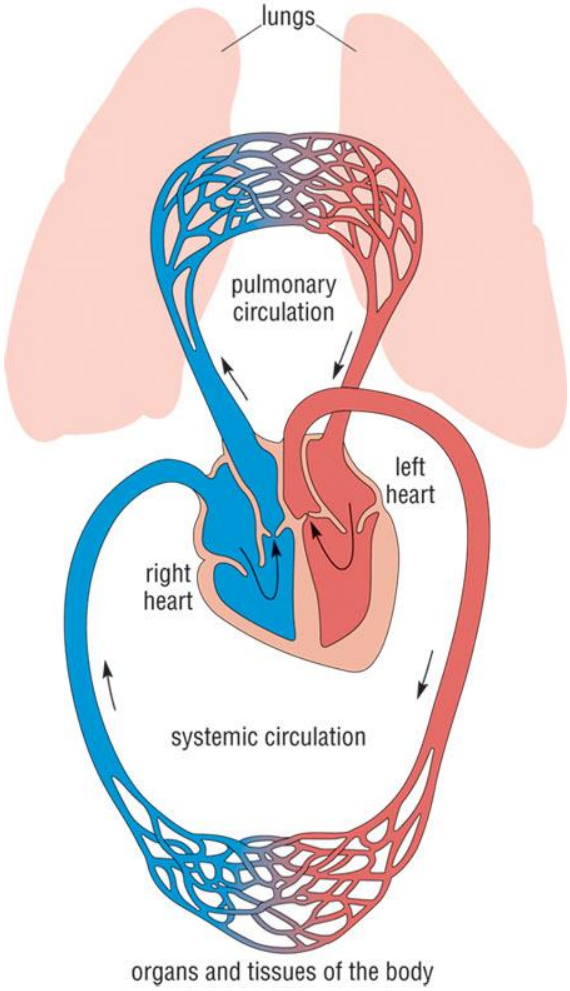

Figure 3.1. The cardio-circulatory system of the body

3.2 Heart anatomy

The human heart is a muscular pumping organ located medial to the lungs along the body's midline in the thoracic region. It has a weight of approximately 250-300 g and a size similar to a closed fist [18]. The heart is divided into a left and a right side. Each side of the heart consists of two chambers, the atrium and the ventricle, separated by an atrioventricular (AV) valve: the mitral and the tricuspid valves on the left and right sides, respectively. The anatomy of the heart is depicted in figure 3.2.

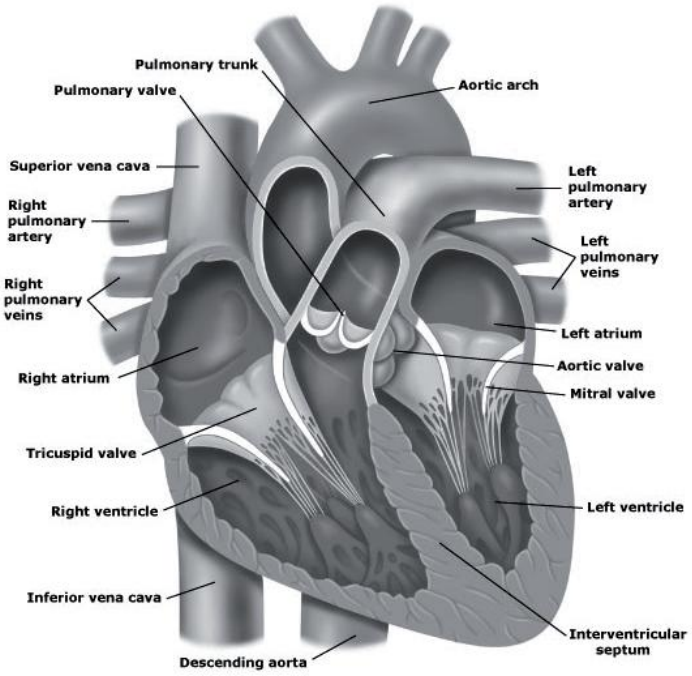

Figure 3.2. Anatomy of the heart

The left side of the heart delivers oxygen-rich blood to the body (systemic circulation) passing through the aortic valve to the aorta, whereas the right side pumps blood through the pulmonary valve and the pulmonary artery for an oxygen refill in the lungs (pulmonary circulation). The four heart valves act as inlet and outlet check-valves for the ventricles, allowing unidirectional flow and preventing backflow by being passively opened and closed due to pressure gradients.

3.2.1 The cardiac cycle

The right and the left sides of the heart operate as two serial pumps, performing the pumping work fairly synchronously in the normal heart. The cardiac cycle consists of the two main phases: systole, referring to the period of ventricular contraction and ejection of blood out of the ventricles, and diastole, being the period of ventricular relaxation and filling. In the figure 3.3, the systole and diastole phases are shown.

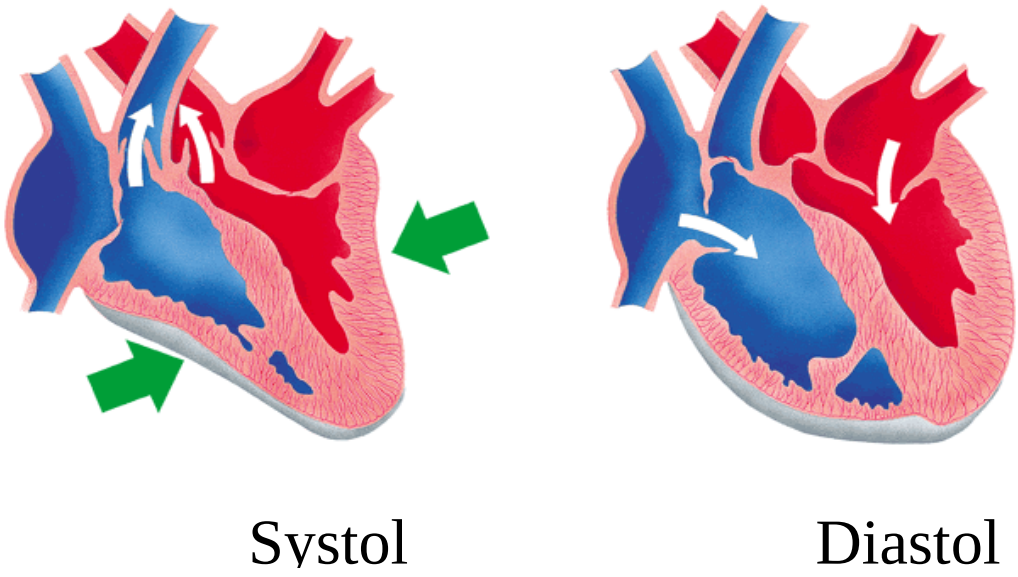

Figure 3.3. The systole and diastole phase of the heart

The myocardial contraction is initiated by automatic generation of an electrical impulse in the sinus node located in the superior lateral wall of the right atrium. The contraction results in a pressure rise within the ventricles. The phase when pressure increases most rapidly is called the isovolumic contraction time (IVCT), since all valves in the heart are closed and the ventricular volume is constant. When the pressures in the ventricles exceed the pressures in the aorta and the pulmonary artery, the aortic and pulmonary valves open and the ventricles eject blood. The blood travels along the cardiovascular system, driven by the pressure gradient generated by the myocardium. Blood from the body and the lungs starts to fill the atria of the heart, simultaneously with ventricular ejection. The pulmonary and aortic valves close when the pressures in the aorta and the pulmonary artery exceed the ventricular pressures.

When the ventricular myocardium starts to relax, the ventricular pressures drop rapidly. Once again, all valves in the heart are closed during the isovolumic relaxation time (IVRT). The pressures in the

Blood-filled atria increase, which leads to mitral and tricuspid valve opening to let the blood flow into the ventricles. During the first part of the ventricular filling phase, the blood flows as a result of the pressure gradient between the atria and the ventricles. This phase is called the fast filling phase or the early diastolic wave (E-wave). The filling continues after the E-wave, but at a reduced rate during the phase called the diastasis [19]. This phase is followed by atrial contraction during the atrial diastolic wave (A-wave), contributing to the ventricular filling by lifting the AV-plane. The pressures inside the

ventricles rise with the increased filling and, finally, the blood is pushed up against the mitral and tricuspid valves, forcing them to shut. Thereafter a new cardiac cycle can begin. Myocardial perfusion mainly occurs during diastole, as a consequence of increasing resistance in the coronary arteries during systole.

3.3 Cardiovascular function

The most important factors governing the function of the circulatory system are volume, pressure, resistance, and flow. Blood flow is determined by two factors: a pressure difference between the two ends of a vessel or group of vessels, and the resistance that blood must overcome as it moves through the vessel or vessels. The relation between pressure, resistance, and flow is expressed by the equation $F = P/R$, in which F is the blood flow, P is the difference in pressure between the two ends of the system, and R is the resistance to flow through the system. In the circulatory system, blood flow is represented by the cardiac output (CO), affected by the viscosity of blood and determined by the cross-sectional area of a vessel.

Cardiac output (CO) is the term used to describe the amount of blood pumped by each ventricle per minute. The left ventricle and the right ventricle have the same cardiac output despite the differences in their architecture – it must be that way or an accumulation of blood would exist on one side of the circulatory system causing catastrophic consequences. Cardiac output is calculated by the following formula, $CO = SV * HR$, where SV is stroke volume and HR is heart rate. A non-athlete pumps about $20 – 25\ L$ of blood per minute [20].

Stroke volume is the amount of blood ejected from the heart by each heartbeat, and the heart rate is the number of times the heart beat in one minute. Stroke volume is related to the strength of contraction of the ventricle. The average ventricle contraction leaves some blood volume left within the ventricle. The stronger a ventricle's contraction, the less blood is left once systole is over [20].

The amount of stroke volume can be changed in three ways. The first way is by changing the initial volume within a ventricle at the start of systole (also known as the end-diastolic volume (EDV)). The Frank-Starling Mechanism is the formal name given to describe the relationship between stroke volume and end-diastolic volume. An increase in the amount of blood occupying a ventricle after diastole results in an increase in contraction. The

stronger contraction is a result of the increased amount of blood creating an increased tensile preload on the muscle fibres of the ventricle, creating a greater force of contraction. The Frank-Starling Mechanism kicks in when there is an imbalance of rate of blood flow between separate sides of the heart. If one side of the heart begins to pump blood at a faster rate than the other, the side of the heart with the slower rate of blood flow will demonstrate an increase in venous return, creating a higher EDV in the ventricle, instigating a stronger contraction resulting in a greater stroke volume [20].

The second way is by input from the sympathetic nervous system. The sympathetic nervous system mobilizes the body's resources during times of stress. When greater cardiac output is required, the body can create stronger ventricular contraction that results in greater stroke volume [20].

The third way stroke volume can be changed is through a change in arterial pressure in which the ventricles must empty into. An increase in afterload (the pressure exerted by the arteries onto the ventricle) usually decreases stroke volume because the increased load prevents full contraction of the ventricle's muscle fibres [20].

3.4 Cardiovascular diseases

Cardiovascular diseases (CVDs) are a group of disorders of the heart and blood vessels. Cardiovascular disease still kills more people in Europe and North America than any other disease. It is the number one cause of death among women and men in the United States and many other developed countries [21-23]. The statistics from developing countries paint a similarly bleak picture. There were approximately 17 million deaths due to CVD in 2003 accounting for one third of all deaths in the world. For example strokes kill nearly 6 million [24].

CVDs include:

- Coronary heart disease or coronary artery disease – disease of the blood vessels supplying the heart muscle;
- Cerebrovascular disease - disease of the blood vessels supplying the brain;
- Peripheral arterial disease – disease of blood vessels supplying the arms and legs;

- Valvular disease – damage to the heart muscle and heart valves from rheumatic fever, caused by streptococcal bacteria;
- Congenital heart disease - malformations of heart structure existing at birth;
- Deep vein thrombosis and pulmonary embolism – blood clots in the leg veins, which can dislodge and move to the heart and lungs.

3.4.1 Coronary artery disease

Coronary artery disease (CAD) is the term for atherosclerosis in the coronary arteries. Atherosclerotic disease is the development of artery wall thickening and calcification, due to accumulation of lipids within the arterial intima resulting in atherosclerotic plaques. Atherosclerosis leads to increased peripheral resistance in the vascular system resulting in higher work-load for the myocardium and, in some cases also to a severe narrowing of the vessel lumen due to building of focal plaques leading to obstruction of the blood flow (stenosis). This can lead to myocardial ischemia, which is a lack of oxygen as the result of a perfusion imbalance between supply and demand. Prolonged ischemia can lead to myocardial infarction, i.e. regional myocardial cell death/necrosis [25].

CAD is usually the underlying cause of ischemia and myocardial infarction. Stable CAD is associated with chronic stenosis/-es in the coronary arteries, leading to symptoms, most often chest pain (angina) due to ischemia at a certain workload. Moreover, stable CAD is characterized by unchanged or slowly progressing symptoms over time. A sudden change of symptoms is associated with unstable CAD, often due to a plaque rupture leading to thrombus formation in the artery. When a plaque ruptures and subendothelial vessel structures come into contact with the blood, a thrombus formation is trigged, creating a dynamic stenosis or occlusion in the coronary artery. Unstable CAD carries a high risk of cardiac death and/or myocardial infarction and requires urgent medical treatment.

3.4.2 Cerebrovascular disease

Cerebrovascular disease is a disease of blood vessels supplying the brain and it causes a group of brain dysfunctions. The most important cause is Hypertension; it damages the blood vessel lining, endothelium, exposing the underlying collagen where platelets aggregate to initiate a repairing process which is not always complete and perfect. Sustained hypertension permanently changes the architecture of the blood vessels making

them narrow, stiff, deformed, uneven and more vulnerable to fluctuations in blood pressure. The results of cerebrovascular disease can include a stroke or occasionally a hemorrhagic stroke. Ischemia or other blood vessel dysfunctions can affect the person during a cerebrovascular incident [26].

3.4.3 Peripheral arterial disease

Peripheral arterial disease is a progressive disease which includes stenosis and occlusions in the peripheral arterial bed. The commonest manifestation of PAD is in the lower limbs and it can be symptomatic or asymptomatic. In the legs, the symptoms range from intermittent claudication (IC) to critical limb ischemia (rest pain, ulceration and/or gangrene). Most cases of PAD are, however, asymptomatic. Depending on the site of the arterial tree affected, the patient may also present with mesenteric angina (abdominal pain after meals), transient ischemic attacks or stroke, renal failure (renal artery disease) or myocardial infarction. Common manifestation of arterial disease is in the lower limbs, where, patients present with IC. IC manifests as muscle pain in the lower limbs on exercise. The muscle groups affected will depend on the level of arterial tree occluded. Aorto-iliac occlusive disease patients will have thigh or buttock pain and femero-popliteal occlusion will present with calf muscle group pain. More importantly, atherosclerosis may cause or worsen multi-level disease in segments of the arterial tree that are already diseased, so that the same patient may have both aorto-iliac and femero-popliteal disease. The pain rapidly improves on cessation of exercise/walking.

PAD risk factors are almost identical to those of developing atherosclerosis disease elsewhere. The most important risk factors are smoking, the male gender and diabetes. [27]

3.4.4 Valvular disease

Valvular disease refers to the improper functioning of the valves of the heart for various reasons. For individuals who have mild versions of valvular disease, undergoing thorough examination by a trained physician is usually the only way to diagnose the problem. Valvular disease will often be diagnosed by a doctor when an abnormal sound known as a murmur signals the malfunctioning of a valve initiating further investigation [28].

A mild problem with a heart valve can take years to grow to become congestive heart failure because the heart is able to adjust its own performance to make up for problems with the valve. Problems with other parts of the cardiovascular system that force the heart to work even harder together with mild valvular malfunction is usually what causes the heart to weaken [28].

The regularity of valvular disease is not clearly defined in the medical world. While almost one in twenty persons have a mild congenital form of what is known as mitral valve prolapse (the mitral valve does not cover the annulus completely), only one in half a million people suffer from valvular disease that affects adequate pumping to the body by the heart. Diseases of the valves are named by identifying the affected valve and whether the valve is stenotic (narrowed) or regurgitant (leaking). Mitral valve stenosis is an example of the nomenclature for a given valvular disease [28].

Common causes of valvular disease include congenital defects (a malformation during fetal development), calcium deposits that form as people age, and valvular infections. Less commonly, the deterioration of valvular supportive tissue (the valve no longer seals tightly due) as well as aortic aneurysm (the dilated aorta is too wide for the aortic valve to cover sufficiently) can also cause disease of the valves. Valvular disease affecting the left side of the heart is a much more serious problem than disease of valves on the right side due to the much higher pressure loads that must be withstood on the left side of the heart [28].

Rheumatic fever and infectious endocarditis are two infectious diseases that can cause disease of the heart valves. Rheumatic fever is caused by the same strain of bacteria that causes strep throat and can infect the heart valves if improper treatment allows for spreading of the bacteria to the heart. The bacteria cause inflammation of the lining of the heart and heart valves, almost always in the mitral valve, and half of the time in the aortic valve.

Stenotic valves can be caused in many ways – heart attack, congestive heart failure, aging, or cardiac/aortic aneurysm. In all cases, the support structures of the valve stiffen and the valve loosens resulting in valvular disease and allowing for regurgitation of blood [28].

Mitral stenosis is caused most often by Rheumatic fever, and less frequently by the aging process that results in the calcification of the valve. Severe cases of mitral stenosis cause a backup of blood in the left atrium, distending the atrial wall. The atrium in turn attempts to compensate for the overfilling over time by thickening so that it can pump blood more forcefully. An enlarged left atrium may inherit rhythm irregularity known as atrial

fibrillation where the atrium no longer contracts. Eventually, blood backs up through the pulmonary vein and into the lungs causing pulmonary edema. Pooled blood in the atrium can also clot. If a small piece of the clot in the atrium breaks off into the bloodstream, it could lead to infarction in some other region of the body [28].

Aortic stenosis is commonly caused by the aortic valve only having two leaflets. A bicuspid aortic valve becomes stenotic more easily because it more easily calcifies. Aortic stenosis causes the left ventricle to undergo hypertrophy to generate the much higher pressures that the diseased valve imposes on the ventricle to force blood into the body. Eventually the left ventricle hypertrophy leads to congestive heart failure with all its aforementioned symptoms [28].

3.4.5 Congenital heart disease

Congenital heart disease (CHD) is among the most common congenital abnormalities and involves structural anomalies of the heart and/or related major blood vessels. Many types of heart defects exist, most of which either obstruct blood flow in the heart or vessels near it, or cause blood to flow through the heart in an abnormal pattern. CHD arises in the first trimester of pregnancy, occurring often and in many forms. It is the leading cause of infant mortality [29] and contributes to 30% to 40% of all deaths during infancy and early childhood [30].

The morbidity varies with the severity of the CHD and can be quite serious and life threatening. The multiple surgeries needed to correct the anatomical defects can be debilitating. Furthermore, the quality of life of these patients is often compromised due to severe physical as well as psychological problems.

Over the past decades the diagnosis, medical care and surgery have considerably improved the prospects for children with CHD and resulted in a significant decrease of CHD mortality and morbidity [31]. Nowadays approximately 85% of children with CHD survive. Therefore, the primary prevention of CHD would be a big step forward, being only possible when more insight is gained into the embryogenesis of the heart and the role of genes and environmental factors.

CHDs appear in many forms and affect most parts of the heart. Cardiomyopathies, conduction-system disease and laterality defects, are inherited and sometimes present at birth, but are often not considered CHDs because of their distinct clinical presentation.

CHDs are associated with other anomalies or occur as part of a syndrome, but are most frequently present as an isolated malformation.

3.4.6 Deep vein thrombosis

Deep vein thrombosis is a serious condition with potentially fatal consequences. Many patients in both hospital and the community are at increased risk of DVT, and it is therefore important for nurses to understand the condition and how to recognize it.

Veins have a hollow core (lumen) through which blood flows from the tissues back to the heart. They contain valve cusps and are composed of three layers. The inner layer is composed of endothelial lining, the middle layer is composed of smooth muscle and elastic tissue, and the outer layer is composed mainly of elastic and collagenous fibers. In figure 3.4, the components of a vein are shown.

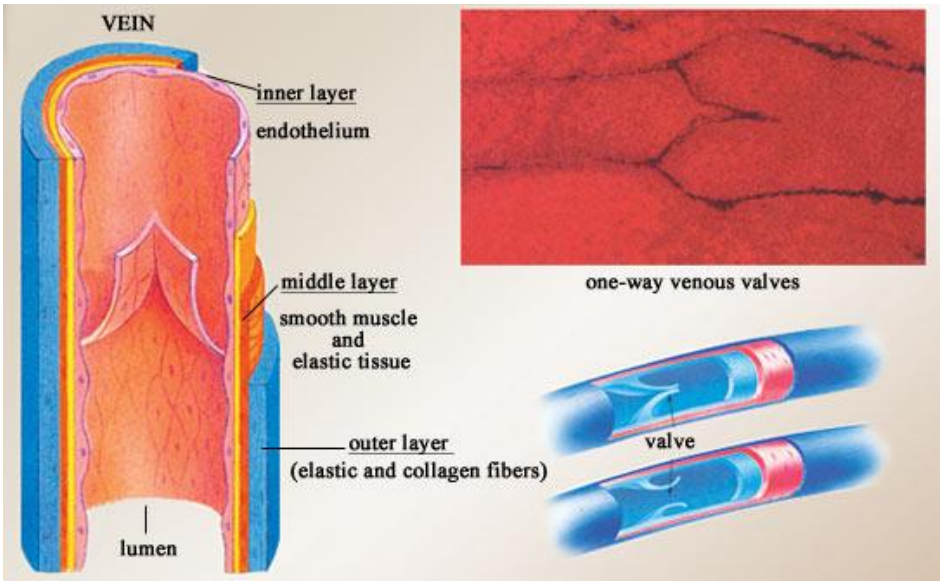

Figure 3.4. The components of a vein

Venous blood flow is assisted by respiration, which causes pressure changes in the thorax and abdomen, and by skeletal muscles and valve cusps. During mobilization the skeletal muscles of the lower limbs contract, causing the valves to open and forcing blood towards the heart (the calf muscle pump). When the muscles relax, the valves close to prevent backflow. In figure 3.5, the skeletal muscle pump is depicted.

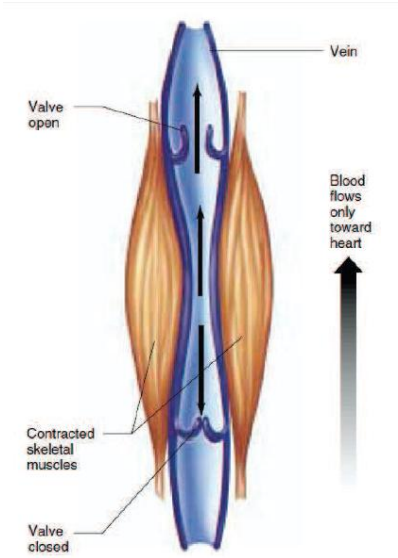

Figure 3.5. The skeletal muscle pump

DVT is the formation of a thrombus in a deep vein. Venous thrombosis are comprised mainly of fibrin and red blood cells. Although it usually affects the leg veins, DVT can occur in the upper extremities, cerebral sinuses, hepatic, and retinal veins. In figure 3.6 the schema of the deep vein thrombosis is shown.

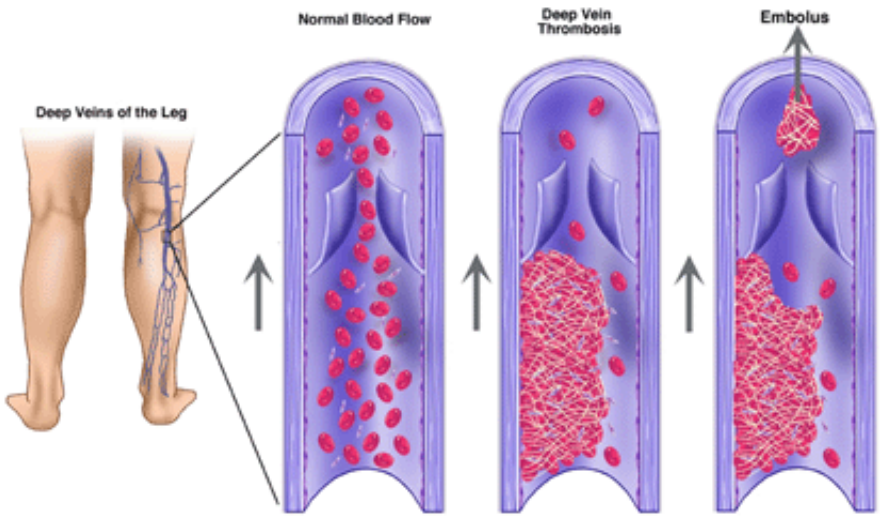

Figure 3.6. Schema of the deep vein thrombosis

It is usually caused by a combination of predisposing factors known as Virchow's triad after the German pathologist who discovered them:

- Venous stasis: immobility reduces the effectiveness of the calf muscle pump and can lead to stasis (slowing of blood flow) and pooling of blood behind the valve cusps;
- Vein wall trauma/dilation: local trauma (for example, orthopaedic surgery or leg fracture) to the endothelial lining of the vein wall activates clotting by triggering the release of tissue factor. Venous dilation, which may occur intraoperatively, can cause endothelial damage resulting in the exposure of collagen and activation of clotting;
- Hypercoagulability: a variety of hereditary and acquired causes of increased coagulability, such as pregnancy, malignancy, and thrombophilia.

All hospital patients should be assessed for clinical risk factors of DVT. The risk in surgical and orthopaedic patients is well recognized but medical patients (for example patients with myocardial infarction, stroke, or heart failure) are also at high risk and should receive thromboprophylaxis as appropriate.

3.5 Deep vein thrombosis prophylaxis

The basis of DVT prophylaxis is to target the triad of predisposing factors: venous stasis; vein wall trauma/dilation; and hypercoagulability.

- Mobilisation and breathing exercises

Nurses can encourage mobilisation and leg exercises in at-risk patients in order to activate the calf muscle pump. Breathing exercises will also help venous return. Patients should be advised to observe for signs and symptoms that suggest DVT and inform nurses if concerned.

- Antiembolism stockings

Antiembolism stockings (AES) provide continuous stimulation of linear blood flow, prevent venous dilation [32], and stimulate endothelial fibrinolytic activity [33].

- Anticoagulants

Anticoagulants such as low-molecular-weight heparin (LMWH) increase the action of antithrombin and inhibit a number of coagulation proteins. LMWH can be administered in a prophylactic dose, usually via subcutaneous injection, with a predictable anticoagulant response. In moderate-risk patients use of AES may be combined with anticoagulants to minimize risk. Patients require careful observation as anticoagulants can cause bleeding, and any side-effects should be reported.

- Intermittent pneumatic compression

Intermittent pneumatic compression (IPC) is a device to produce defined compression/relaxation patterns on limb surface to improve the venous return and to prevent of the deep vein thrombosis in the lower limb. This action can be done by a given number of actuator to stimulate mechanically the limb. So, by replacing striate muscle pump on limb veins, the venous return may recover in the immobilized patients. In the next section the IPC device is described completely.

4. IPC DEVICE

This chapter presents general information about intermittent pneumatic compression (IPC) device. The general structure and the background of using IPC device to recover cardiovascular system are explained. In addition, the designed IPC device is described and the experimental results of the effectiveness of the device in cardio circulatory function are expressed.

4.1 General structure of an IPC device

IPC device is a device for exerting an intermittent pressing action on the lower limb, to the aim of improving the venous return in impaired people, like paraplegics. However, the same concept could concern any device aimed at exerting a compressing action, like a massage for lymphoedema treatment or sports recovery.

A typical structure of such a device could be the one depicted in figure 4.1. In this case it is provided with a given number of inflatable bladders (*a*), included into shells (*b*, *c*), and acting on the skin of the calf and foot. The shells could be rigid or, more conveniently, a sort of sleeves, flexible but inextensible, so self-adapting to the shape and size of the limb but also avoiding stretching and therefore directing all the pneumatic energy towards the limb.

The control system can be arranged with several levels of complexity; basically it must include a group of valves (*d*) and a programmable logic controller, i.e. a PLC (*e*); for given applications it may be convenient to include also some sensors, for dynamic monitoring of air pressure inside bladders or contact pressure to the skin.

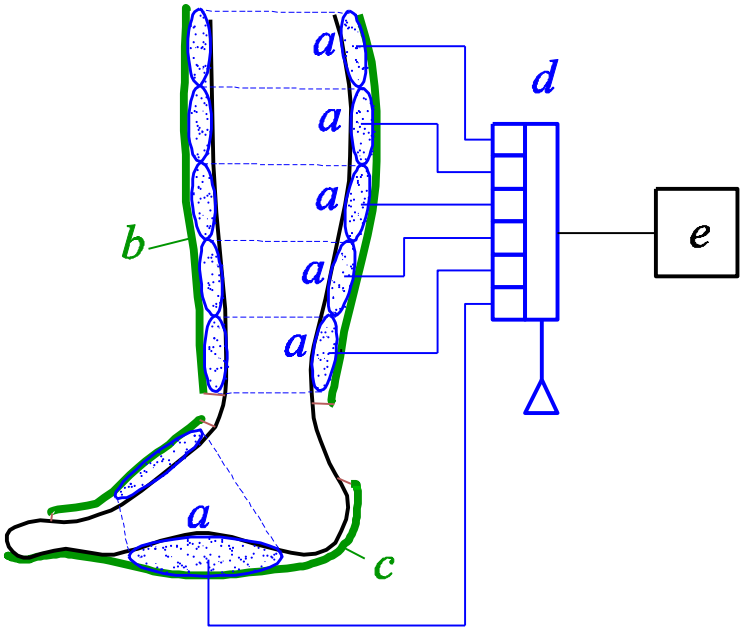

Figure 4.1. Typical configuration of an IPC device

The operating of the device is simple: by inflating the bladders with the compressed air, the pressure can be applied to the limb surface. Moreover, the programmable logic controller (PLC) controls the valves with a defined time sequence, so as to arrange the sequential acting to the bladders and generate a peristaltic and centripetal pressure wave on the limb.

4.2 Background of using IPC (literature review)

During any physical activity, the intermittent contraction of the limb muscles exerts important pumping actions on physiological systems such as the muscular, cardiovascular or lymphatic system. When the muscular efficiency is compromised for some reason, its function can be mimicked by a mechanical device properly conceived.

Although the various forms of mechanical intermittent compression of limbs have a 70-year history of published clinical effectiveness, a complete knowledge of the cause and effect process is not yet fully reached.

One of the first significant commercial devices based on real physiological evidence was the ColWil pump developed in the sixties. Many other devices were developed since that

early system, with different characteristics and to accommodate different medical applications [34].

Today in various therapeutic situations the use of an Intermittent Pneumatic Compression (IPC) system may be recommended: lymphoedema treatment, deep vein thrombosis prevention, management of venous leg ulcers, sport recovery, critical limb ischemia, improving of walking distance in patients with intermittent claudication.

Johansson et al. [35] effected a lymphoedema treatment by an IPC device for the arm (Lympa-Press, Liljenberg Medical AB, Malmo, Sweden) employing a 9 compression cells, 40-60 mmHg for 2hour/day for two weeks 5days/week, and made a comparison with a corresponding manual treatment. They refer no significant difference between the two methods, thus demonstrating the possibility to substitute the manual operation with an automatic mechanical system.

Partsch [36] focuses on the importance of using IPC devices in immobile patients, because their active venous calf muscle pump does not work. He stresses a lack of specific references in literature and lists many parameters being influenced by an IPC (venous pressure and velocity, foot/calf venous volume, skin blood flux and many others). He highlights the need to understand which IPC system is most suitable for which application.

Another field of use is sports recovery: Wiener et al [37] examined the effect of IPC on the legs for the recovery of fatigued Tibial Anterior muscles. After an IPC treatment, the muscle fatigue was monitored by surface EMG, showing significant improvement with respect to manual passive treatment. For this experience, a LYMPA.WAVE® system was used, provided with 7 bladders and operated at maximum pressure of 80 mmHg, used for 3 minutes after training, performing 2 cycles/min with 21 s inflation and 9 s deflation.

Similarly, Waller et al [38] made a pilot study aiming to demonstrate that IPC devices may be beneficial to the warm-down activities of athletes. They compared two different treatments with low pressure (20:15:10 mmHg) and high pressure (70:65:60 mmHg) and concluded that “athletes undertaking IPC as part of their training regime should be able to increase their training volume with a reduced risk of discomfort and injury”.

A pair of recent review articles, Comerota [39] and Nelson et al. [40], underlines that in various researches an IPC device can be used for the management of advanced chronic venous disease, specifically Venous Leg Ulceration. They underline that different devices with different pressure levels, duration per day and duration of treatment have been performed. Comerota suggests that use of IPC as an adjunct to sustained compression may

be the optimal choice for treating patients with VLUs, however a number of questions remain, for example the type of compression. Nelson et al. conclude that there is no robust evidence that IPC improves ulcer healing when compared with continuous compression alone or when added to a standard regimen of compression bandages. There is only some generic indication that "fast" IPC therapy has more effectiveness than "slow" therapy.

Various researchers (Flam et al. [41], Christen et al. [42], Froimson et al. [43]) investigated the effectiveness of several commercial IPC devices for the prevention of deep vein thrombosis. In general they observed positive results, although each device was used with very different settings, as concerns pressure values and cycle times, thus indicating a poor knowledge of the relationship between the characteristic and setting of the device and the effect on the human.

Morris et al.[44] tried to evaluate the variety of available systems, with different compression techniques and sequences, in order to individuate appropriate choice criteria for each patient. They conclude that rapid inflation, high pressure and graded sequential IPC show particular augmentation profiles, but there is no evidence that such features improve the prophylactic ability of the device. According to them, the most important parameters are the patient compliance and the appropriateness of the site of compression. In particular, as regards to the extent of the bladders, they prefer the asymmetric solution, with smaller bladder placed only at the back of the limb, rather than bladders extended circumferentially around the whole limb. This is because smaller bladders require limited size pumps and allow higher operating frequencies.

A research by Dai et al. [45], oriented to a more quantitative study, defines a method to model the deformation of a limb under different cuffs (circumferentially symmetric and asymmetric) and to examine the stress distribution within the tissues and the corresponding venous blood flow. With a 2D FEM model, they found that asymmetric compression would generate larger blood flow velocities and shear stresses than circumferentially symmetric compression. However, no consideration is made on dynamic effects.

Malone et al. [46] made a comparison between five IPC devices, two of standard type (low pressure: ranging from 40 to 50 mmHg, slow dynamics: 1min cycle, inflation 11-12 s) and three high pressure (160, 160, 120 mmHg), rapid (22, 22, 30 s cycle, inflation 2 s) compression systems. They evaluated the maximal venous velocities at the common femoral vein and at the popliteal vein and observed an increase for all devices. The comparison between the two kinds of devices showed an increased velocity response to

the high-pressure, rapid inflation device. Thus, this research raises a question about the need to understand the dynamic behaviour of the device, considering the effect of two parameters: pressure level and inflation/deflation time. Actually, these parameters are correlated: if inflating time is very short, the contact pressure between leg and device could not reach the supply pressure value.

The need to relate the supply pressure with the real operation pressure (i.e. the contact pressure between leg and bladder) as a function of the device characteristics and the work cycle timing is an important topic, poorly investigated.

This crucial point was caught by Lurie et al. [47]. Their study attempted to investigate the relationships between the interface pressure produced by IPC devices, the deformation of extremity tissues produced by this pressure, and changes in venous blood flow, by use of magnetic resonance imaging and duplex ultrasound scans in addition to pressure measurement. They used Venaflow® (Aircast Inc, Summit, NJ) (6 s inflating with 0,3 s delay between the two chambers, rapid deflating, at 52(distal), 45 (proximal) mmHg and WizAir® (MCS Medical Compression Systems Ltd, Or Akiva, Israel) (slow inflation and slow deflation at 80 mmHg). They concluded that, while in the past the difference between hemodynamic effects produced by various IPC devices has been attributed only to the different levels of the air supply pressure, the patterns of pressure actually applied to the extremity might be different due to different materials and construction of the garments. They also conclude that "further investigation of biomechanical mechanisms of IPC is needed to guide the development of better engineering solutions …"

Summarizing, this review highlights the lack of a general methodology to study and develop an IPC device with physical and dynamical characteristics suitable for the intended application.

In particular, the dynamic behaviour of the device in response of the control command is practically ignored.

4.3 Commercial IPC devices

In the market, there are some devices to treat the lymphedema diseases and also to improve the cardio circulatory system. These devices work based on the pneumatic compression. In the following, some of the devices are described.

- **VenaFlow**

VenaFlow provides intermittent pneumatic compression (IPC) suitable for cases of deep vein thrombosis. The device operates using a sequential and graduated compression to increase the speed of the blood, reduce stasis and therefore promote the reabsorption of body fluids.

The device consists in electronic device (figure 4.2) , to which are connected , by means of a system of pipes , a series of sleeves , inflating and deflating conduct the business compressive . In particular, the system can act at three different levels depending on the number of sleeves to which are connected: the simplest case with only one foot (figure 4.3 a), to the case of more extensive than expected to act at the level of the leg (figure 4.3 b), or thigh (figure 4.3 c).

Figure 4.2. The electronic system and the connecting pipe of the VenaFlow

Figure 4.3. The VenaFlow device for acting on the foot (a), calf (b) and limb (c)

In each case the activity of the compression part by a level distal to continue in the most proximal. The pressure cycles, consisting in successive inflations/deflations sleeves are

automatic and their peaks increase gradually through the first five minutes of operation. Moreover, the system is equipped with an alarm system in case of failure or malfunction. The normal actual pressure of the device is between 40-50 mmHg.

The main drawback in the use of the device suggest not to use it for patients with heart failure, pulmonary edema , thrombophlebitis, severe atherosclerosis , infection or extreme deformity of the leg [48].

- **Bio-Arterial plus**

Bio arterial plus is an Intermittent, Sequential, Pneumatic Compression System that sequentially compresses the lower extremity in patients suffering primarily from arterial ulcers, ischemia or intermittent claudication. The system is designed to deliver pressures of 120 mmHg for two to three treatments per day. It increases arterial blood flow in both the popliteal artery and at the tissue level. Through effective compression, resultant evacuation of venous blood from the lower limbs enables replacement with substantial volumes of oxygenated arterial blood. In the figure 4.4, the Bio-Arterial plus device is shown.

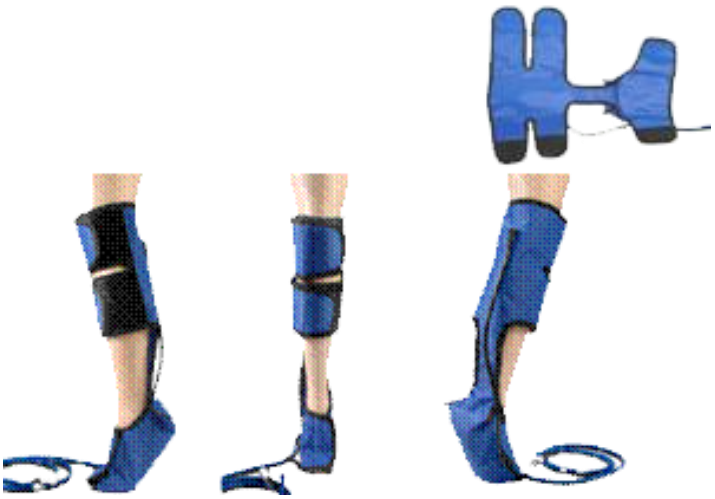

Figure 4.4. Bio Arterial Plus device

Every cycle takes 20 seconds, so every minute there are three cycles. The inflation takes 4 seconds ±0.5 s, while the deflation period takes 16 seconds ±0.3 s. It should be noted that the delay between the foot and calf is1 second ± 0.5 seconds. This tool is not recommended for patients with limb infected, suspected deep venous thrombosis, arterial

thrombosis, inflammatory episodes of phlebitis or pulmonary embolism and venous and lymphatic return undesirable (such as congestive heart failure) [49].

- **Flexi-Touch system**

The Flexi- touch is a pneumatic compression device, advanced and lightweight, suitable to the stimulation of the lymphatic system. This system allows not only the treatment of lymphedema from home and chronic edema, but also the prevention of their progression, eliminating many of the complications that result from such disorders, including recurrent soft tissue infections and chronic fibrosis.

Unlike traditional compression pumps that press on the affected areas, the system Flexi-Touch promotes the natural circulation of the fluid through the lymphatic system, to the healthy areas of the body. Therefore, its action is different because it proposes the aim of exploiting the lymphatic system for the transport of fluids from the areas of the affected limb impaired to the healthy regions of the body in which the fluid can be absorbed and treated naturally. The mechanism to stimulate the lymphatic system of the Flexi-Touch has been clinically proven [50] and has been observed to be more effective than the simple pneumatic compression [51, 52].

The Flexi-Touch provides a dynamic pressure in a rhythmic manner and gentle on the skin, using up to 27 to 32 chambers, through fifteen different programs for the treatment of upper and lower body. The program is selectable by using a display, in order to provide a customized treatment and efficient. The loading phase lasts only a few seconds for the chambers and a full treatment of the leg takes about 45 minutes. In the figure 4.5, the Flexi-Touch device is depicted.

Figure 4.5. The Flexi-Touch device

- **Mobility-1**

MOBILITY-1 is the only intermittent pneumatic compression device for lymphedema and chronic venous insufficiency (CVI) that allows patient mobility. It applies graduated sequential pressure within a fully mobile pneumatic device. Its application is important for patients that suffer from various disorders who do not benefit from static compression dressings. The main advantages are the full patient mobility with a small fully portable compressor, the adaptation to the leg anatomy in real time, the improvement of capillary filtration rate, the high patient compliance achievement, the edema reduction and prevention, and the promoting of lymphatic drainage with an optimal pressure calibration. The application of pressure has two different modes; the first permits the application of pressure sequentially from the feet to the top of the leg, while the second mode applies the pressure with a sequential and overlapped application of pressure between the bladders [53]. In the figure 4.6, the Mobility-1 device is shown.

Figure 4.6. The Mobility-1 device

- **Lymphastim BTL**

The principle of operation of Lymphastim consists of a pneumatic pressure therapy. The applicator with special sleeves and pants in several superimposed. The device makes a gentle massage which encourages the natural circulation of the lymph in the human body, similar to the manual lymph drainage through the hands of a therapist.

It is used in various fields such as sports rehabilitation and medicine, and rheumatology clinics to Lymphology, in health resorts, hotels and SPA centres of aesthetics. The system

allows Lymphastim significant advantages because it is a therapeutic method known and clinically approved, with immediately visible results. Moreover, the treatment is well received by patients and the body is not unnecessarily burdened with medicines.

Lymphatic drainage offered by the system allows you to drain the lymph within the lymphatic vessels, causing the natural flow from the peripheral parts of the body. Hence it reduces swelling and pain caused by the excessive amount of lymph and metabolites in the limbs. Lymphastim also helps the healing and regeneration of muscle tissue, increasing the tone and elasticity of the skin.

It is a 12-channel device with easy-to- use user interface with colour touch screen 5.7 ". BTL has encyclopedia with medical and aesthetic protocols, sequences, pre-set programs, internal memory to store up to 100 user-defined programs (thus allowing for specific treatments and custom). It can set the continuous pressure from 20-160 mmHg with adjustment of the gradient, and pressure control separate for each chamber (their operating activities is shown on the display).

It is a system easy to wear, the connection of the applicators is simple and is equipped with a compressor reliable and silent [54]. In the figure 4.7, the Lymphastim BTL device is depicted.

Figure 4.7. The Lymphastim BTL device; the compressor and sleeves (a), the device worn by a patient (b)

- **BALLANCER**

The BALLANCER is a device designed for aesthetic applications such as body care, slimming and cellulite reduction. The lymphatic drainage massage produced by the system, is used for the treatment before and after liposuction, to reduce edema post-surgery and the swelling for the treatment LPG cellulite. The BALLANCER mimics the movement of a manual massage giving the feeling of two hands which move simultaneously. In figure 4.8, the BALLANCER device is depicted.

Figure 4.8. The compressor and the body of the BALLANCER device

It is therefore a specific device for an effective massage aesthetic tire with applications not only at the level of the lower limbs but also superior, simply connect the device with the corresponding supplement. The technical characteristics of the compressor allow: a pressure adjustment from 20 to 80 mmHg, a peristaltic cycle of 35 minutes. The size of the compressor is reduced (14.5 x 30.5 x 38.5 cm) with a weight of only 5.1 kg, this allows ease of transport.

There are some cases in which the using of the device are not recommended; in presence of pain, in the case of atherosclerosis or vascular ischemia, heart failure, or in case of suspected presence of deep vein thrombosis, thrombophlebitis, gangrene, dermatitis, infected ulcers or inflammatory processes [55].

- **LymphaWaveTM 301**

This device is particularly indicated for the treatment of lymphatic problems, suffering with localized lymphedema and venous ulcers. The cycle of peristaltic LymphaWaveTM promotes lymphatic and venous return, making it particularly suitable for post-traumatic edema, edema of venous origin, ulcers in the postoperative course of perforator ligation or

stripping of the Saphenous vein in the post- mastectomy lymphedema with scars. In figure 4.9, the LymphaWaveTM device is depicted.

Figure 4.9. The LymphaWaveTM device

The pressure can be adjusted from 20 to 80 mmHg, according to medical indication, making the device safe even for a home use; specifically for the treatment of lymphatic problems.

Technical characteristics of the compressor include a pressure adjustment from 20 to 80 mmHg, a peristaltic cycle of 30 s (4s break), with a maximum time of use around 120'.

It is not recommended to use in the presence of pain, in the case of atherosclerosis or vascular ischemia, heart failure, gangrene, dermatitis, ulcers and infected in the presence of inflammatory processes [56].

- **Aviafit**

Aviafit is a small and portable intermittent pneumatic compression device, designed for all those who live in a situation of limited mobility; at home, in the office or on the road. The device is designed to be used by surgical patients from the beginning of the surgery, during hospitalization, up to when patients are no longer at risk of thrombosis. Among those most at risk of thrombosis can cite smokers, overweight people, and pregnant women, at risk of abortion or undergo hormone treatments.

The portability allows the treatment for more than 20 hours a day continuously, the system is a safe alternative (it has no known side effects) and effective alternative to anticoagulant drugs. Aviafit clinically tested and uses to prevent stagnation of blood clots in the blood, stimulates the circulation in the legs and then prevents the onset of deep vein

thrombosis and helps to reduce swelling in the legs and ankles. The set includes 2 units by means of straps to tie around the two legs (one leg) at the level of the calf muscle (over or under clothing). Figure 4.10 shows the Aviafit device.

Figure 4.10. The Aviafit device

In several clinical studies published, Aviafit has shown that it is able to increase the peak velocity of the flow in the veins. It was also verified that it is able to provide the same hemodynamic benefits of conventional intermittent pneumatic compression devices, highlighting the benefits for the prophylaxis of thromboembolism, increased compliance in rehabilitation and home care. The measured increase is equivalent, and in some cases superior, to that measured using compression devices stationary [57].

4.4 The designed IPC device

In this study based on the previous IPC devices and their deficiency, we decided to design the prototype to cover all philological and mechanical aspects. In addition, the prototype must consider the convenient and the conditions of the patients.

Two IPC prototypes were designed in the laboratory of the Mechanical engineering department of PoliTo, that in the following sections those are described.

4.4.1 Prototype 1

This prototype was the first device that made in the laboratory. It includes 6 bladders, a rigid body to support the bladder, the electrical control system, and the pneumatic circuit. In the figure 4.11, the prototype 1 is depicted.

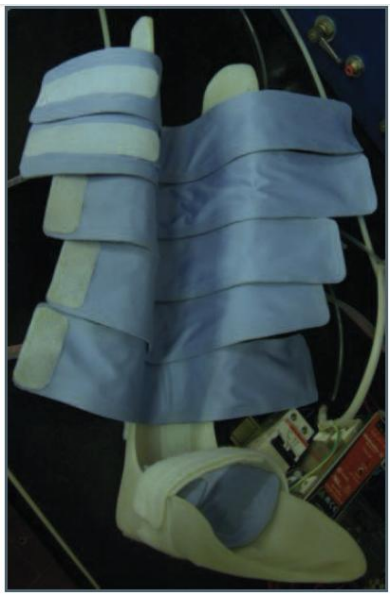

Figure 4.11. The first prototype made in the laboratory

The prototype was tested on the volunteer persons with cooperation of the Caliari University and the positive effects on the cardiovascular system were reported.

To characterize this device we faced several problems about its rigid body. Due to the rigid body, the adaptability of the device on the leg and using of the maximum air energy exerted to the leg ignored. Moreover, it causes the gap between the bladder and the skin and this value may be different in the persons and it depends on the shape of the leg. Therefore, the characterization of the device in presence of this undetermined value is not so accurate.

Another problem was the displacement of the device. To move the device and transport of that, the weight of the rigid body makes some difficulties. So, we decided to optimize the prototype and making a new one to remove the uncertainties and more convenient in the displacing.

4.4.2 Prototype 2

The second prototype has the objective to overcome the limitations of the previous one, especially for what concerns the problems of fit and adaptability to the shape and dimension of the limbs, in order to improve the effectiveness of the air energy to the muscle at the level of interface. In this prototype, instead of the rigid body, the flexible and inextensible tissue is used to support the bladders. The inextensibility of the tissue causes the expansion energy of the bladders only affect on the limb size. And the

flexibility of the tissue allows to the device to adapt as much as possible to the anatomy of the limb. In the figure 4.12, the second prototype is shown.

Figure 4.12. The second prototype made in the laboratory

Also in the figure 4.13, the whole system used in this study is depicted.

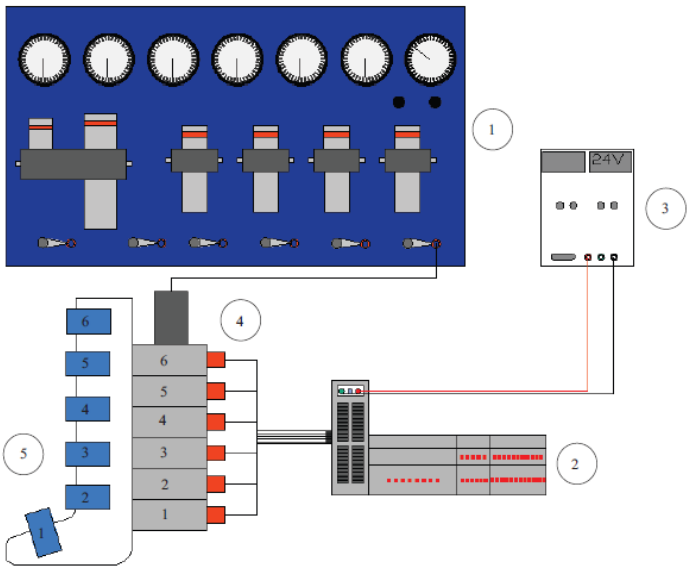

Figure 4.13. The whole system of the IPC device

In the system, the pressure source or air compressor *1*, compresses the air until the given value of the pressure and by using the elastic pneumatic pipe the compressed air transit to the micro-electric valves *4*. There are 6 micro-electro valves to connect each bladder to

the pressure source in inflating or to ambient in deflating. The signal for opening and closing of the valves, come from the PLC *2*, which is supplied by electrical source *3*.
In the following each components of the system is described more.

4.4.2.1 The bladders

In the IPC devices, the mechanical action is provided by pneumatic energy through the bladders. Bladders are sealed cells which are very strategic element in such devices. In order to optimize the performance, it is convenient that the air energy is directed as much as possible towards the biological tissues of the limb, rather than used to deform the materials of the device structure. To this aim, the bladders should be able to expand with limited or null stretching of the wall and this can be achieved both by proper shaping of the cell and adopting a material which should be compliant but, of course, air-tight. In addition, the number of the bladders and its area are so important to cover the muscle s of the leg and foot.
In our IPC device, the bladders are made of Windtex® tissue and there are 5 bladders for the leg and 1 for the foot. The bladders cover all regions of the leg and foot. Also the bladders are numerated as 1-6 from foot to leg. In figure 4.14, the bladders of the IPC device are shown.

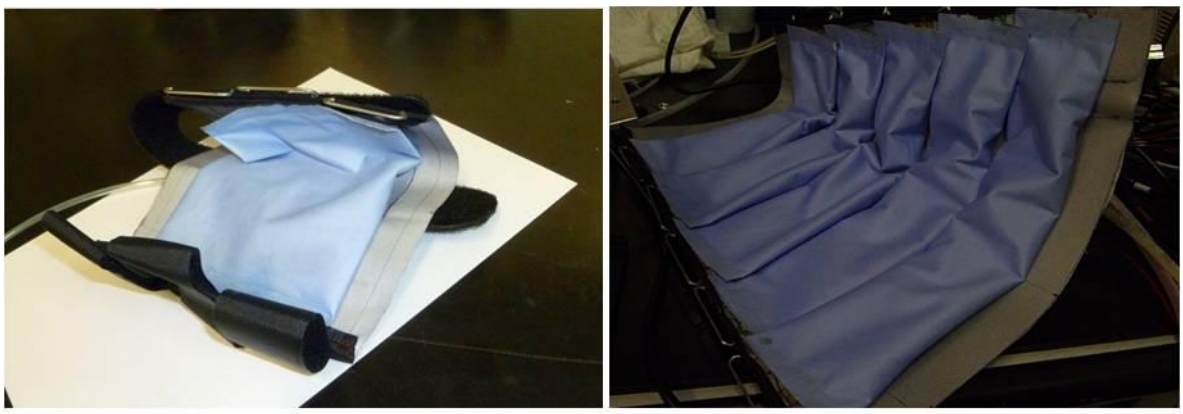

(a) (b)

Figure 4.14. The bladders of the foot (a) and the leg (b)

To optimize the situation in deformation of the bladders towards the leg and cover the whole of the leg, we used several plans for the area of the bladders and how they should attach to the shell. The best was determined when the bladders are rectangular with

different in width and same height equal *5 cm*. To attach the bladders to the shell the bladders fold in the longitudinal direction as *1 cm* on the edge and are glued to the shell. In this case to cover the region of the leg the bladders have overlapping with together about *0.5 cm*. For the foot, the bladder is rectangular with the size *16.5*12 cm* to cover the whole muscle of the foot for normal person. In the figure 4.15 the plan of the bladders are shown.

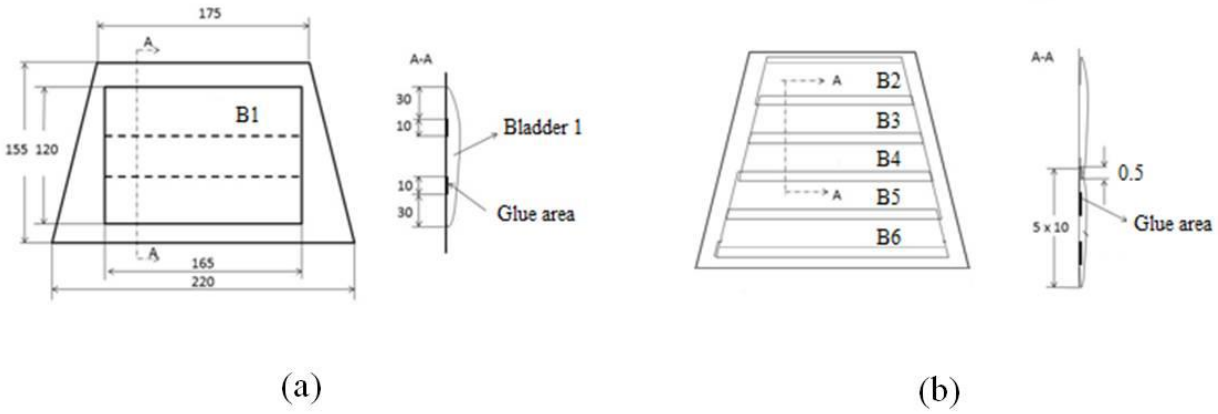

Figure 4.15. The plan of the foot bladder (a) and the leg bladders (b)

4.4.2.2 Programmable Logic Control (PLC)

A programmable logic controller (PLC) is a programmable microprocessor-based embedded designed to perform programming and control of temporal sequential processes. It has the facility for extensive input/output (I/O) arrangements through the implementation of specific functions such as logic, sequencing, timing, counting, and arithmetic. PLCs are categorized by the number and type of I/O ports they provide and by their I/O scan rate. The used PLC in this IPC device belongs to the SIEMENS company and its model is LOGO 24RC. The PLC is used for the electrical commandment of the 12 pneumatic valves (six for each leg). This commandment is proceeding while sending diverse signals configured with different characteristics for the independent opening and closing of the valves. The differences between the signals are basically the duration of the period, the step size, the diphase or overlapping between the six valves, and the breaks inside the periods. The numeration of the valves is ranked in increasing order from bottom to top. Accordingly, the first bladder corresponds to the first pneumatic valve, so that the first bladder is in contact to the foot.

The programs have been used for the opening and closing the valves can be defined as below:

- **Program A**

This program is very fast and each bladder is open for *0.5 s*. Inflating of the bladders in this program are without any overlapping and the cycle for one leg takes *3 s* and for two legs takes *6 s*. In the figure 4.16 the sequence diagram of this program is shown.

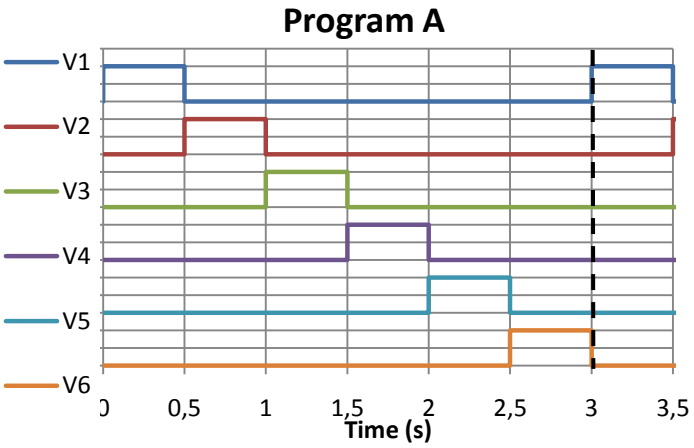

Figure 4.16. The sequence diagram of the program A for one leg

- **Program B**

The program *B* has been proposed in two versions, with *B1* cycle duration *T = 4 s*, and B2, which is the same cycle but slower *T = 7 s*. In the first case, each valve remains open for a period of *0.75 s*, and the valves are opened in sequence one after the other with an overlap of *0.25 s*. When the last valve is closed, the system remains stationary for *0.25 s* before starting the next cycle.

Regarding the program *B2*, the relationships between the valves are the same but in double time. So each valve remains open for a period of *1.5 s* and the valves are opened in sequence one after the other with an overlap of *0.5 s*. When the last valve is closed, the system remains stationary for *0.5 s* before starting the cycle on the other leg. The complete cycle for two legs takes *14 s* in this program. In figure 4.17 the sequence diagram of the program *B2* is depicted.

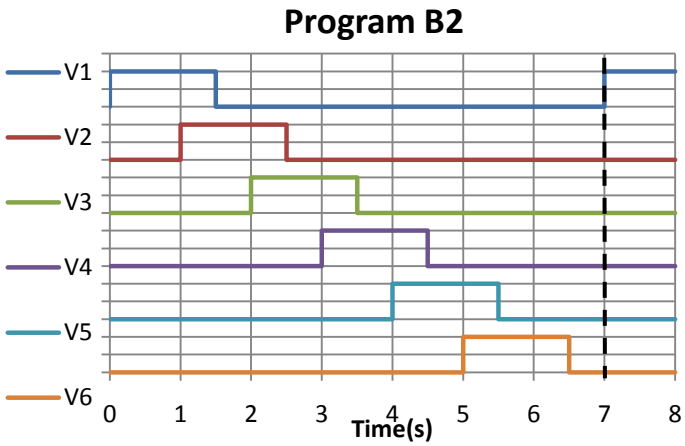

Figure 4.17. The sequence diagram of the program B2 for one leg

- **Program C**

The program C is characterized by a cycle of *6 s*. The activation of the valves is superimposed through the cycle and those are activated progressively from the foot to the leg and remain active until the end of the cycle.

Therefore the first valve (V1) is activated at the beginning of the cycle and is kept open for *6 s*, one second after the second valve is opened while keeping such a state for a duration of *5 s*, and so in a second sequence after another, the other valves are activated until the last which remains open only for a time of *1 s*. At this point after *6 s*, the valves are closed together for one second and after that the cycle is started for the other leg. In this program a complete cycle for two legs takes *14 s*. In the figure 4.18 the sequence diagram of this program is shown.

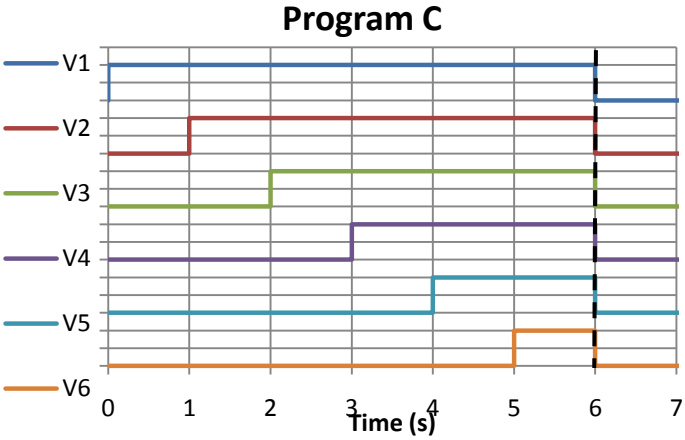

Figure 4.18. The sequence diagram of program C for one leg

- **Program A_ap3**

The program A_ap3 is characterized by a total cycle time of *36 s* (*18 s* per leg). Each valve is opened in sequence (then no overlap), one after the other, starting from the valve controlling the bladder to the foot and ending with the valve to the knee. The time in which the valve remains open is the same for all and that is *3 s*. Once the cycle on one leg, starts on the same loop on the other. Figure 4.19 represents the signals supplied to the individual legs.

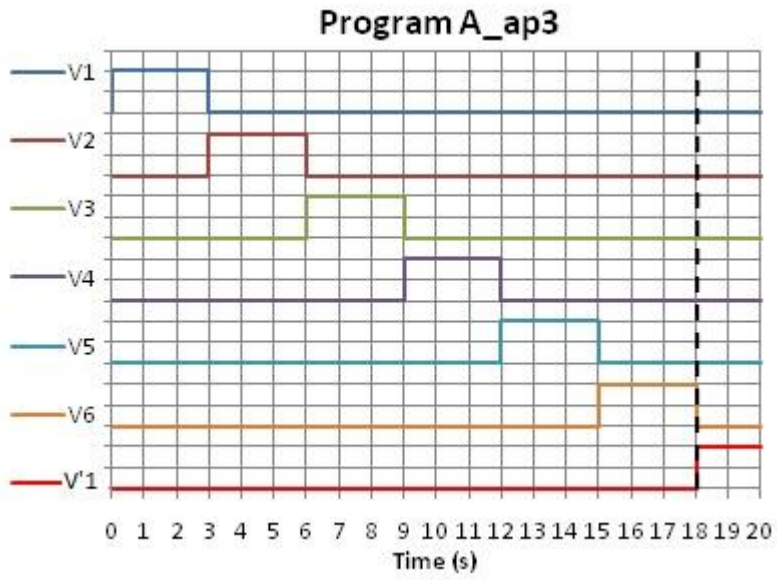

Figure 4.19. The sequence diagram of program A_ap3 for one leg

- **Program B_ap3**

The program B_ap3 is characterized by a total duration of *21 s* (*10.5 s* per leg). Each valve is opened in sequence, at a distance of *1.5* if it remains open for a period of *3 s*. At the end of the cycle starts again on one leg in a similar manner on the other. The configuration of the signals in time for the individual leg is represented in Figure 4.20.

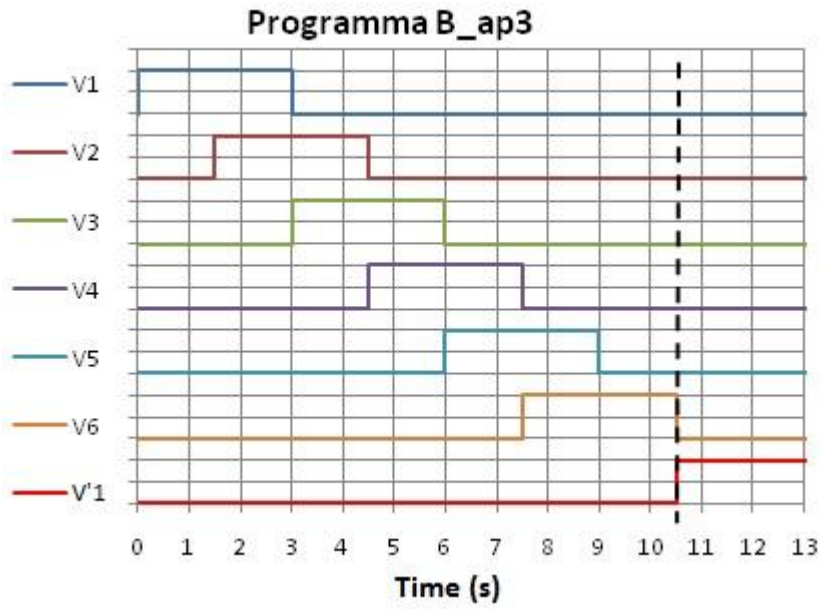

Figure 4.20. The sequence diagram of program B_ap3 for one leg

- **Program B_new**

The program B_new is characterized by a total duration of *13 s* (*6.5 s* per leg). Each valve is opened one after the other at a distance of *0.5* if it remains open for *4 s*. At the end of the cycle starts again on one leg in a similar manner on the other. The configuration of the signals in time for the individual leg is shown in Figure 4.21.

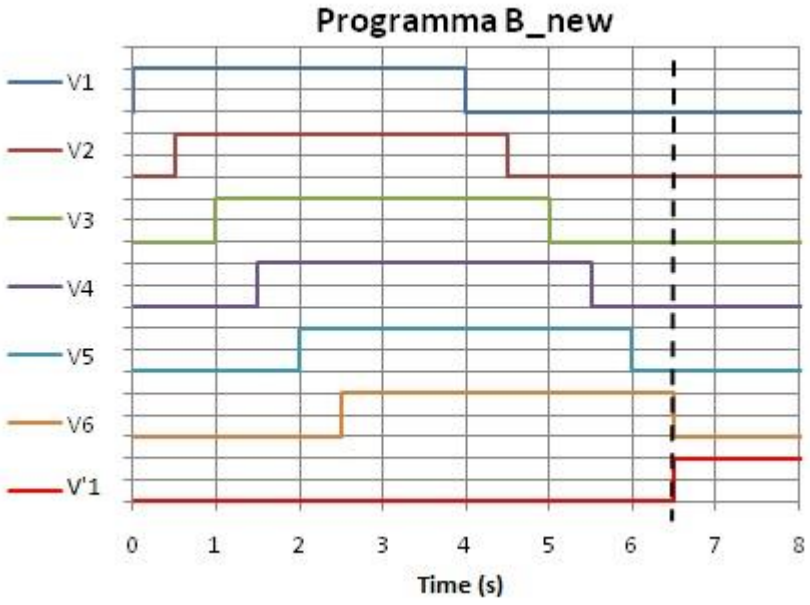

Figure 4.21. The sequence diagram of program B_new for one leg

- **Program C5**

The program C5 is characterized by a total duration of *24 s* (*12 s* per leg). Each valve is opened one after the other (starting from the valve to the foot and ending with the valve at the knee) at a distance of *1*, if they remain active for different times. In particular, the valve *V1* is open for *6 s*, the valve *V2* for *5 s* and from the valve 3 (ie V3, V4, V5, V6) remain active for 4 s. After the closure of all valves on the first leg there is a pause of 3 s, during which all the valves are closed before restarting the cycle on the other leg. The configuration of the signals in time for the individual leg is represented in Figure 4.22.

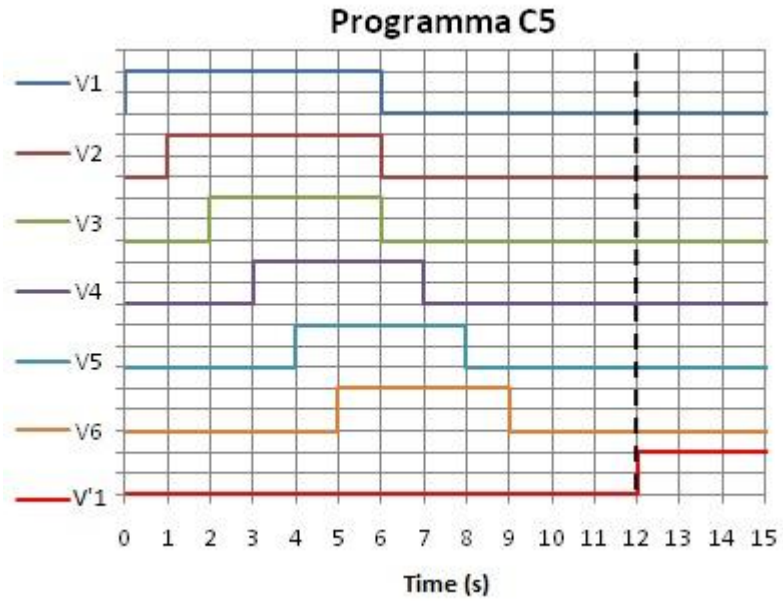

Figure 4.22. The sequence diagram of program C5 for one leg

4.4.2.3 Micro electro valves

The pneumatic valves are an essential component of the device for the control of pressure, flow rate and direction of the air. The air must be controlled in order to inflate and deflate successfully the bladders of the device.

The six pneumatic valves used in the device are solenoid 3/2 way valves. In the figure 4.23, the pneumatic valves are shown.

Figure 4.23. The pneumatic valves used in the device

A solenoid valve has two main parts: the solenoid and the valve. It is an electromechanically operating valve which is controlled by an electric current through a solenoid. The solenoid converts electrical energy into mechanical energy which, in turn, opens or closes the valve mechanically.

In the case of a three-port valve, the outflow is switched between the two outlet ports (exhausted port and the port for the bladder).

4.5 Experimental physiological test of the IPC device

The second prototype was tested experimentally on 19 voluntary subjects in the laboratory of Sports Medicine at the Cagliari University and by Echocardiography *ECG* and Impedance Cardiometry devices the most important parameters of the cardiovascular system were studied.

4.5.1 Study population

A group of 19 male healthy subjects aged between 20 and 35 years (Height: 1.74 ± 0.08 m; Weight: 66.2 ± 8.5 kg) were recruited, none had any history of cardiac or respiratory disease or was taking any medication at the time of the study. Each volunteer gave written consent to take part in this study after they had been given detailed information on the procedures and risks. Subjects were asked to refrain from caffeine, alcohol and physical activity for 12 h, and eating for 3 h, prior to the inflation test. All experiments were carried out in a temperature-controlled room (room temperature set at 22º C, relative humidity between 40-50%). Before, during and after each test routine cardiovascular parameters were assessed. The study was performed according to the Declaration of Helsinki and was approved by the local ethics committee.

4.5.2 Inflating tests design

Before monitoring the cardiovascular response during the activation of the device, each subject was monitored at rest for 3 min to collect baseline values. Then, the IPC device was placed to the subject to collect the data (Figure 4.24). Once the preparation was completed, all volunteers underwent a compression-relaxation protocol.

Figure 4.24. Placement of the device and equipments for the experimental tests

The device operating protocol adopted is the same as program *B_ap3*, the one reported in figure 4.20 in sequence and inflating time. Only the difference is in delay of *3 s* between the two boots; thus the entire cycle including both boots was *27 s* lasting. The inflating relative pressure reached the maximum value of *0.3 bar*. On each thigh an elastic containment stocking was worn to reduce the venous distension coming from the increase of blood flow during the mechanical actuation.

4.5.3 Hemodynamic assessment

Hemodynamic variables were monitored and recorded beat-to-beat by means of an impedance cardiography device (NCCOM 3, BoMed Inc., Irvine, CA) which allows a

continuous non-invasive transthoracic electrical bioimpedance (TEB) assessment throughout all the phases of the protocol [58]. The scheme of using the device and how to assess the hemodynamic variables is sown in figure 4.25.

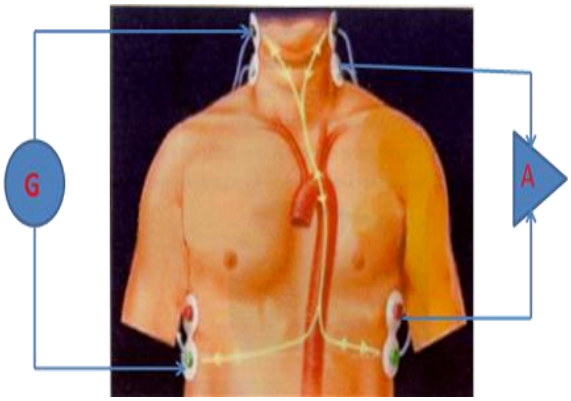

Figure 4.25. Electrical Schema of an impedance cardiography device

According to the figure 4.25, an electrical current generator (G) was connected to the subjects' thorax by two pairs of disposable *ECG* electrodes (green snap fastener): the one pair cervical and the other thoracic, in such a way to inject into the thorax a constant, alternating current (2mA, 70kHz). Other two pairs of electrodes (red snap fastener) were sensing electrodes and were placed respectively *5 cm* below those cervical and *5cm* above those thoracic injecting current. Both pair sensing electrodes were tie up the amplifier section (A) of the impedance device, from which analogical signals of thoracic electrical bioimpedance *Z0* (Ohm) were detected.

Totally, the impedance device was connected to the subject by eight electrodes: two pairs were thoracic and cervical electrodes to inject a constant current (2mA, 70kHz), whereas two other pairs were sensing electrodes placed above the cervical and below the thoracic pairs [59]. The electrical signal was recorded by a digital chart recorder (AD Instruments, PowerLab 8sp, Castle Hill, Australia) [60].

Analog traces of TEB, i.e. the thoracic impedance value (Ω) results from the Ohm law or from ratio between applied voltage difference to the thorax by the alternate current (G in figure 4.25) and the circulating electrical current into thorax collected by an electronic

amplifier (A in figure 4.25). Beat-to-beat values of TEB at the end of cardiac diastole (Z0) were acquired and *Z0* was utilized as an inverse index of LVEDV [61].

The rationale for this choice is shortly presented here so on. Considering the electrical resistors which all together constitute an electrically equivalent model of the thorax, most of they are of solid consistence (muscles, bones, cartilages, vessels, connective tissue of lungs) which, for this, do not vary their mass suddenly. On the contrary, lung air content and intrathoracic liquids content are subjected to cyclical changes. So, changes in equivalent electrical impedance of the thorax, i.e. *Z0*, refer about a like sinusoidal oscillation which shows two harmonics: the main one corresponding to breathing phases and the secondary one, with a lesser amplitude, corresponding to cardiac cycle phases. By utilizing a common electronic band-pass filter the main respiratory harmonic of *Z0* can be excluded and, in this way, observed changes in *Z0* only depends on changes in intrathoracic liquids volume. These in turn depend on both blood volume into heart and thoracic vessel and on extra-vessel water volume. It is expected that, in a healthy subject, extra-vessel water volume does not change significantly, thus *Z0* ought to depend essentially by beat-to-beat variations of thoracic blood volume which reach its relative peak when ventricles get to end diastolic volume. Since blood is a more conducting electrical current tissue, an increase in end diastolic volume induces a corresponding reduction in *Z0*.

4.5.4 Results

Figure 4.26 shows a typical experimental session. In each subject *Z0* values were assessed just before the test beginning (Z0-basal) and just at the end of the test (Z0-test). During tests ECG traces were assessed. Assessed values of Z0-basal were compared with Z0-test values by the Students't-test for paired samples and a value of $P<0.05$ was considered as significant.

As shown by the columns height in the graphs of Figure 4.26, mean values ± SEM of Z0-basal and Z0-test were 26.73 ± 3.88 Ohm and 26.38 ± 3.88 Ohm respectively. Students't for paired samples was: - 4.62 with $P < 0.0002$. So, the mean reduction of Z0-test values with respect to that of Z0-basal values was highly significant.

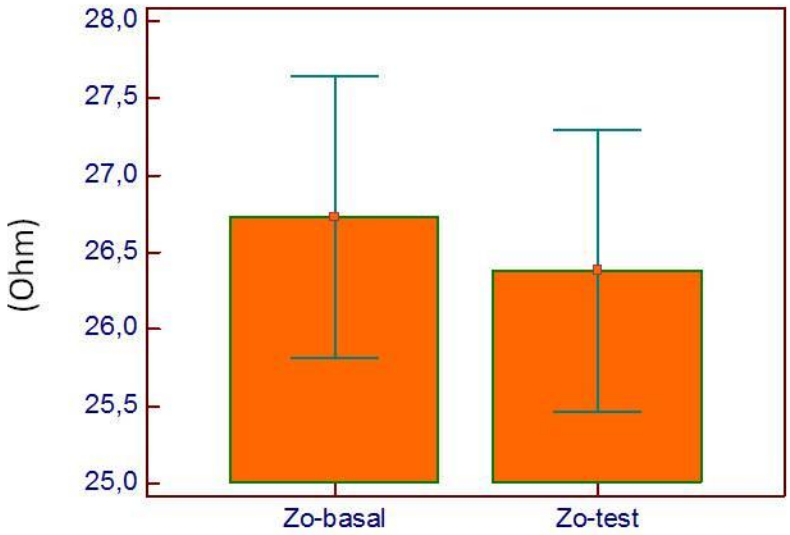

Figure 4.26. The value of Z0 before the test (Z0-basal) and after the test (Z0-test)

Test induced changes in Thoracic electrical impedance. Columns represent mean values of the thoracic electrical impedance respectively before legs compression session (Z0-basal) and just at the end of the compression session (Z0-test). Vertical bar in each column represent SEM. *P < 0.0002 with respect to the Z0-basal mean value.

4.5.5 Discussion

The mechatronic device here tested showed good chances to substitute physiological features in producing sufficient venous return for avoid LVEDV loss in bed-rest, endurance athletes. In fact, a good feedback for this possibility arose from the observed statically significant reduction in Z0 just after a leg compression test which lasted less than 30 s.

Several previous studies support, both in animal and in humans, reciprocal and consistent relationship between Z0 and LVEDV. Luepker et al [62], in anesthetized dogs in which the thoracic extra-vessel fluid was maintained at a constant, found that changes in central blood volume (CBV) were highly correlated with Z0 changes (r = -0,978). They also calculated the following linear regression equation: [Z0 = 101,3 – 0,68 (CVB)] in which it appear that each unitary increase in CBV induced a Z0 decrease of about an half.

Now considering humans, Okutani et al. [63], while applying head up tilt manoeuvres in healthy subjects, showed that when head up was reached the Z0 rose up to +9.5% than the pre-test value. Moreover, legs venous occlusion while recovering supine position showed that Z0 fall but its final value was higher than that recovered without occlusion. Since in these subjects legs venous occlusion reduced LVEDV, the fact that Z0 correspondingly did not recover pre-test, lower values demonstrates that it is inversely correlated to a reached LVEDV. This latter conclusion is also supported by the observation that, passing from standing to supine position, a group of healthy subjects showed ultrasonographic images of left ventricle which indicates a LVEDV increase of about 24% while Z0 fall of about 7% or a reduction of about one third of Z0 at each unitary increase in ventricle volume (personal observation).

Recently [64] it has been found that during passive recovery following repeated bouts of supramaximal exercise at a cycle ergometer, Z0 progressively increased during passive recovery (+1.6 ± 0.4 Ω at the 10th minute of recovery) since the absence of pedalling after a strenuous cycling exercise may result in a serious blood pooling into leg veins [65]. On the contrary, when in the same experiment an active recovery was done Z0 did not increase (+0.05 ± 0.3 Ω at corresponding time points of passive recovery period), and the difference between these two kinds of exercise recovery was statistically significant ($P < 0.05$).

Our actual results showed that the applied compression protocol induced a Z0 reduction of about -1.3% with respect to the pre-test value. Considering that: i) in a previous study [66] in which distance runners performed a cycle ergometer incremental exercise, their highest reduction in Z0 (-4.5%) was reached when workload was 50% of that maximum; ii) in another study [67] a group of endurance athletes who also performed an upright bicycle test at about 50% of maximum workload (their heart beat was 130/min) the LVEDV showed its maximum increase of 33 mL which was +23% of corresponding rest value; iii) speculating now with a proportional approach it can be deduced that, if -4.5% Z0 (from reference 30) ought to correspond to+23% LVEDV (from [67]) then -1.3% Z0 (in the present research) ought to correspond to an extrapolated LVEDV increase of about 10%.

In addition, increasing of the LVEDV about 10% causes the cardiac output CO and stroke volume SV increase about 9.4% and 16% respectively [68,69].

5. MATHEMATICAL MODEL OF THE IPC DEVICE

Mathematical modelling of a system means describing the system by using the mathematical concepts and formulations. The purpose of the modelling is to predict the behaviour of the system in static or dynamic situation and determine the effectiveness of the different parameter on the performance of the system. The mathematical model includes the linear or nonlinear differential equations, operators such as algebraic operators, and a sort of variables and uncertainties. In other words, the mathematical model can connect the input and the output of a system by mathematical equations.

The reliability of results depends on the number of variables and interactions considered, as well as the presence or absence of factors of uncertainty which may affect the operation of the system and the initial data. As much as the variables and physical parameters choose accurately, the results of the mathematical model are close to the experimental one. Therefore, to have the reliable and accurate mathematical model, it is necessary to understand the variables and their relationships as well as determining the physical parameters of the system.

An accurate mathematical model of the IPC device is a fundamental tool for understanding the physical behaviour and setting all structural and functional parameters.

The model must consider all physiological and mechanical principles which have to be harmonized for the expected therapeutic methodology.

It is supposed that the basic requirement for a given therapeutic protocol is the application of a rhythmic pressure to a limb; the pressure must be automatically controlled as regards in particular the frequency and the maximum/minimum levels.

A conceptual block diagram of the system may consider a single module with one bladder supplied by one pneumatic valve, as depicted in figure 5.1. The bladder and the limb together form the so called "Human-Machine System".

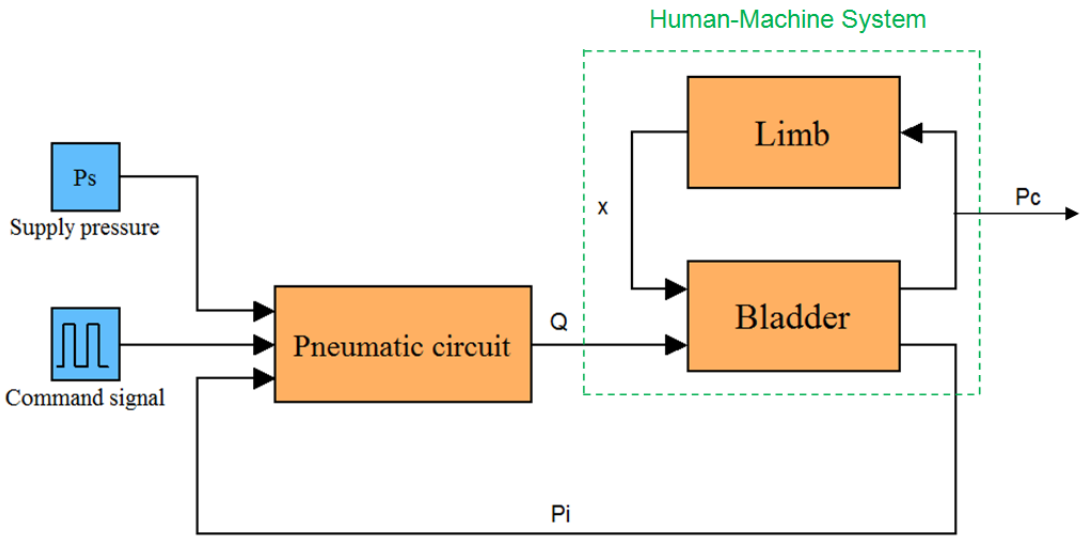

Figure 5.1. Conceptual block diagram of the system

The micro electric valve is supplied by a given pressure source P_S and is commanded by a digital on-off signal; the air flow Q from the valve inflates the bladder, producing a variation of the internal air pressure P_i and of the contact pressure P_C on the limb; this latter is then deformed by an amount x which in turn affects the volume of the bladder. The bladder pressure P_i also influences the mass flow rate Q.

The contact pressure P_C is the physical quantity which must be controlled.

To model the whole of the system, it is required to characterize all subsystems and determine their parameters. In the following, the modelling procedure is described.

5.1 Modeling of the pneumatic circuit subsystem

The pneumatic circuit subsystem for one bladder comprises a 3-port electro-pneumatic mini-valve, connected to a supply source on one side and to the bladder on the other side. The switching of the valve between its two operating conditions connects in turn the bladder either to the supply source or to the exhaust.

To model the pneumatic system it is necessary to express the air mass flow rate through the valve as a function of the supply and bladder pressures, and of the operating

conditions. This can be done by using the formulation defined by the ISO 6358 Standard [70], which considers the two possible conditions of sonic and subsonic flow. The figure 5.2 shows the typical shape of a valve flow curve for fixed upstream pressure P_1 and variable downstream pressure P_2. The symbol Q_C indicates the critical flow rate. One must consider that, depending on the valve condition, the bladder inner pressure P_i can correspond either to the downstream pressure P_2 (when the bladder is inflated and the upstream pressure is the supply pressure P_S) or to the upstream pressure (when the bladder is deflated and the downstream pressure is the ambient pressure P_A).

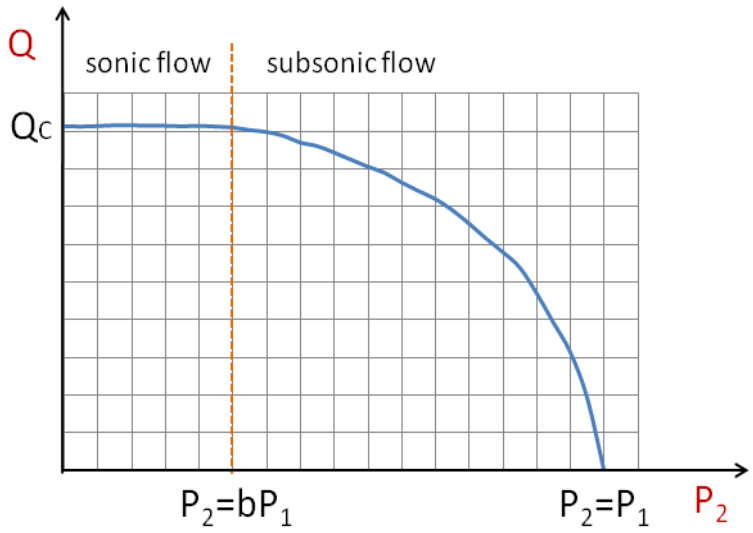

Figure 5.2. The flow curve of a pneumatic valve

According to the above Standard, the valve flow rate can be analytically expressed by interpolating functions:

$$Q = C \cdot P_1 \cdot H\sqrt{1-\left(\frac{r-b}{1-b}\right)^2} \quad \text{for subsonic flow}$$
$$Q = C \cdot P_1 \cdot H \quad \text{for sonic flow} \qquad (5\text{-}1)$$

Where: C is the valve conductance, H is a corrective factor depending on the inlet air temperature (H=1 at standard conditions, with P_1=1.013 bar and T=273 K); $r=P_2/P_1$ is the actual pressure ratio; b is the critical pressure ratio (when P_2 reaches the critical value $P_{2CR}=b\cdot P_1$).

The valve coefficients *C* and *b* can be evaluated by the experimental characterizing of the valve.

5.1.1 Characterizing of the pneumatic micro-electro valve

Characterizing a valve can be done by determining its flow curve. In this case, since the valve use for the inflating and deflating, characterizing the valve can be done in the two conditions. In the following the coefficients C and b for both inflating and deflating will be obtained experimentally.

- **Inflating condition**

The schematic of the system to obtain the flow curve of the valve in this condition shows in figure 5.3.

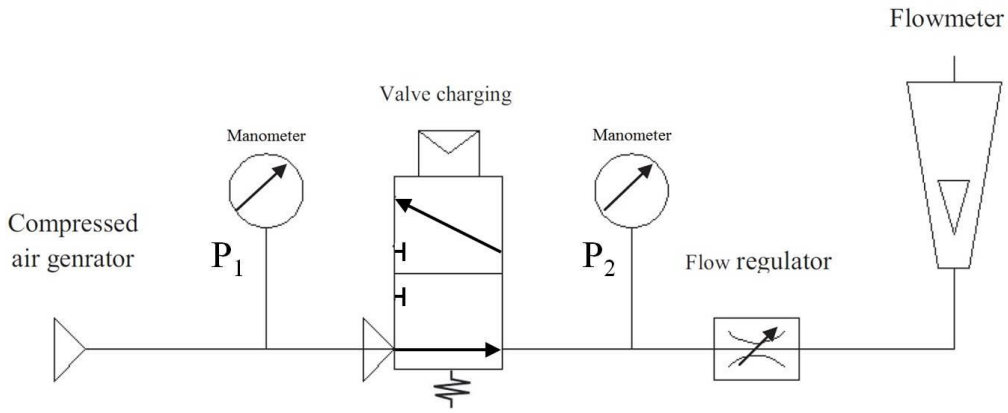

Figure 5.3. Schematic of the system to obtain the flow curve in inflation condition

At the first the flow regulator is close and flow meter indicates no flow rate. So the upstream and downstream pressure of the valve are equals (P1=P2). By progressively opening the flow regulator, the pressure P_2 will decrease and the flow rate up to a critical point at which the flow rate becomes constant even if the flow regulator is opened further. This critical corresponds to the sonic condition of the flow. Once the flow regulator is completely open, the maximum flow rate is constant from critical point and the value of downstream pressure is *0, $P_2 = 0$.*

According to equation 5-1, The valve conductance (C) is the ratio between the maximum flow rate (Q_c) and absolute inlet pressure (P_1) under sonic flow condition at a temperature of *20°C*. In addition, critical pressure ratio (b) is the ratio between the output absolute

pressure (P_2) and the inlet absolute pressure (P_1) at which the flow becomes sonic. (b = $\frac{P*_2}{P_1}$)

To characterize the valve and determining valve conductance (C) and critical pressure ratio (b) in the inflating condition, the experimental tests (as it is shown in Figure 5.3) have been done in three different inlet pressures and their flow curves are shown in figure 5.4.

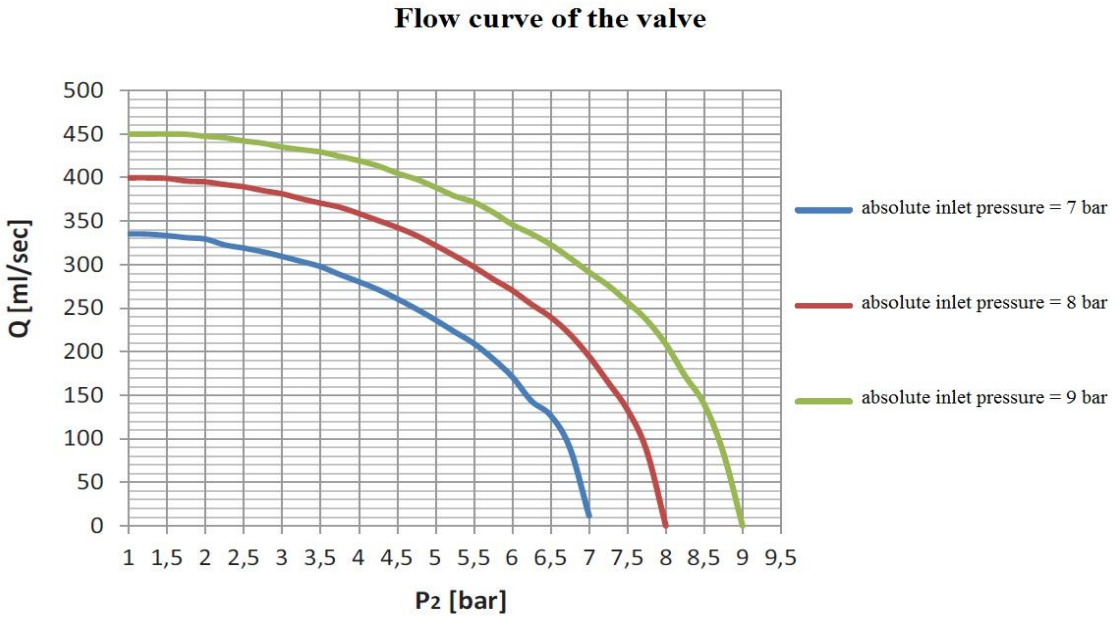

Figure 5.4. Experimental flow curves of the valve for three inlet pressure

According to the figure 5.4, the valve conductance and critical pressure ratio can be obtained for each flow curve and the mean value of them can be considered as properties of the valve. So, the parameters *C* and *b* for the valve in the inflating condition are:

C = 50 ($\frac{ml}{s.bar}$)

b = 0.02

Once the parameters *b* and C are obtained, it is used to develop the correspondent equation 5-1, in order to calculate the flow rate *Q*. Moreover the pressure ratio *r* can be obtained by the ratio between the downstream pressure *P2* and the upstream pressure *P1*.

- **Deflating condition**

In this condition, the schematic of the system which is used to characterize the valve is shown in figure 5-5.

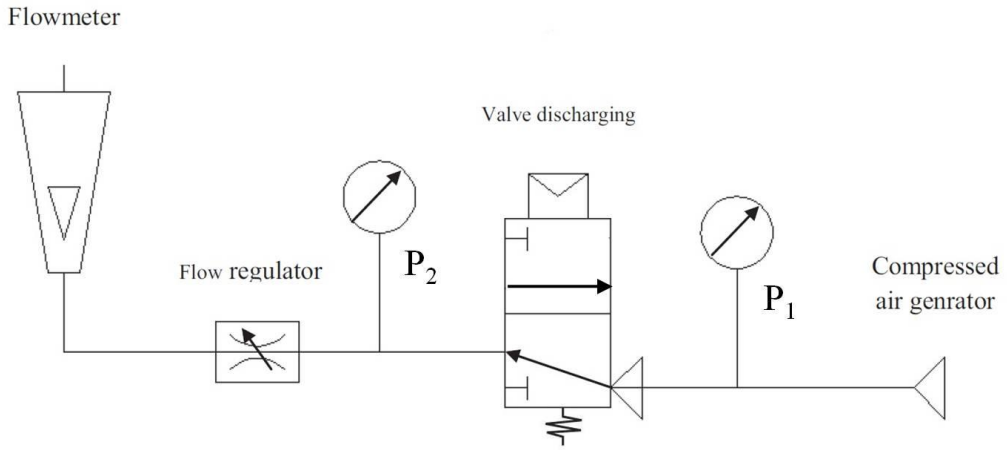

Figure 5.5. Schematic of the system to obtain the flow curve in deflation condition

The process of obtaining *b* and *C* in the deflating condition is the same as inflating condition. The coefficients in this condition are calculated as:

C = 50 ($\frac{ml}{s.bar}$)

b = 0.2

According to the value of the *C* and *b* in both inflating and deflating condition, it can be deduced that the conductance *C* is independent of the valve operation.

By calculating the coefficients *C* and *b*, and substituting in the equation 5-1 for subsonic condition, the flow rate *Q* can be obtained. Also the mass flow rate can be obtained by multiplying the flow rate to the density of the air.

$$q_m = Q * \rho \qquad (5\text{-}2)$$

Where ρ is the density of the air in the normal conditions.

After determining the all parameters of the pneumatic circuit system, it is possible to implement the mathematical model in the SIMULINK ambient. Figure 5.6 shows the system is implemented in the SIMULINK ambient.

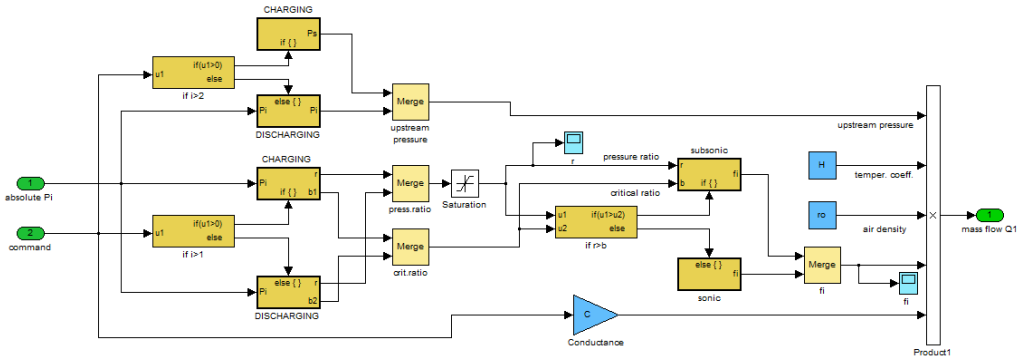

Figure 5.6. The implemented pneumatic circuit system in SIMULINK

5.2 Modeling of the human-machine subsystem

The Human-Machine System represents the interaction between the bladder and the limb. A possible schematization of the system is shown in figure 5.7. The bladder is considered as a compliant closed volume supported by the device shell; the limb is schematized as a compliant body (the muscle) supported by the bone.

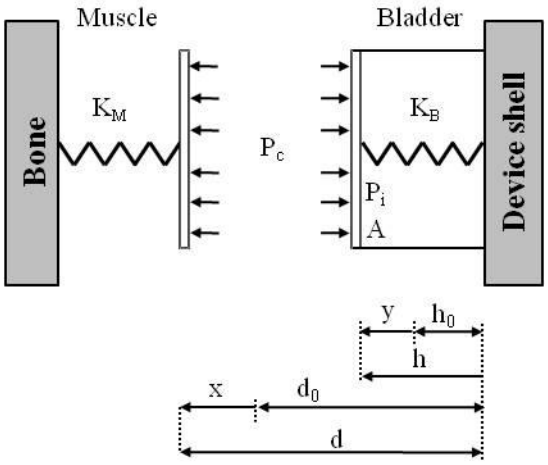

Figure 5.7. Scheme of the human-machine subsystem

The main mechanical characteristics are the transversal muscular stiffness K_M and the bladder wall stiffness K_B. P_i is the pressure inside the bladder; P_C is the contact pressure between bladder and limb. x and y represent respectively the deformation of limb and bladder under the effect of the pressure. The actual height of the bladder is indicated as h, whose initial value (no pressure in bladder) is h_0; d represents the actual distance (gap)

between the shell and the limb, with initial value d_0; in case of skin-bladder contact, $h=d$. The initial values h_0 and d_0 represent the "rest condition" of bladder and limb respectively, i.e. when a null pressure is acting on the system.

The physical behaviour of the bladder can be described by the scheme of figure 5.8. The internal pressure P_i depends on the mass flow rate Q coming from the valve and on the deformation y of the bladder; the contact pressure P_C on the limb depends on the inner pressure P_i and on the deformation y. The relationship between the bladder deformation y and the limb deformation x can be determined by a discussion of the contact condition.

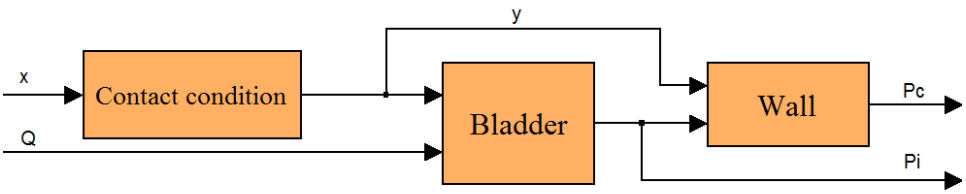

Figure 5.8. Scheme of physical behaviour of the bladder

The flow continuity equation for the bladder can be written as:

$$Q = \frac{W}{RT}\frac{dP_i}{dt} + \frac{P_i A}{RT}\frac{dy}{dt} \tag{5-3}$$

Where Q is the air mass flow rate entering the bladder, P_i is the absolute air pressure, W is the actual volume of the bladder, R is the air constant, T is the absolute temperature, A is the bladder-limb contact area.

The volume of the bladder can be expressed as:

$$W = A(h_0 + y) \tag{5-4}$$

The equation (5-3) is nonlinear; its integration allows the calculation of the absolute bladder pressure P_i but requires the knowledge of the bladder deformation y.

In the following, a capital letter P indicates an absolute pressure, while pressures relative to ambient will be indicated by a small p.

The difference between p_i and p_C depends on the stiffness of the bladder wall and is a function of its expansion, as expressed by the following equation:

$$p_C = p_i - K_B y \tag{5-5}$$

To evaluate the bladder stiffness K_B it is worth mentioning that, because of the bladder material, the elastic term $K_B y = p_B$ is existing only when the bladder wall is stretched. The variation of the bladder elastic force with respect to the bladder height can be experimentally valued by inflating the bladder in no-constraint condition, as represented in figure 5.9.

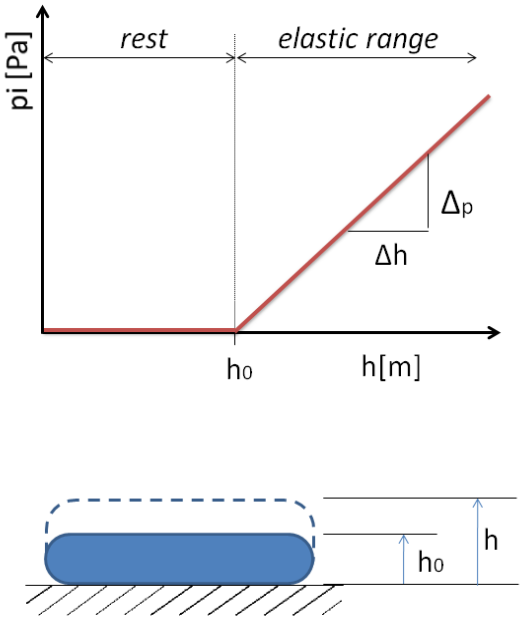

Figure 5.9. Evaluation of the bladder elastic stiffness

In this way, a variation in the inner pressure determines variation of the height, according to a given trend; this function can be approximated by two straight lines, so individuating a "height at rest" h_0, reached at an almost null inner pressure, and an "elastic range" in which the bladder wall is stretched and the height increases with the pressure. Therefore, the equation (5-5) can be split to consider the full range of the bladder expansion:

$$p_C = p_i \qquad for\ h \leq h_0 \tag{5-6}$$

$$p_C = p_i - K_B(h - h_0) \qquad for\ h > h_0$$

The actual value of K_B depends on the wall material and also on the shape and dimension of the bladder. By way of example, a rectangular bladder of 5 by 30 cm sides, made of Windtex®, presents an average $K_B = \Delta p/\Delta h$ of about $5{\cdot}10^5\ Pa/m$.
According to the figure 5.7, from the muscle side, it is possible to write:

$$p_C = K_M x \tag{5-7}$$

The determination of the transversal muscular stiffness K_M is a very crucial point. The value of this parameter is subjective and depends on the muscular condition of the limb. No information about that is available in literature and very few researchers, like Dai et al. [45] tried to experimentally measure this characteristic. A possible way to determine it is described by the scheme of figure 5.10.

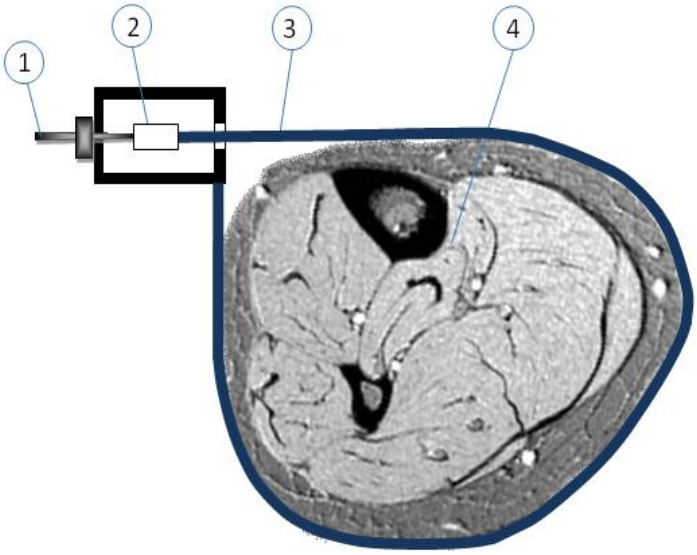

Figure 5.10. Scheme of experimental setup to evaluate the transversal muscular stiffness

In such a device, a tension *T* is applied to a strip *3* wrapped around the limb *4*; the tension is regulated by a screw device *1* and measured by a load cell *2*. In the figure 5.11, the 3-D scheme of the device and how applying to the leg is shown.

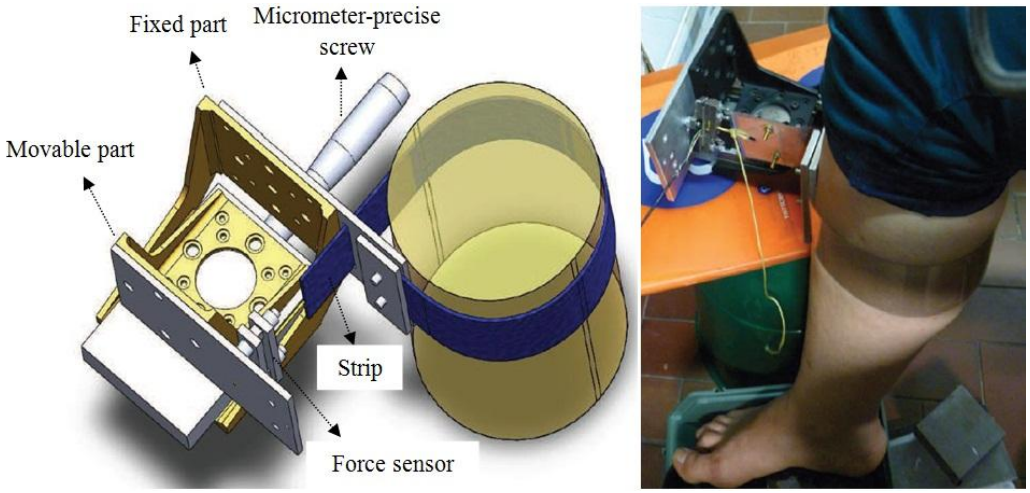

Figure 5.11. The 3-D scheme of the device is used to measure transversal muscle stiffness

When the tension T is applied, the limb deforms by a given amount, depending on its muscular stiffness. The applied contact pressure can be calculated considering the muscular tissue as a fluid mass, as depicted in figure 5.12, by the following equation:

$$p_C = \frac{T}{r \cdot l} \tag{5-8}$$

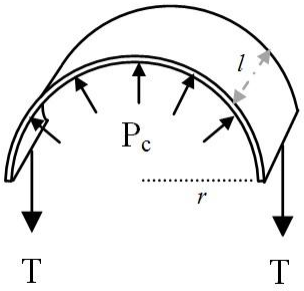

Figure 5.12. The string applies contact pressure to limb by tension T

Where r is the radius of the limb and l is the height of the strip. The muscular stiffness is measured and expressed as:

$$K_M = \frac{\Delta p_C}{\Delta r} \tag{5-9}$$

Experimental tests on three different subjects provided values of muscular stiffness that in the following is described.

5.2.1 Experimental measurement of the transversal muscle stiffness K_M

The experiments were repeated by three members of our group, each of them with different ergonomic conditions. During the process, some parameters were obtained: the length of the circumference described by the strip around the leg (L), the initial distance of the movable piece with respect to a reference point, the displacement of the movable piece measured with the bearing micrometre (ΔD), the tension in the sensor thread measured with the force sensor (T), and the height of the strip (l). According to the physical principle described before, the muscular stiffness can be calculated by equation (5-9).

The parameter Δr is calculated with the difference between the initial radius of the circumference described by the strip around the leg (r_0) and the value of the current radius (r).

$$\Delta r = r_0 - r \tag{5-10}$$

The current radius of the circumference (r) is calculated as the difference between the initial length of the circumference (L_0) and the displacement of the movable piece (ΔD), divided by twice the value of pi (π).

$$r = \frac{L_0 - \Delta D}{2\pi} \tag{5-11}$$

And the pressure is obtained by:

$$p = \frac{T}{r \cdot l} \tag{5-12}$$

As a result, the pressure will be calculated as the coefficient between the tension measured in the force sensor, and the product of two factors: the current radius of the circumference described by the strip around the leg (r), and the height of the strip (l).

The measurements were repeated between two and three times for each member and the results are shown in figure 5.13.

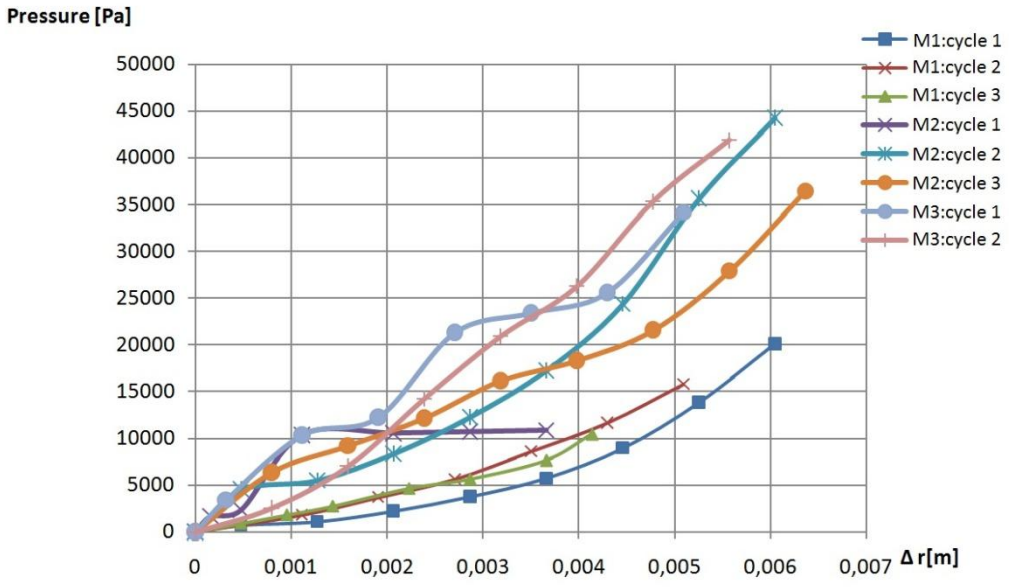

Figure 5.13. Pressure as a function of Δr corresponding to 3 members

According to the figure 5.13, the value of the transversal stiffness of the muscle can be in the range $3*10^6$ - $7*10^6$ (Pa/m).

5.2.2 Characterizing the contact between bladder and limb

The integration of equation (5-3) requires expressing the bladder deformation y as a function of pressure P_i. To do that it is necessary to detect if there is contact between bladder and limb.

The existence of the contact can be determined by calculating and comparing the values of the bladder height $h=h_0+y$ and the total gap $d=d_0+x$ (with reference to figure 5-7). Therefore to characterize the contact, it can be divided into two conditions: contact and without contact.

- **Without contact**

In this case, there is no contact between the bladder and the limb. It means, the gap between the shell and the limb is more than the total height of the bladder after air

supplying (*h<d*). Therefore, the radial deformation of the limb is zero (*x=0*). In the figure 5.14, the without contact condition is depicted.

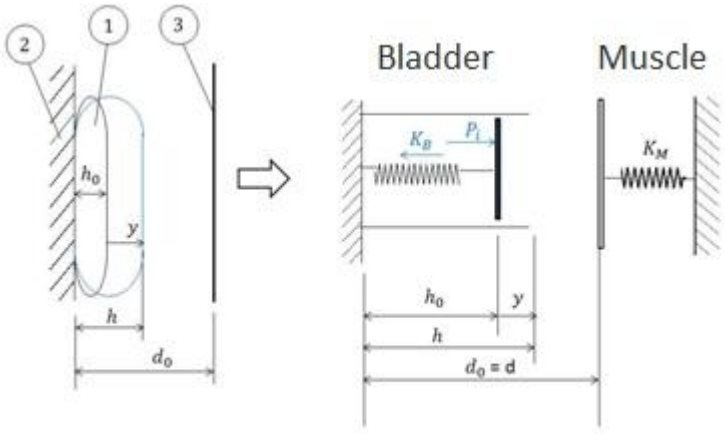

Figure 5.14. The without contact condition - The gap between shell 2 and the limb 3 is more than the height of the bladder 1 after air supplying

The deformation of the bladder *y* can be obtained by considering the static equilibrium for the bladder wall.

$$p_i - K_B\, y = 0 \quad \rightarrow \quad y = \frac{p_i}{K_B} \tag{5-13}$$

- **With contact**

In this case, the gap between the shell and the limb is less than the total height of the bladder after supplying (*h > d*). Therefore, there is contact between the bladder and the limb and the radial deformation of the limb is not zero (*x≠0*). Moreover, in this condition, there is contact pressure in the contact areas. In the figure 5.15, the contact condition is depicted.

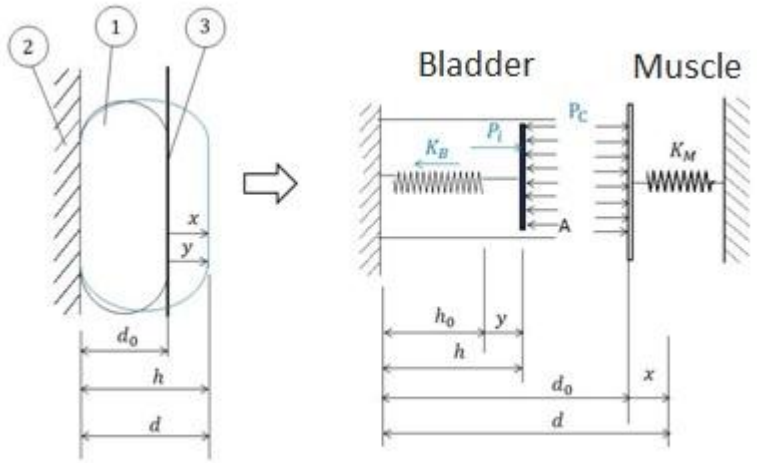

Figure 5.15. The contact condition - The gap between shell 2 and the limb 3 is less than the height of the bladder 1 after air supplying

By considering the equilibrium for the bladder wall and skin, the following equations can be expressed for this condition.

$$x = \frac{p_C}{K_M} \tag{5-14}$$

$$y = \frac{p_C}{K_M} + (d_0 - h_0) \tag{5-15}$$

With p_C expressed as per equation (5-6).

The two conditions for the contact characterization are implemented in the MATLAB-SIMULINK as it shows in figure 5.16.

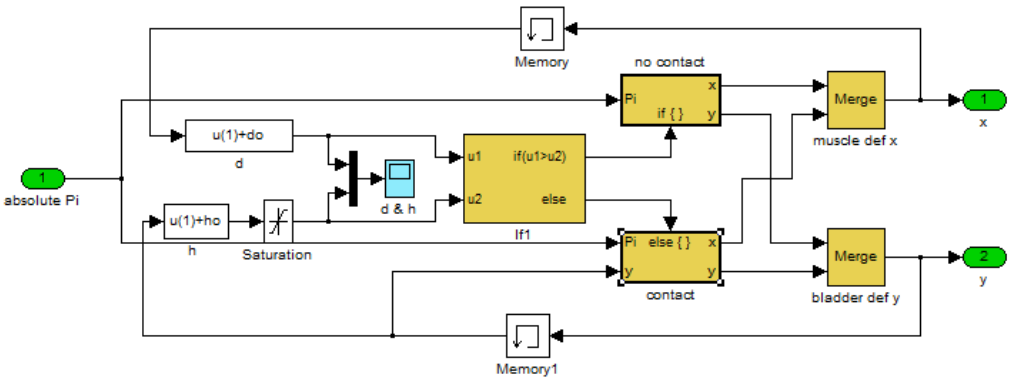

Figure 5.16. The contact characterization implemented in MATLAB-SIMULINK

5.3 Simulation of the whole model

The mathematical model with all subsystems which were characterized in the previous sections is implemented in the Simulink as figure 5.17.

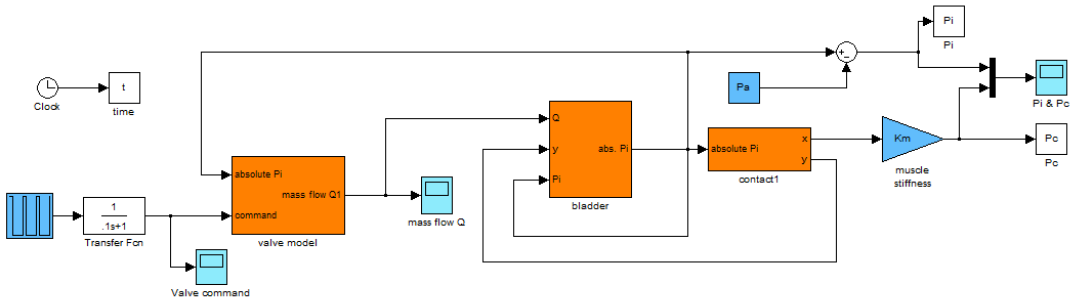

Figure 5.17. The implemented model of the IPC device in MATLAB-SIMULINK

The inputs of the model are the command signal and the supply pressure p_s and the outputs are the bladder pressure p_i and the contact pressure p_c.

5.4 Validation of the mathematical model

In order to verify the effectiveness of the mathematical model, it has been numerically simulated for the bladder number *3* of the IPC prototype. The physical and operating conditions for the system are shown in table 5-1.

Table 5-1. Experimental and simulated conditions

Parameter	***Symbol***	***Value***	***Unit***
Absolute supply pressure	P_S	$1.5 \cdot 10^5$	Pa
Absolute ambient pressure	P_A	$1 \cdot 10^5$	Pa
Contact area of the bladder	A	0.015	m^2
Pneumatic conductance	C	$3 \cdot 10^{-10}$	$m^3/(s \cdot Pa)$
Critical pressure ratio	b	0.02 (inflating)	

		0.2 (deflating)	
Temperature	T	293	K
Temperature coefficient	K_T	1	
Bladder height at rest	h_0	0.006	M
Initial shell-limb gap	d_0	0.01	M
Bladder stiffness	K_B	$5 \cdot 10^5$	Pa/m
Muscle stiffness	K_M	$7 \cdot 10^6$	Pa/m
Inflating time	ti	4	S
Total cycle time	t_C	13	S

A validation of the numerical model has been made by comparing the simulation with the experimental registration of the dynamic bladder pressure during the operation of a prototype.

The figure 5.18 shows the experimental registration of the relative internal bladder pressure in comparison with the one simulated by the numerical model in the same condition. The figure reports also the contact pressure calculated by the model.

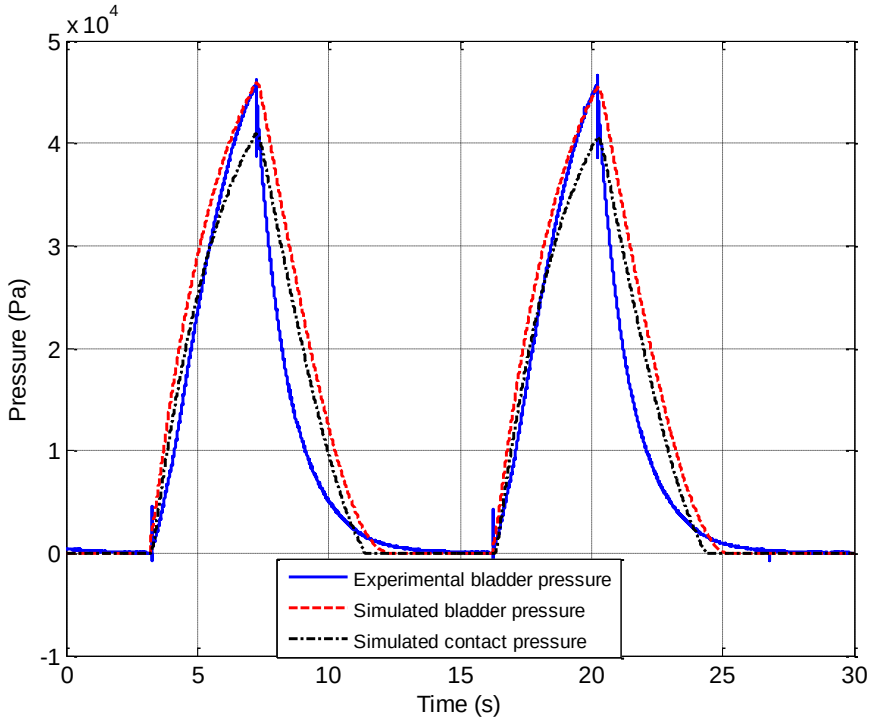

Figure 5.18. Comparison between the real and simulated relative bladder pressures

According to the figure 5.18, the following remarks may be done:

- The inflating condition is well simulated: the model reaches the same value of the bladder pressure with quite a similar dynamic behaviour.
- The simulation of the deflating phase shows some difference from reality: this could mainly due to the identification of the bladder stiffness, which is considered constant in the model but should be more likely defined as increasing with the pressure.

In general, the model is able to simulate the main dynamic behaviour of the bladder thus providing a tool useful to foresee the dynamic evolution of the internal pressure and the contact pressure on the limb, as a function of the main physical characteristics of the device and the control conditions.

5.5 More simulations of the mathematical model

The model has been used to simulate the sensitivity of the device to the variation of several parameters. All simulations have been made by varying one parameter at a time starting from the “nominal condition” reported in table 5-1.

The figure 5.19 reports the maximum values of the relative bladder pressure and the contact pressure, as a function of the initial shell-limb gap d_0, the bladder height at rest h_0, the bladder inflating time t_1 and the relative air supply pressure p_S .

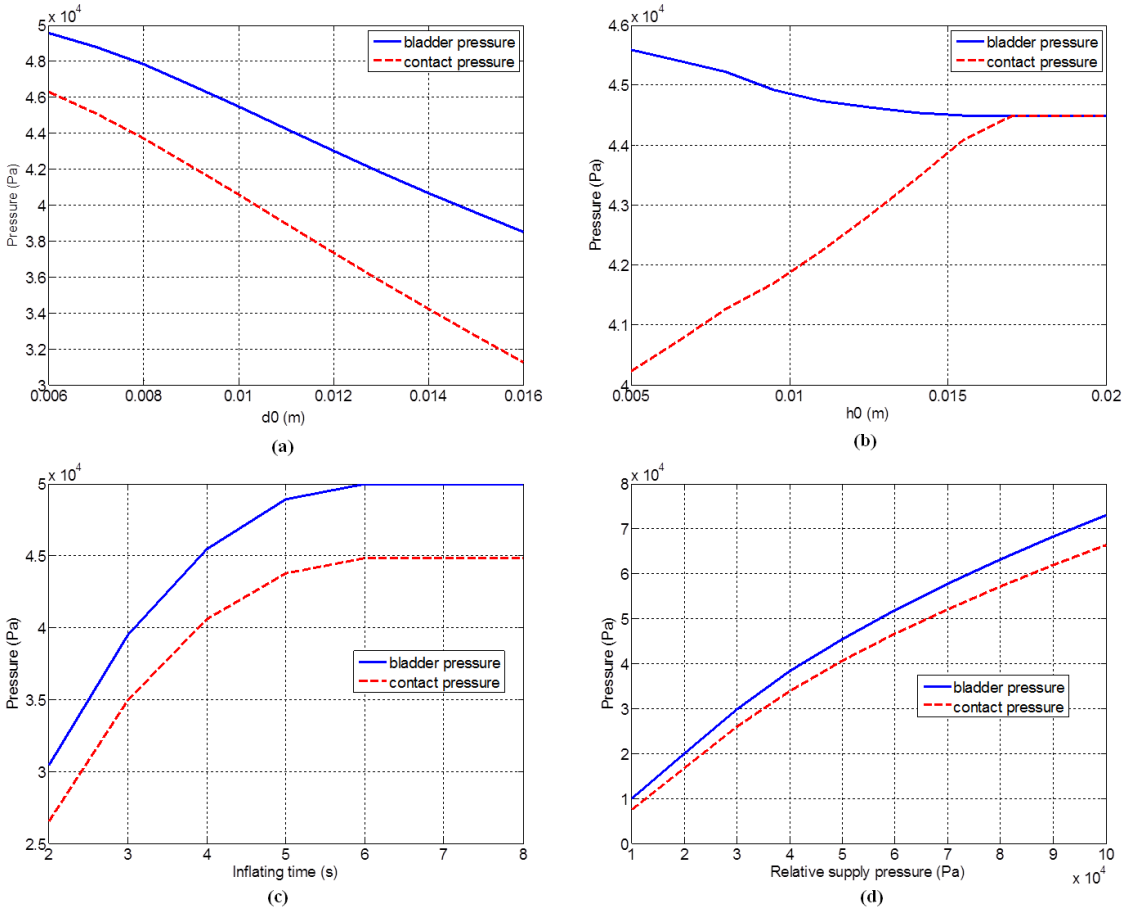

Figure 5.19. Maximum values of bladder pressure and contact pressure as a function of: initial shell-limb gap d0 (a); bladder height at rest h0 (b); inflating time t1 (c); relative air supply pressure pS (d)

Moreover, the model has been used to simulate the dynamic evolution of bladder pressure and contact pressure supposing a very fast command cycle, with *1 s* inflating time and *1 s* deflating time. The result is reported in figure 5.20 and shows behaviour of the device similar to the *tetanus* phenomenon in skeletal muscles.

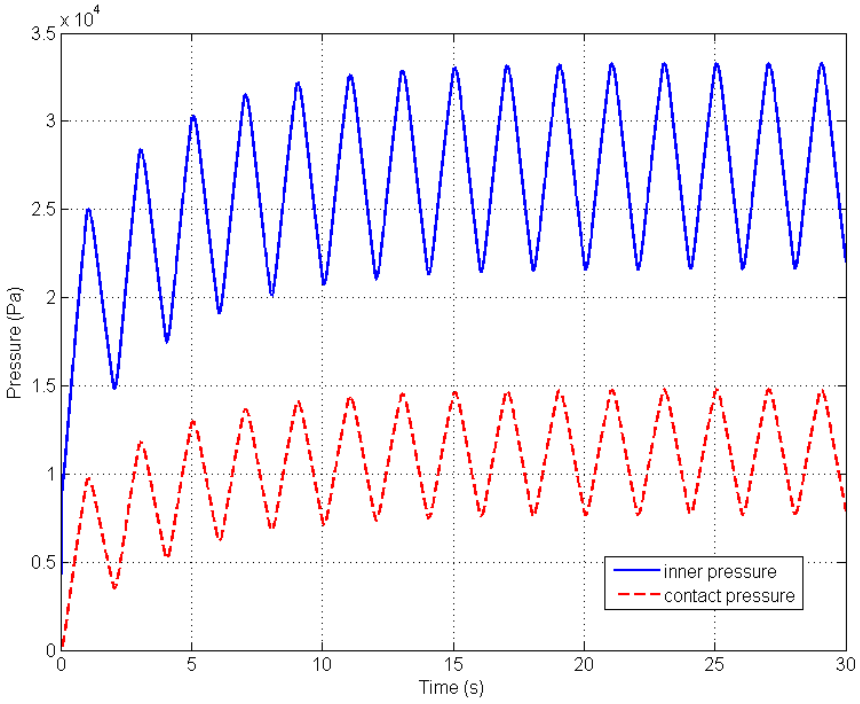

Figure 5.20. Bladder pressure and contact pressure for a fast command cycle

According to the figures 5.19 and 5.20, it can be deduced that the model is sensitive to the variation of the parameters and highlights the way this latter influence the action on the human. Thus, it is possible to obtain important indications on the values that must be respected in the design phase of the device.

For instance, figure 5.19(a) shows the influence of the initial gap on the device performance, this demonstrates the importance of considering the anatomical aspects in the development of the device. Also it shows that by increasing the initial gap, the exerted energy to the limb decreases and as a result the maximum bladder pressure and contact pressure are decreased too.

The figure 5.19(b) gives indications on the shape and material of the bladder: a high value of the parameter h_0, convenient for the performance, can be achieved both using a soft material and choosing a shape allowing high dilatation with no stretching of the wall. The enhancement of the h_0 causes the deceasing in the distance between the bladder wall and the skin. Therefore, more energy can exert to the limb and the contact pressure increasing.

From figures 5.19(c) and 5.20, it is possible to get indications on the relationship between the control command and the characteristics of the pneumatic circuit, including the bladder volume, the air supply pressure and all the pneumatic components. From such

simulations, it is possible to foresee the dynamic performance of the device and recognize the maximum operating velocity that can be reached by the device. For instance in figure 5.19(c), it can be observed that the optimum inflating time is *6 s* to reach the value of supply pressure in the bladder. Increasing this value after *6 s*, does not have any influence on the exerted pressure and only it wastes the energy.
Figure 5.19(d) shows how the device performance may be influenced by the value of the air supply pressure, for a given configuration of the physical parameters and the control law.

5.6 Specification of the initial gap d_0 and transversal muscle stiffness K_M for the model

Initial gap d_0 and transversal muscle stiffness K_M are two parameters that cannot be determined exactly. The value of d_0 depends on the fastening of the IPC device and its adaptability to the leg anatomy of the person. On the other hand, the value of K_M , as mentioned before, depends on the condition of the muscle and the region of the leg. As it can be observed in section (5.2.1), the experimental tests on three persons showed a range of the value for K_M. Therefore, to have the exact results and to do the more actions on the system such as controlling of it, it is necessary to know the best value of the parameters, which are close to real condition.

The following steps can describe a method to estimate the values of K_M and d_0 for using in the obtained model of the IPC device:

1. Simulation of the model for different combinations of K_M and d_0 values, and generating a table reporting the maximum value of p_i in terms of K_M and d_0;
2. Obtain the experimental value of p_i by applying the device to the person for a given number of cycles;
3. Find the experimental maximum value of p_i in the table of step 1, and individuate a corresponding combination of K_M and d_0 for the model.

The simulation results for the maximum inner pressure p_i of the bladder in terms of the different values of K_M and d_0 are shown in the figure 5.21 and table 5.2.

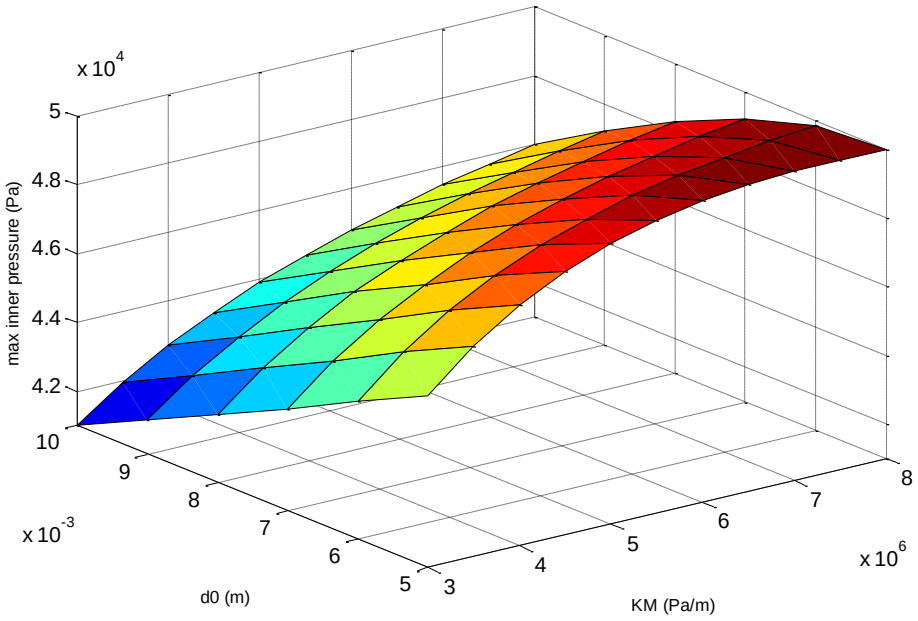

Figure 5.21. The maximum value of the inner pressure pi of the bladder in terms of d0 and KM

Table 5-2. The maximum value of the inner pressure of the bladder in terms of d0 and KM

KM ($\frac{Pa}{m}$) / do (m)	3.0E+06	3.5E+06	4.0E+06	4.5E+06	5.0E+06	5.5E+06	6.0E+06	6.5E+06	7.0E+06	7.5E+06	8.0E+06
0.005	46011	47133	47998	48658	49153	49511	49757	49909	49985	50000	50000
0.006	45009	46124	47012	47720	48285	48734	49087	49364	49575	49732	49849
0.007	43939	45029	45914	46641	47241	47738	48152	48498	48787	49028	49229
0.008	42982	44024	44879	45591	46189	46693	47125	47494	47812	48087	48326
0.009	41985	42971	43787	44471	45050	45546	45974	46346	46672	46958	47212
0.01	41008	41933	42701	43347	43898	44372	44785	45146	45464	45747	45999

In addition, the experimental result for the bladder in two cycles is depicted in figure 5.22.

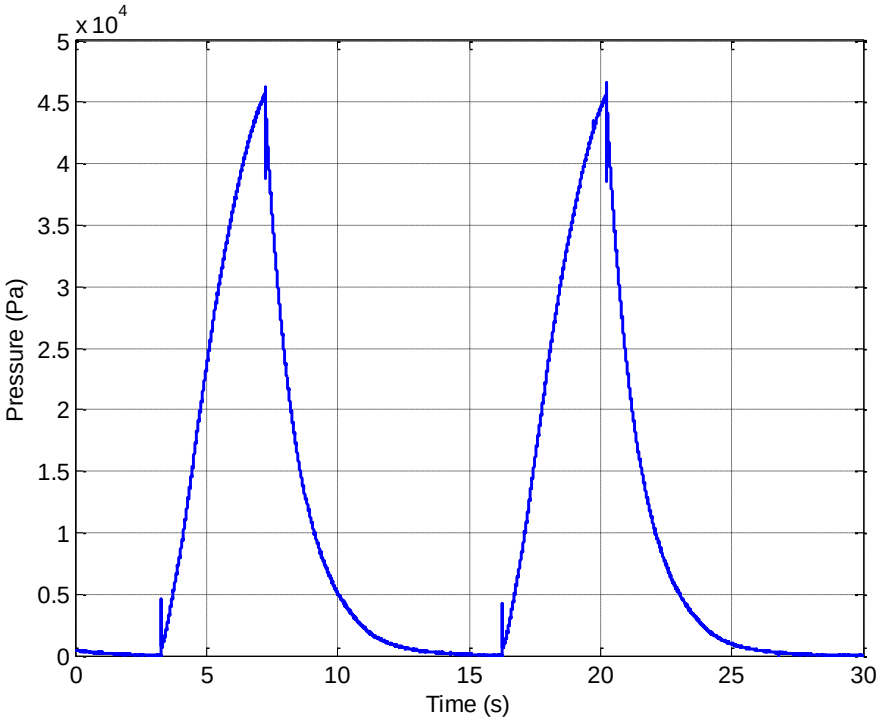

Figure 5.22. The experimental record of the inner pressure of the bladder pi

As it can be observed from figure 5.22, the maximum value of experimental P_i is *45320 Pa*. According to the table 5.2, this exact value is not in the table but there are some values close to it, included in the green zone of table 5.2. How to choose the best values depends on the conditions of the bladder. The region of the leg, where the bladder is acting, is an important parameter. For instance, for the bladders *4* to *6* the value of the muscle stiffness K_M is smaller than that of bladders *2* and *3*. Because in the upper region of the leg, there is muscular tissue, while in the lower part there are ligaments and bone. Also for the d_0, the adaptability of the device for the bladders *4* to *6* is better than the bladders *2* and *3* and the value of the gap between bladder and skin in this region is less. The other parameter can be affected to select value from the table, is the type of the person. Obviously, the muscle stiffness is different between the normal person, patients and an athlete or between young people and old people. Totally, according to the mentioned parameters, therapist can select the value of K_M and d_0 for the simulation, based on the experimental record of p_i.

In the case analysed here, the bladder is number *3* and the best selection could be $K_M = 7*10^6$ *Pa/m* and $d_0 = 0.01$ *m*. This simulation was shown in the figure 5.18 and the figures validate the proposed method.

6. CONTROL OF THE IPC DEVICE

In this chapter, based on the mathematical model, two control strategies are developed for the IPC device. The aim is to create a desire pressure pattern on the limb surface. This latter have been done by using PID controller with proportional components for regulating the pneumatic quantities of the system, and also regulating the inflating time of the bladders.
In addition, the experimental test for controlling the device base on the PID controller is presented.

6.1 Control of the IPC device by regulating inflating time

The value of inflating time t_i is an important parameter in the IPC device and has a significant role in the operation of the device. Selecting the wrong value for inflating time may causes applying the different pressure from the required pressure on the limb. The inner pressure of the bladder does not reach to the desired value when the inflating time is less than the required one. In this case, the device does not have the positive influence on the cardio circulatory system. On the contrary, if the value of inflating time is more than the required one, the pressure on the limb increases and its tissues and vein may be damaged. Therefore, the control of inflating time can increase the performances of the device to have the best results.

To understand the influence of the inflating time on the inner pressure of bladders, the inner pressure of a bladder for 3 and 4 seconds inflating times are experimentally registered and shown in the figure 6.1.

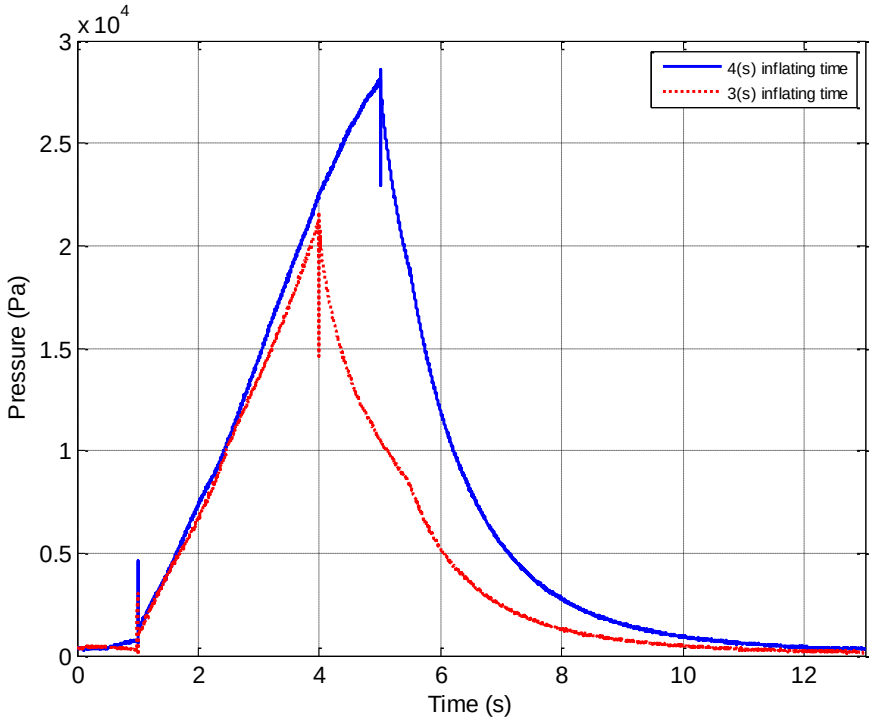

Figure 6.1. Inner pressure of a bladder for two different inflating times (4 s and 3s)

As it can be observed in the figure 6.1, in the same condition, one second different in the inflating time causes about 5000 Pa difference in the inner pressure of the bladder. Therefore, controlling the inflating time in such IPC device is required.

In the following, two methods (offline and online methods) based on the mathematical model are proposed to control the value of the contact pressure p_c by regulating the inflating time t_i.

6.1.1 Offline method

In this method, the control of the contact pressure between bladder and skin can be implemented by determining the time constant of the bladder. In this case, time constant τ is the constant represents the time that takes the contact pressure to reach 1-1/e ≈ 63.2% of the value of supply pressure. Equation (4.1) shows the definition of the time constant.

$$P_{actual} = P_s \left(1 - e^{-\frac{t}{\tau}}\right) \qquad (6\text{-}1)$$

The procedure of the method is that, at the first, the model is simulated for two or three cycles. Then, the time constant of the bladder can be determined and apply to the model to simulate the next cycle operations. In figure 6.2 the first two simulated cycles for the bladder is depicted.

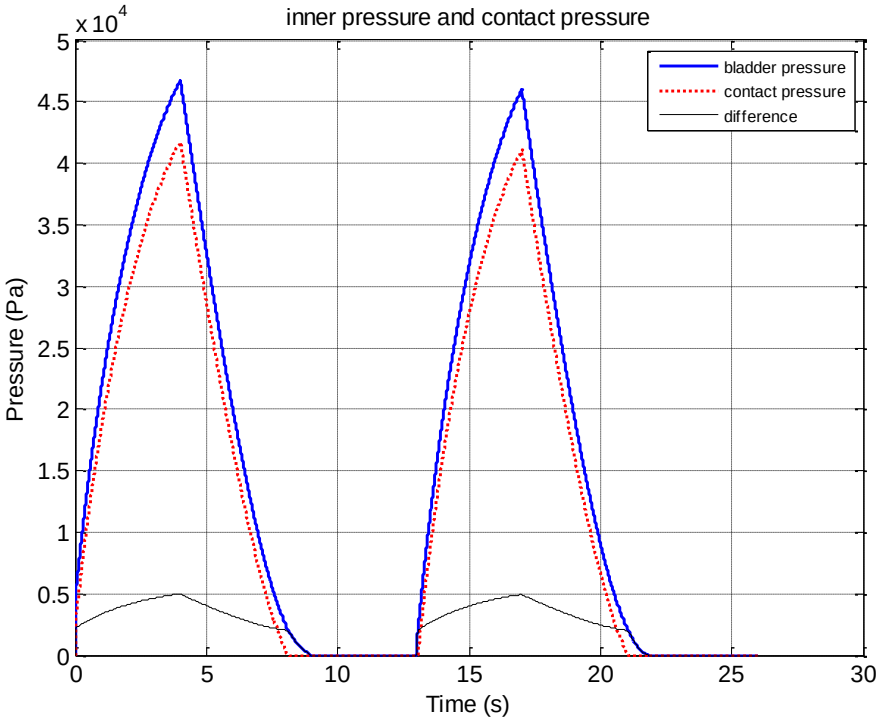

Figure 6.2. The inner and contact pressure of a bladder in two cycles

In the simulation the supply pressure p_s considered as $5*10^4$ *(Pa)* relative to the ambient pressure, So the time constant of the bladder can be calculated as $\tau = 2.437(s)$. If the desired contact pressure p_d is considered as $3.5*10^4$ *(Pa)*, the required time to inflate the bladder can be obtained by substituting the value of the P_s and P_d in equation 6-1. The desired time t_d can be obtained as: $t_d \approx 1.2\,\tau = 2.92\ s$.

By using the obtained desired inflating time, the system can be simulated for several cycles. In figure 6.3 the simulated cycles by using the desired inflating time is shown.

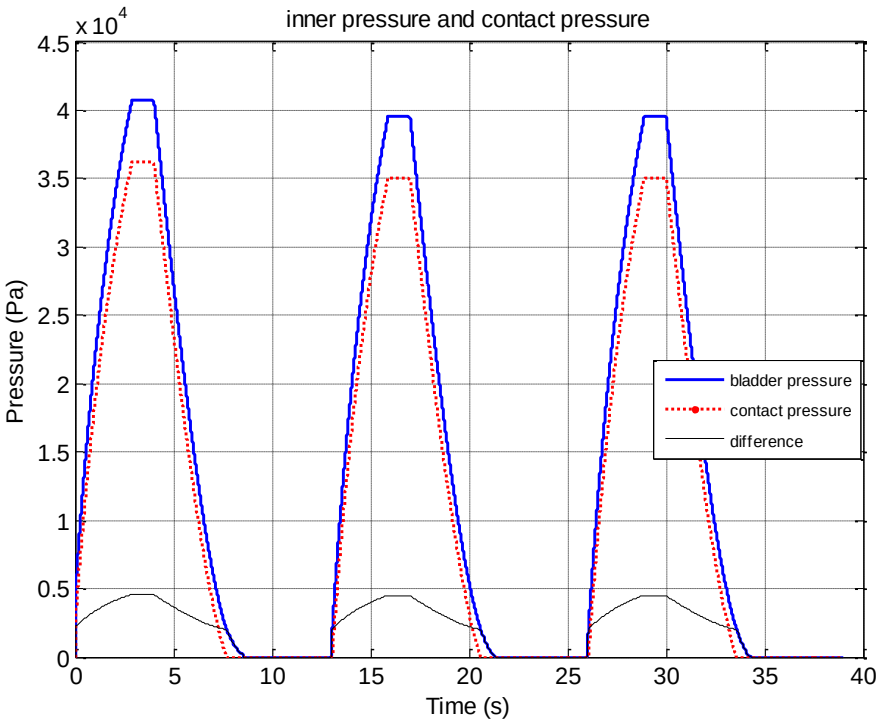

Figure 6.3. The simulated cycles for the bladder by using the desired inflating time

According to the figure 6.3, the bladder inflates until the desired inflating time t_d, and then PLC commands the valve to change the state, to the steady state to keep the inner pressure constant. Therefore, the contact pressure remains constant until *4s*; and after that the discharging will be started.

Keeping the contact pressure in the desired value, helps to apply the desired force on the muscle for more times and it has positive effect to recover the cardiovascular efficiency. To increase the time of the applying desired pressure to muscle, it is possible to increase the whole time of the keeping pressure or increasing the supply pressure.

6.1.2 Online method

In this method, the contact pressure p_c is measured automatically through the simulation and in the same time, it is compared with the desired one. If the contact pressure is less

than desired one, the bladder continues to be charged, else the charging valve will be closed and the value of the contact pressure remains constant until the end of the inflating time. After the whole time of the inflating, the discharging valve will be opened and the deflating will be started. This control procedure can be done by PLC to update the command signal every moment. In this method opposite of the Offline method, the simulation of the model to determine the time constant before operating the device is not required. The scheme of the online method is depicted in the figure 6.4.

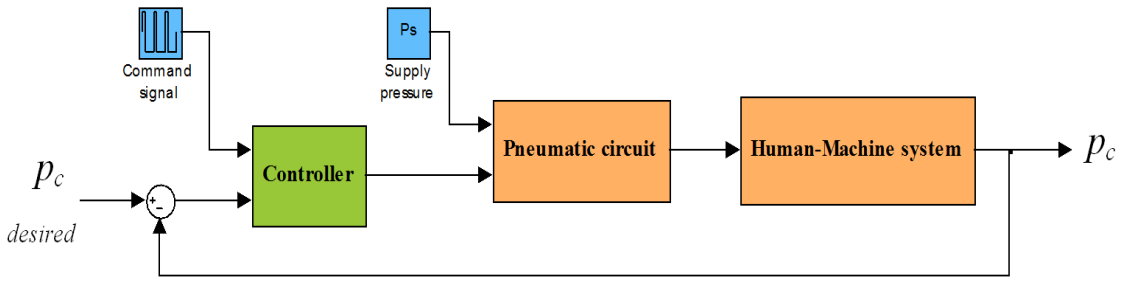

Figure 6.4. The Scheme of the online method

In the figure 6.5, the simulated contact and inner pressure of the bladder in the on line method is depicted.

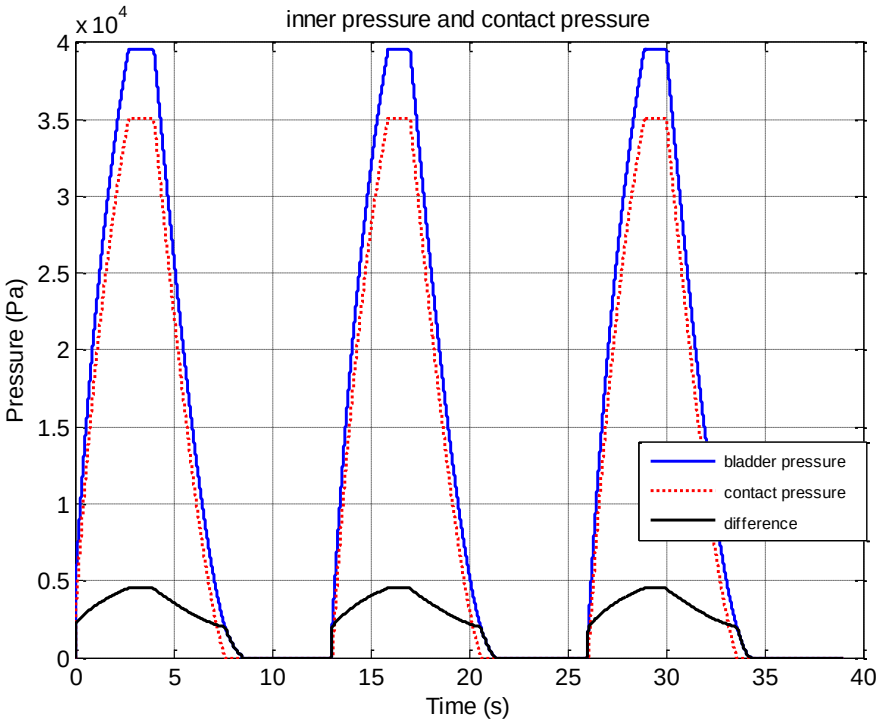

Figure 6.5. The simulated contact and inner pressure of the bladder in the online method

As it can be observed in the figures 6.3 and 6.5, control of the contact pressure and inserting its desired value for more time are achieved. Regarding to the results of both control methods (Offline and Online), it can be deduced that for each cycle of the simulation the bladder can apply on the limb the desired contact pressure about *1.5(s)*, which is about *37%* of the inflating time. Since the rising time in each cycle is constant, by increasing the inflating time, the rate of having the contact pressure on the limb will be increased. For instance, if the inflating time is considered as *7s*, about *65%* of the inflating time, system works on the desired value. While without controlling the contact pressure (Figure 6.2), the system only passes the desired value and goes over until the end of the inflating time. Having the pressure more than the proper value may damage the device by exploding the bladder or the limb tissue like vessel rupture.

6.2 PID control of the IPC device

6.2.1 General description of PID controller

Proportional-Integral-Derivative (PID) is well-established and popular technique for many real-world control problems. This is due to its simplicity from both the design and the parameter-tuning point of view [71]. Since the invention of PID control in 1910 (Elmer Sperry's ship autopilot) [72], and Ziegler-Nichols's tuning methods in 1942[73], the popularity of PID control has grown all over the world. In this method, the proportional, integral and derivative terms are summed to calculate the output of the controller. Defining *e(t)* and *u(t)* as the input (error) and output of the controller respectively, the PID algorithm is:

$$u(t) = K_P \cdot e(t) + K_I \cdot \int_0^t e(t)dt + K_D \cdot \frac{d}{dt}e(t) \tag{6-1}$$

And its transfer function is:

$$G(s) = K_P + K_I \frac{1}{s} + K_D s = K_P \left(1 + \frac{1}{T_I s} + T_D s\right) \tag{6-2}$$

Where K_P, K_I and K_D are proportional, integral and derivative gains respectively; T_I is the integral time constant and T_D is the derivative time constant. The action of the three terms can be described as [74]:

1. The proportional term: providing an overall control action to the error signal through the all-pass gain factor.
2. The integral term: reducing steady-state errors through low-frequency compensation by an integrator.
3. The derivative term: improving transient response through high-frequency compensation by a differentiator.

In addition, the individual effect of increasing each term on the closed-loop performance is shown in Table 6-1.

Table 6-1. Effect of the gain increasing on the closed-loop response

Closed-loop response	Rise time	Overshoot	Settling time	Steady-state error	Stability
K_P	Decrease	Increase	Small increase	Decrease	Degrade
K_I	Small decrease	Increase	Increase	Large decrease	Degrade
K_D	Small decrease	Decrease	Decrease	Minor change	Improve

Several methods can be used to tune the PID control loop, based on the dynamic model parameters. Manual tuning, Ziegler-Nichols [73-78], Cohen-Coon [77,78] and software tools are the usual methods to tune the PID controller. Depending on the value of the terms, PID controller can be called PI and PD controller in the absence of the derivative and integral terms respectively.

6.2.1.1 Ziegler-Nichols (Z-N) method

This pioneer method, also known as the close-loop or on-line tuning method was proposed by Ziegler and Nichols in 1942. Like all the other tuning methods, it consists of two steps:

1. Determination of the dynamic characteristics, or personality, of the control loop
2. Estimation of the controller tuning parameters that produce a desired response for the dynamic characteristic determined in the first step, in other words, matching the personality of the controller to that of the other elements in the loop.

In this method the dynamic characteristic of the process are represented by the ultimate gain of a proportional controller and the ultimate period of oscillation of the loop. It usually determinate the ultimate gain and period from the actual process by the following procedure:

- Switch off the integral and derivative terms of the feedback controller so as to have a proportional controller.
- With the controller in automatic (i.e., the loop closed), increase the proportional gain until the loop oscillates with constant amplitude. Record the value of the gain

that produces sustained oscillation. To prevent the loop from going unstable, smaller increments in gain are made as the ultimate gain is approached.

To tune a controller using the Z-N method the integral and derivative elements of the PID controller are ignored. The proportional element is used to find a K_u that will sustain oscillation. This value is considered as the ultimate gain. The period of oscillation is the P_u, or ultimate period. Consequently, Z-N settings are reasonable to apply in controller tuning using table 2.1.

Table 6-2. Controller Settings Based On the Z-N Method

Control type	K_P	K_I	K_D
P	0.5 K_u	0	0
PI	0.45 K_u	1.2 K_P/P_u	0
PD	0.8 K_u	0	$K_P P_u/8$
PID	0.6 K_u	2 K_P/P_u	$K_P P_u/8$

6.2.2 Application of PID controller to the model

The scheme of the system in presence of the PID controller can be described as shown in figure 6.6.

In the IPC device, the contact pressure p_c is considered as output controlled value, while for the regulated value, there are two distinct possibilities. Supply pressure p_S and mass flow rate Q are two different quantities that can be regulated by PID controller to track the reference p_C. In the following, both methods to control p_C based on regulating p_S and Q are described.

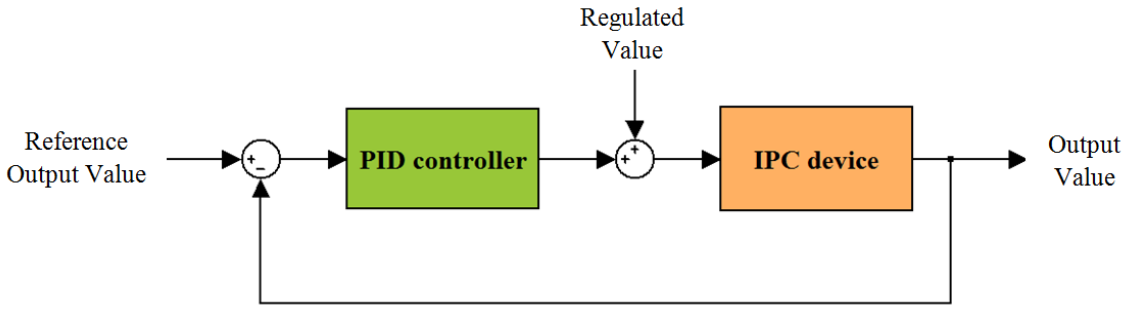

Figure 6.6. The scheme of the system with PID controller

6.2.3 System control based on regulating p_S

In the simulation and experimental validation shown in figure 5.18, the supply pressure to the system was kept constant and equal to $5 \cdot 10^4$ *Pa* relative. The value of the internal bladder pressure and the contact pressure was then determined by the natural dynamic characteristic of the pneumatic circuit and by the inflating/deflating times commanded by the PLC. If a feedback was available (e.g. the contact pressure or the inner bladder pressure), the supply pressure to the system could be regulated by a PID closed loop controller for optimal tracking of the desired value. This can be done by proper integration of an electro-pneumatic pressure proportional valve (PPV) into the system. Such component will transform the electrical input signal sent by the controller into the supply pressure to the IPC device.

Figure 6.7 shows the block scheme of the single-bladder system with supply pressure controlled by pressure proportional valve (PPV).

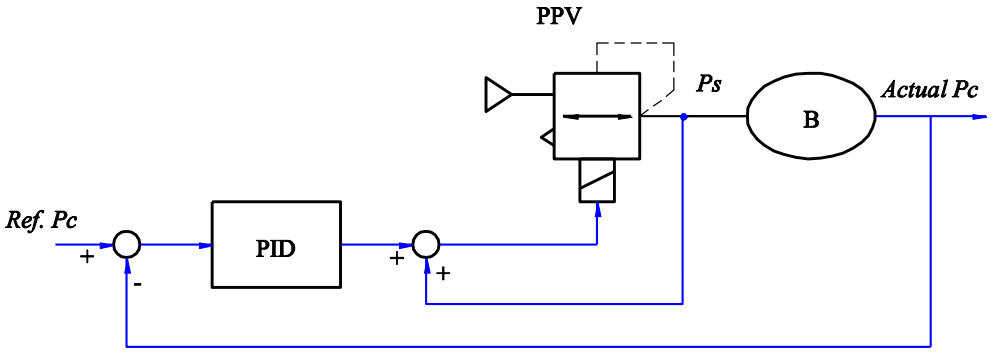

Figure 6.7. Block scheme of the system with supply pressure (Ps) controlled by pressure proportional valve (PPV); contact pressure (Pc) is the outlet from bladder (B)

Figure 6.7 shows the block scheme of the single-bladder system with supply pressure controlled by pressure proportional valve (PPV).

To design the PID control, the mathematical model of the PPV has been integrated in the model. The parameters of the device were maintained as reported in table 5-1. The model of the PPV can be represented by the block diagram shown in figure 6.8 [79], where *Kv* is the flow coefficient, *Tv* is the time constant and *Cv* is the interior capacity of the proportional valve. P_{in} and P_{out} are the input and the output pressure of the proportional valve respectively. For a commercial proportional valve type Festo MPPE-3-1/4, which has been considered in simulations, the parameter values are $Kv=5\cdot10^{-7}$ $(m^3/Pa.s)$, $Tv=0.01$ (s) and $Cv=1.43*10^{-8}$ (m^3/Pa).

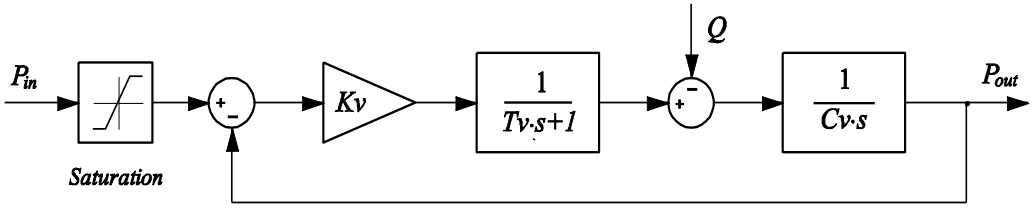

Figure 6.8. Block diagram of a pressure proportional valve

To tune the PID controller, the mix method of Ziegler-Nichols and manual tuning has been used. Since the whole system is represented by a highly non-linear and stiff mathematical model, the first step, consisting on the determination of PID coefficients (K_P, K_I, K_D) by means of Ziegler-Nichols methods, was not sufficient to produce satisfactory results. Thus the first attempt values were changed by further manual fine-tuning, according to the criteria of Table 6-1, for an optimal result.

With a reference contact pressure of $3.5*10^4$ (Pa) relative to the ambient in inflating and zero in the deflating state, the best tuning was found with the coefficients: $K_P= 0.03$, $K_I = 0$, $K_D = 0.0044$, i.e. in this case the best solution corresponds to a PD controller.

In figure 6.9, the reference and the actual contact pressure of the controlled system are shown. The graph reports also the error, i.e. the difference between reference and actual pressure.

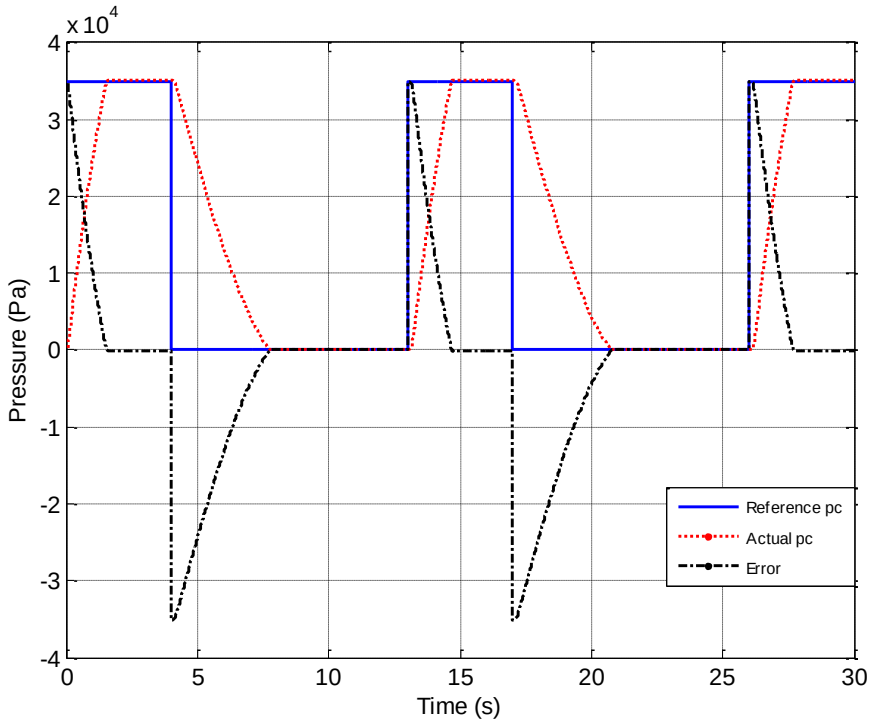

Figure 6.9. The reference and actual contact pressure of the bladder with PD control of the supply pressure

The results of figure 6.9 show the effectiveness of the control: the actual pressure reaches the desired value in less than 2 seconds and it is maintained until the end of the inflating phase.

To obtain this result, the controller must command in a proper way the proportional valve: this is testified by figure 6.10, which shows the variation of the absolute supply pressure P_S, operated by the pressure proportional valve. At the beginning of the inflating phase, the supply pressure reaches the saturation level (2 bar absolute), so speeding as much as possible the rising of the bladder and contact pressures.

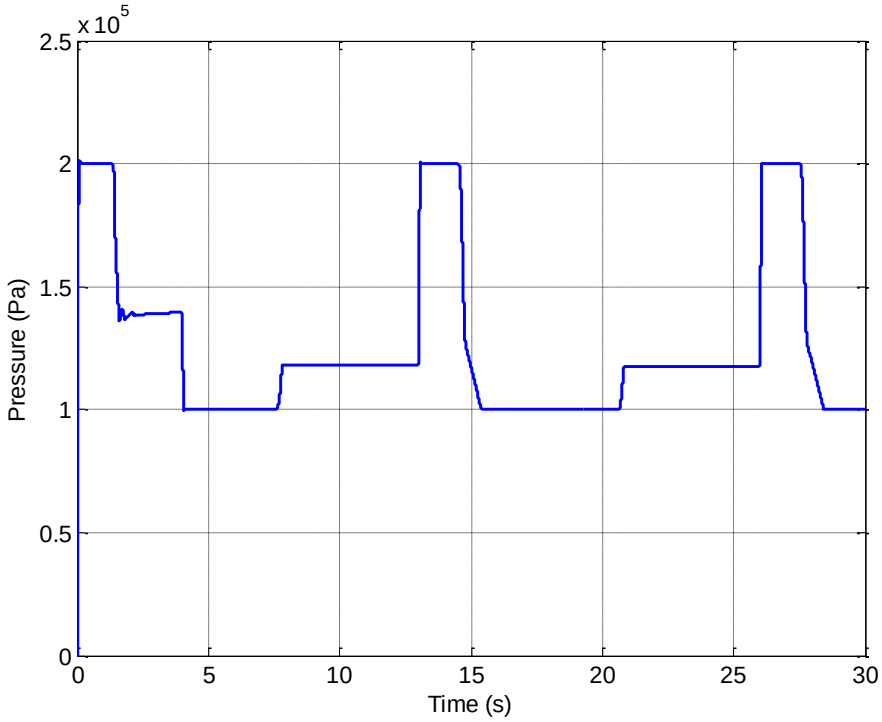

Figure 6.10. The variation of the supply pressure controlled by the proportional valve

The saturation level of the supply pressure, which can be set by the controller, determines the response speed of the system, in particular the rising time of the bladder pressure. Defining the rising time as the time required for actual bladder pressure to rise from 10% to 90% of the reference value, figure 6.11 shows the variation of the rising time versus the saturation level of the supply pressure, as calculated by the mathematical model. Therefore the curve of figure 6.11 can be used to choose the most convenient value for the saturation level of the pressure proportional valve.

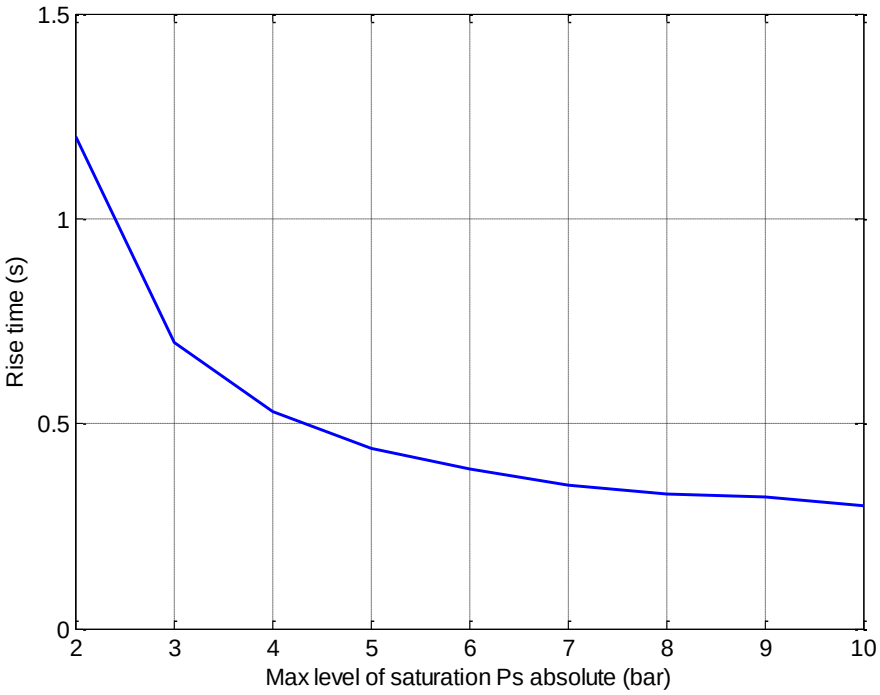

Figure 6.11. Variation of the rising time versus the saturation level of Ps

A further sensitivity analysis was performed to investigate the influence on system performance of the transversal muscle stiffness KM, which was recognized as a very critical parameter to be identified. Like in the previous case, the rising time of bladder pressure in inflating phase was considered to represent the IPC dynamic performance. Figure 6.12 represents the variation of the rising time in terms of variation of KM.

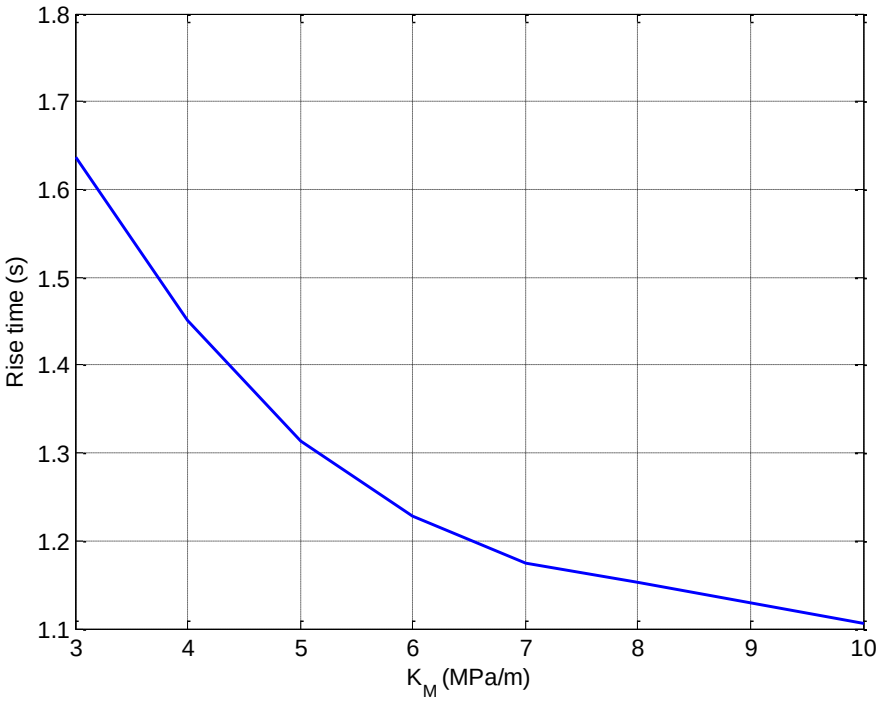

Figure 6.12. Rising time versus transversal muscle stiffness KM

Figure 6.12 shows the result of the analysis: for KM varying from 7 to 3 MPa/m, the rising time increases of about 38%. This is certainly a noteworthy indication, which suggests the search for more effective control solutions in the continuation of research.

6.2.4 Control of the system based on regulating Q

The air pressure inside the bladder can be controlled directly by regulating the air flow rate. In this case, the supply to the bladder must be controlled by an electro-pneumatic flow-proportional valve (FPV), commanded by the PID control. In fact, referring to equation (5-3), the mass flow rate Q entering the bladder is directly related to the derivative of the pressure; therefore, to control the pressure it will be necessary to act on the valve conductance C, as defined in equation (5-1).

Figure 6.13 shows the scheme of such a system. In particular, FPV is a 3-way flow proportional valve, whose conductance C can be regulated in analogical way by the controller.

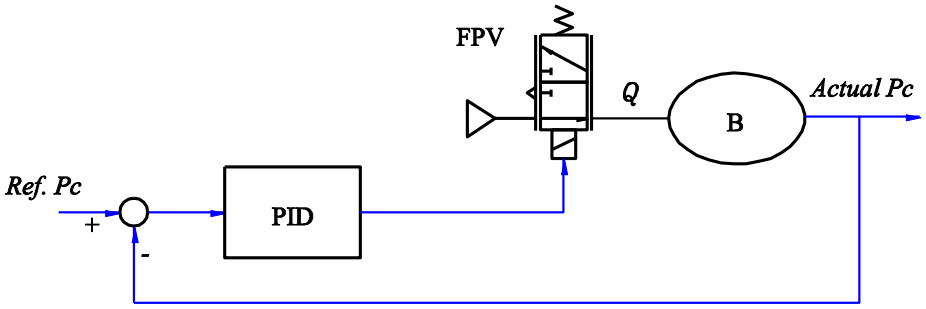

Figure 6.13. Scheme of the single-bladder system with PID controller and flow proportional valve (FPV)

Figure 6.14 shows a block scheme of an electro-pneumatic flow-proportional valve [80], where *K* is the electro-pneumatic gain and *Tv* is the time constant of the valve. Referring to a commercial proportional valve type Martonair SPGB 18913, the characteristic values are: $K=1*10^{-9}$ $m^3/Pa/s/A$ *and* $Tv=0.1$ *s*.

Applying to the system the mixed Ziegler-Nichols plus manual tuning method previously described, the PID coefficient has been calculated. The optimal result has been obtained with $K_P=0.005$, $K_I=0$ and $K_D=0.001$.Also in this case the best configuration corresponds to a Proportional-Derivative PD controller.

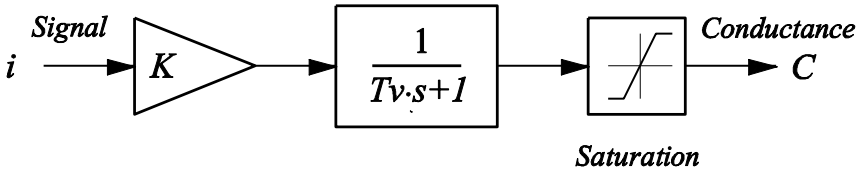

Figure 6.14. Block diagram of a flow proportional valve

The mathematical model including the optimized PID controller and the flow-proportional valve has then been simulated. Figure 6.15 reports the result of the simulation, showing a comparison between the actual and reference contact pressure, as well as their difference (error). The result is very similar to the one produced by the control with regulation of the supply pressure: this confirms that also the solution with flow regulation is theoretically able to control the device in an effective manner.

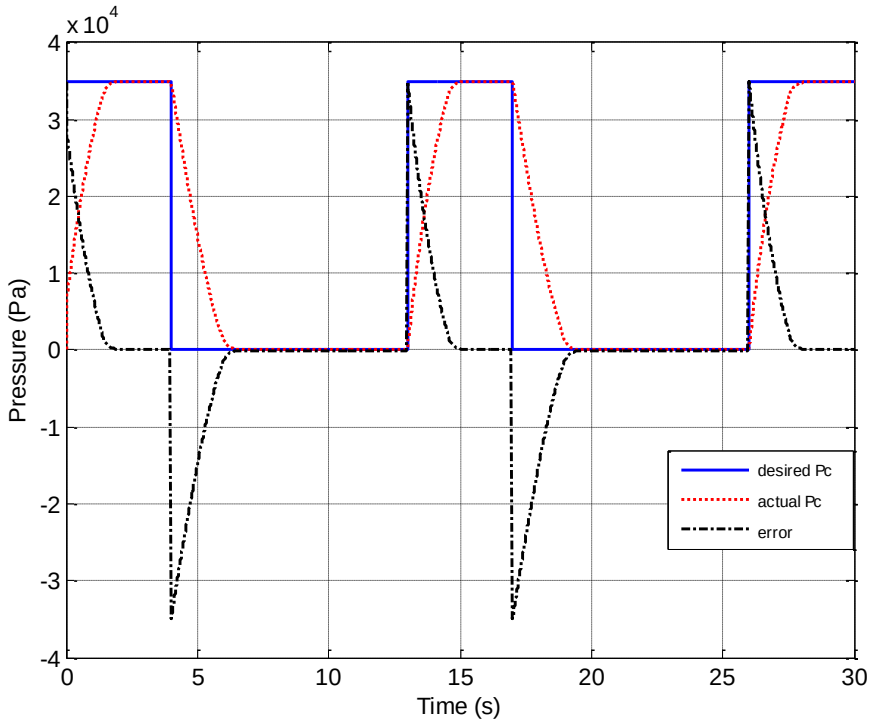

Figure 6.15. The reference and actual contact pressure of the bladder with PID control and the flow rate regulated by a proportional valve

Figure 6.16 shows the variation of the valve conductance, under the regulation of the PID controller. A positive value corresponds to inflating condition, and vice-versa.

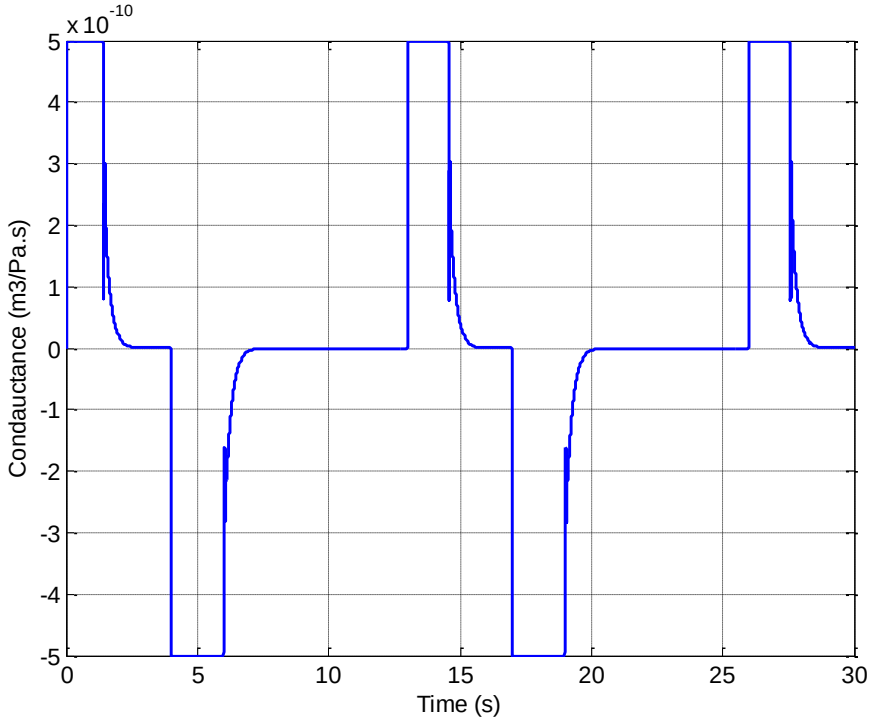

Figure 6.16. The variation of the valve conductance

6.2.5 Parallel control of 3 bladders by one pressure proportional valve

In section 6.2.3 the way to control a single bladder with one pressure proportional valve and a PID controller was described. Actually, an IPC device includes a given number of bladders, which must be controlled in a coordinated way, in order to generate a definite pressure pattern on the limb surface. It is supposed that the device should generate a peristaltic and centripetal pressure wave, i.e. proceeding from distal to proximal position, in order to facilitate the venous blood return to the heart. To this aim, the activation sequence of the bladders must follow the same logic. Thus a definite reference pressure must be tracked in any bladder. In addition, for cost and complexity reasons, it would not be permissible to have a proportional valve for each bladder. Therefore, a system of three bladders controlled by one PID controller and one pressure proportional valve has been studied and simulated.

For such a multi-bladder system the controller, acting as a PLC, must switch among the bladders, commanding the proper on-off control valve, selecting the proper contact pressure feedback and sending the proper pressure reference to the PID controller. A possible scheme of the system is presented in figure 6.17, where , posing n=1,2,3, *Bn* are

the bladders, *Vn* are the corresponding on-off control valves, *Pn* are the bladder-limb actual contact pressures, *PPV* is the pressure-proportional electro-valve.

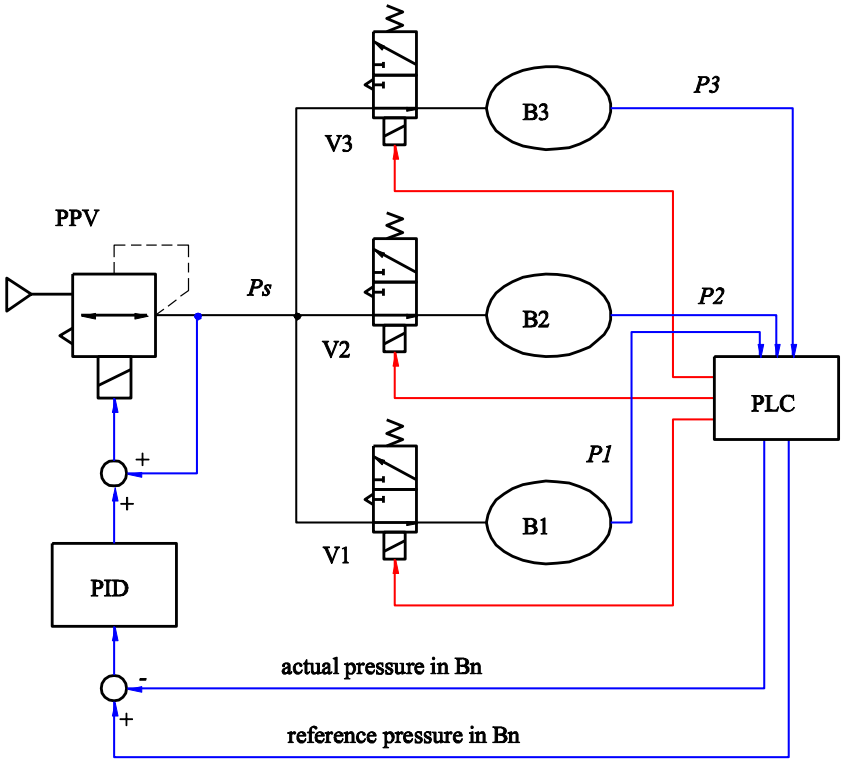

Figure 6.17. 3-bladder system with one pressure-proportional valve (PPV) controlled by PID

In the model the three bladders have been configured with different parameters, including the contact area *A*, the transversal muscle stiffness K_M of the leg region where the bladder acts on, and the gap between the bladder and leg d_0. The values of such parameters, which are shown in table 6-3, were selected in such a way as to represent possible variations due to muscular condition, location of the bladder on the limb and different device dressing that may occur using the actual prototype. In particular, with parameter values of table 6-3, the system is configured in such a way as to present increasing response time from bladder 1 to bladder 3.

Table 6-3. Parameters of the 3 bladders

	Contact area *A* (m^2)	Muscle stiffness K_M (Pa/m)	Gap d_0 (m)

Bladder 1	0.014	7.10^6	0.006
Bladder 2	0.017	6.10^6	0.009
Bladder 3	0.02	5.10^6	0.012

The inflating and deflating times, imposed by the PLC for each bladder, are 4s and 9s respectively, and the three cycles were shifted to produce a peristaltic effect, as it is shown in the command sequence of figure 6.18. When command is OFF the reference pressure is *0*, when command is ON the reference pressure is set at a defined value for all bladders.

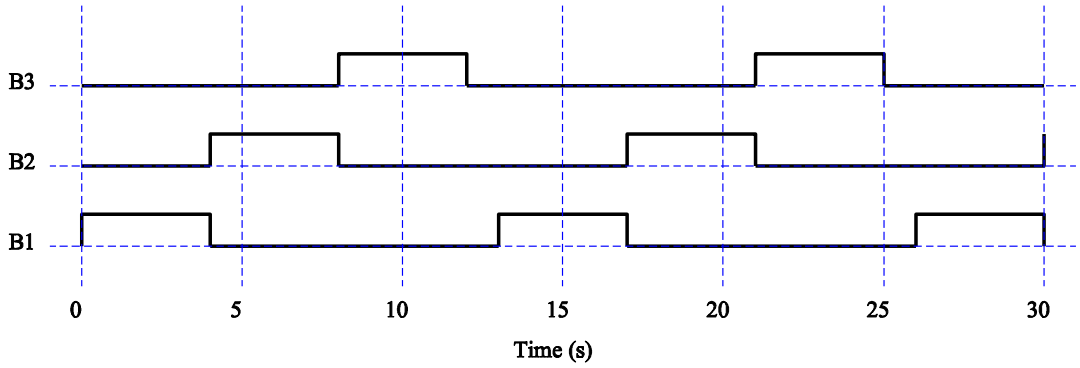

Figure 6.18. Command sequence of the three bladders

The system has been simulated in two conditions:

a) Without proportional valve and PID control: each control valve *Vn* is supplied at $0.5*10^4$ *Pa* relative pressure

b) With proportional valve and PID control: the absolute supply pressure to the valves *Vn* is regulated by the proportional valve and is saturated at $2*10^5$ *Pa*; the relative reference pressure to the PID is set to $3.5*10^4$ *Pa* in inflating state and *0* in deflating state, for all bladders.

Figure 6.19 shows the simulation results without PID controller (a) and with PID controller (b).

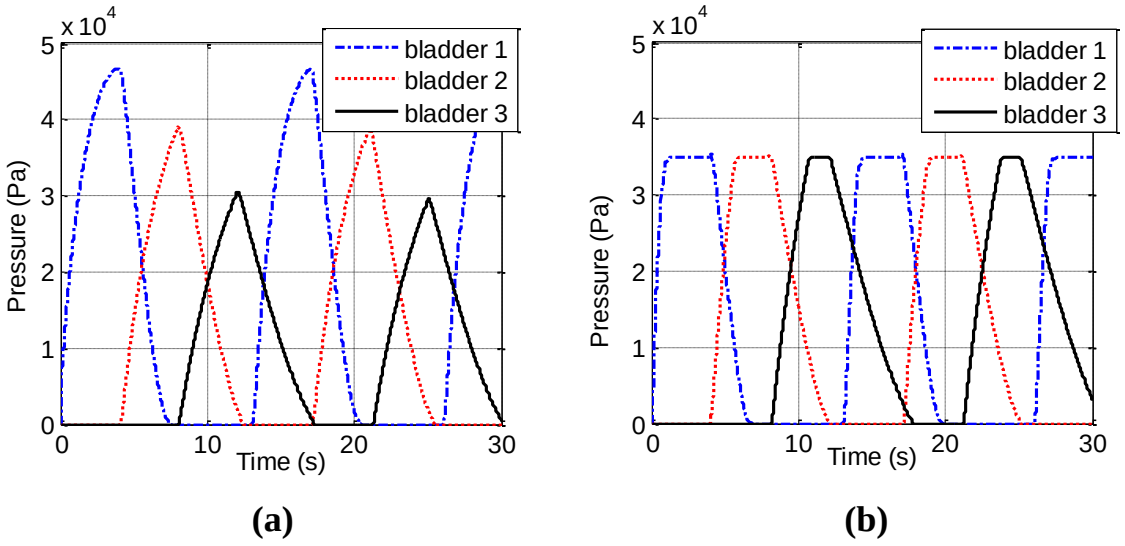

Figure 6.19. Simulation of the multi-bladder system in absence (a) and in presence (b) of the PID controller

The simulation shows that an effective control of the bladder actions is almost impossible without a feedback control system, since the dynamic behaviour and the maximum level of the pressures are affected by a number of randomness that are difficult to evaluate properly. As it can be observed in figure 6.19(a), the dynamic behaviour and the maximum level of the contact pressure are very different among the bladders, that it is due to the differences imposed to the bladder parameters. On the contrary, when the PID controller acts on the system (figure 6.19 (b)), the contact pressure tracks much better the reference one, which is set at $3.5*10^4$ *Pa*, in each bladder. Obviously the feedback controller gives better result, and simply including feedback in the control of on/off valves would guarantee achieving of the desired pressure, but the use of a pressure proportional valve provides advantage also for the system dynamics and general tracking: in this case the bladders can be supplied with pressure much higher than the desired internal value, thus reducing the rising time and allowing to maintain the desired value for a defined period, as highlighted by figures 6.10 and 6.11.

Due to the difference in the bladder parameters, the dynamic behaviours of the three bladders are still different, as highlighted by the rise and fall times, but each bladder can reach the reference contact pressure and maintains it for a significant time: totally, in a cycle of 13 s, the bladders 1, 2 and 3 can stay about 8s in the reference contact pressure, that is equal to 62% of the whole time. You should also consider that the tuning of the PID coefficients has been made for only one bladder, but gives acceptable results for the

whole system, thus testifying the ability to compensate in some extent also uncertainties like the actual value of the transversal muscle stiffness and the limb/device gap.

6.3 Experimental tests of the PID control of the device

In the section 6.2 the PID control for the mathematical model was described and the results showed the effectiveness of the control strategy on the device. Those simulations were implemented for both single and multi-bladder systems. In this section the experimental test based on the obtained data of the section 6.2 is explained. In the following the experimental results for both the single bladder and multi-bladder systems are expressed.

6.3.1 Experimental test to control of the single bladder system

To control the system based on PID controller, the engineering software LabView and the related board National Instrument (NI) are used. The PID control is implemented on the system by means of a NI PCI 6036E board and the Festo proportional valve which is cited in section 6.2.3. A single bladder was placed in a test bench reproducing all conditions of table 5-1, including soft tissue stiffness K_M (transversal muscle stiffness).

The scheme of the experimental control test for the single bladder system is depicted in figure 6.20.

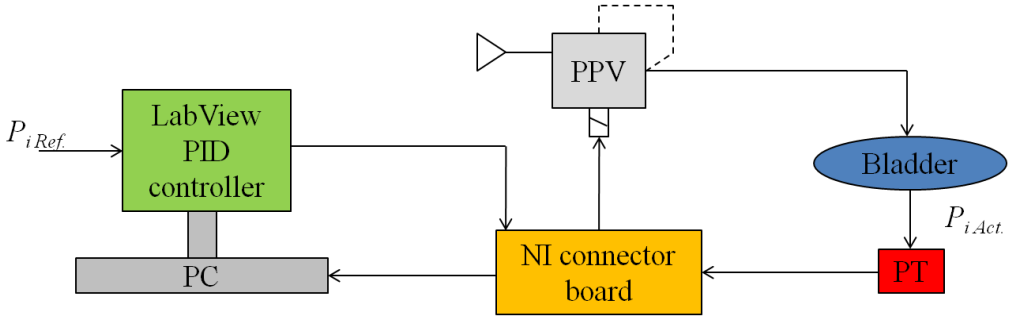

Figure 6.20. The scheme of the experimental control of the single bladder system

In this case, the pressure transducer *PT* measures the inner pressure of the bladder $P_{i\ Act}$ and the obtained data is transferred to the LabView by the *NI* board. The PID control model determines the output signal for the acting on the pressure proportional valve PPV by regarding to the error of the system. The error of the system is the difference between

the reference inner pressure $P_{i\ Ref}$ and the actual inner pressure $P_{i\ Act}$. Moreover the acting signal on the PPV also can be calculated by using the equation 6-1.

The output signal of the PID controller acts on the PPV by NI board after some amplification. Base on the input signal, the PPV regulates the output pressure of the air to enter to the bladder. The mentioned close loop is iterated many times until the inner pressure of the bladder reach to the reference one. And then the control system maintains the desired pressure in the bladder.

The result of the experimental control of the system is shown in figure 6.21. This figure reports the reference and the experimental inner pressure of the bladder. In this test the reference inner pressure is considered as 0.36 *bar* in inflating and 0 in deflating times.

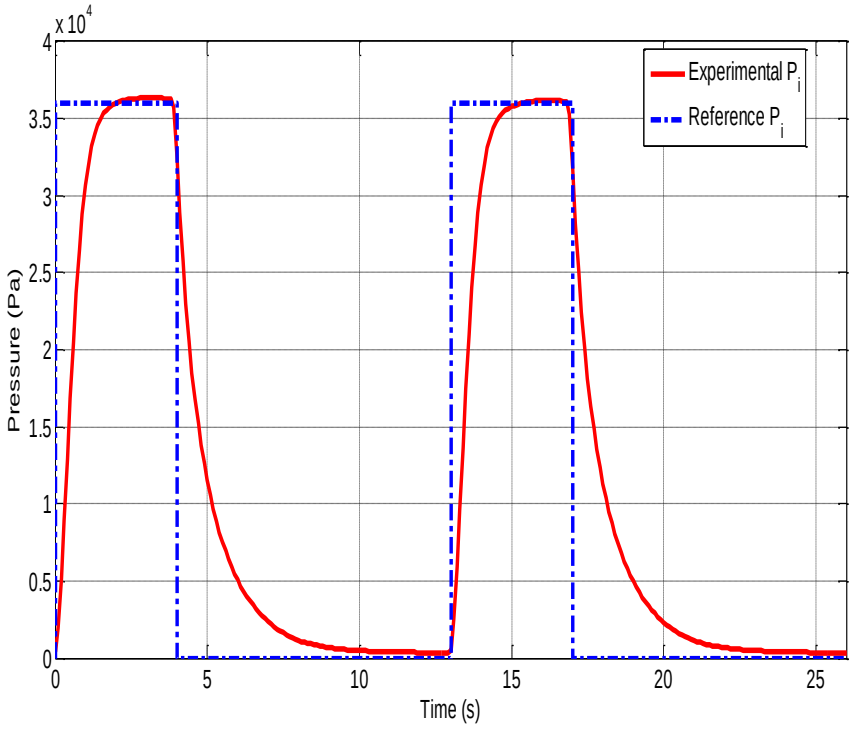

Figure 6.21. The experimental and reference inner pressure of the bladder in presence of the PD controller

To compare the experimental results with the simulation ones (Section 6.2.3), the experimental Pi with the simulated reference and contact pressure of the bladder are represented in figure 6.22.

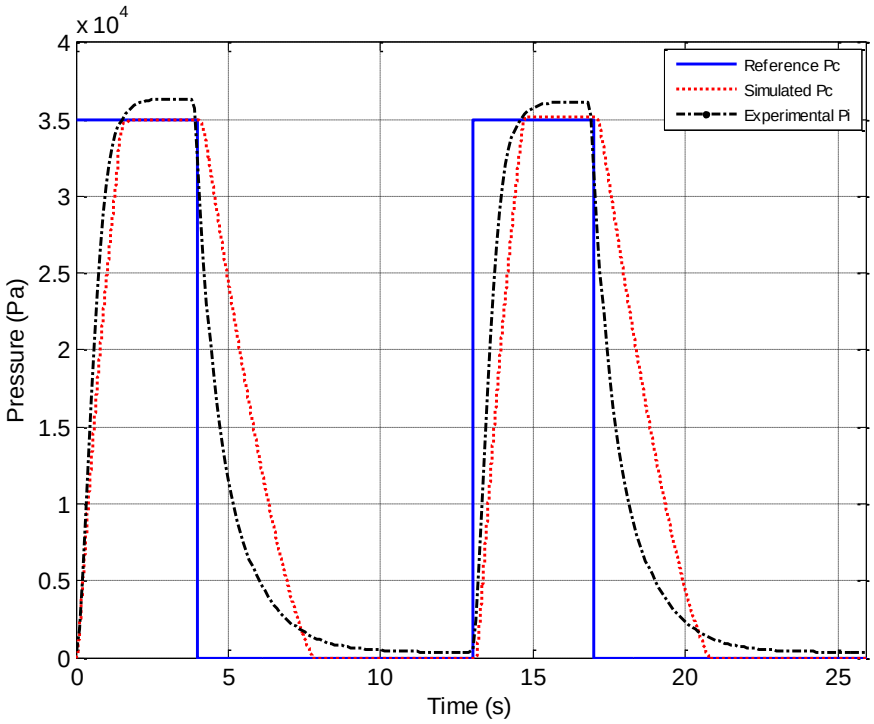

Figure 6.22. Reference and simulated contact pressure with PD control of the bladder supply, compared with the experimental inner bladder pressure

As it can be observed in figure 6.22, there is a good correspondence between the experimental result and simulated one in dynamic behavior of the bladder in the inflating phase. Also it is interesting to note that the controller regulates the inner bladder pressure at a slightly greater than the reference contact pressure, taking into account the bladder stiffness.

About the deflating phase, there is differences in the dynamic behavior of the bladder but in both (experimental and simulation) results the contact and the inner pressure of the bladder reach to the zero before the end of the deflating times and this case is more important to avoid from *tetanus* phenomenon.

Consequently, it can be deduced from the comparison that the simulation results is verified by the experimental one and the figure shows the effectiveness of the proposed control strategy by using PID controller and proportional valve.

According to the figure 6.21, the experimental inner pressure of the bladder reaches to the desired one less than 2 seconds and it is developed the efficiency of the device more than 50%. This is an excellent result, taking into consideration the natural low dynamics of such pneumatic systems.

6.3.2 Experimental test to control of the multi-bladder system

The experimental bench to control the multi-bladder system is developed by the same conditions mentioned in section 6.2.5. For the test, a pressure proportional valve (PPV) and a PID controller are used for whole 3 bladders and the PLC switch among the bladders the command signal which showed in figure 6.18. The scheme of the experimental control test for the multi-bladder system is depicted in figure 6.23.

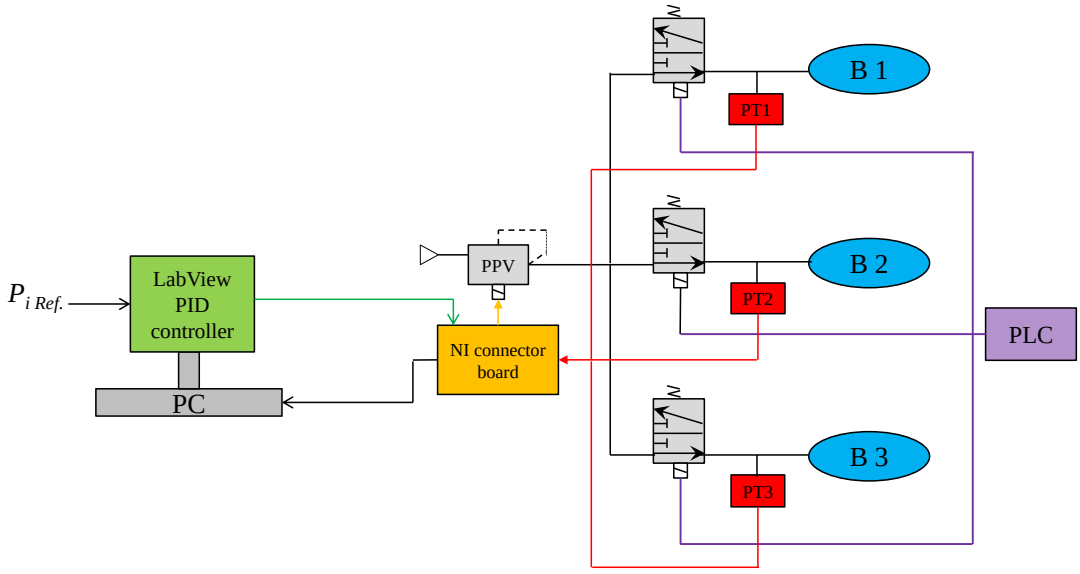

Figure 6.23. The scheme of the experimental control test for the multi-bladder system

The experimental test in this case was done in the same condition with the simulation one (Sec. 6.2.5) and the results are depicted in the figure 6.24. In this test, the inflating and deflating times are considered as *4s* and *9s* respectively for each bladder and the reference value is $0.35*10^5$ *bar*.

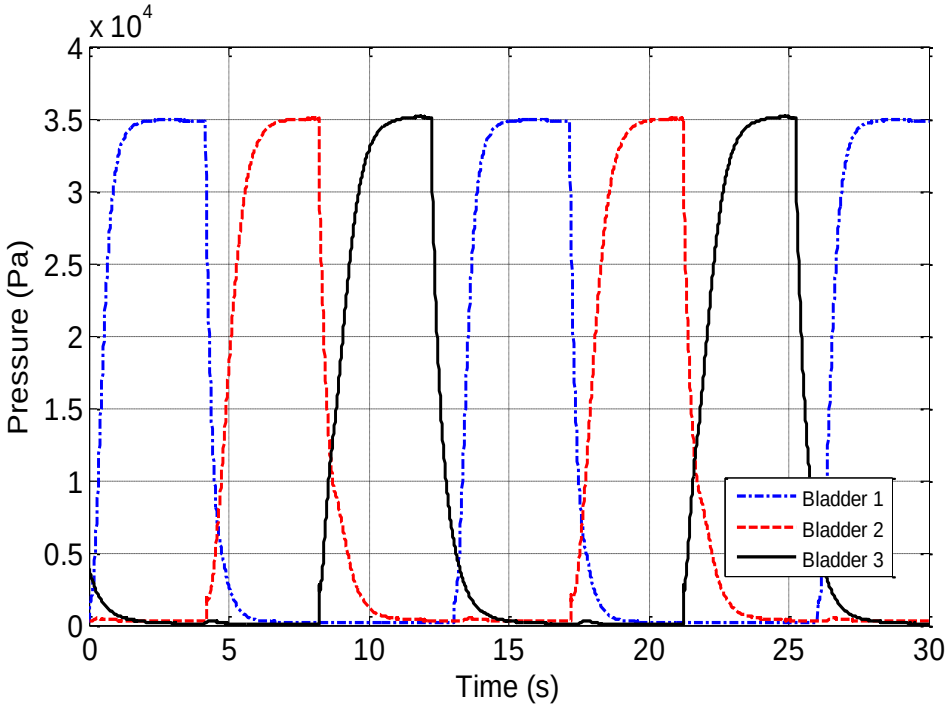

Figure 6.24. The experimental inner pressure Pi for the three bladders in presence of the PD controller

As it can be observed in figure 6.24, the control bench which describe in the previous part, works very good and it can control the inner pressure of the bladders to reach and stay in the reference value. By comparing the experimental results and simulated results (figure 6.19 (b)) for multi-bladder system, it can be deduced that the experimental test verifies the simulation one in both dynamic behaviour of the pressure and the time of remaining in the reference value.

6.3.3 Experimental test for the 3 bladders to simulate the fast mode

This experiment is focused in a closer approximation to the muscle motion and pumping effect in the blood in a healthy human. The objective of this experiment is to achieve a similar performance in our prototype for handicapped people who do not have the lower limbs affected by a disease.

The changes into the period of the cycles try to achieve the similitude with the human walk; tries to get closer to the peristaltic wave the muscles provide in healthy people.

The inflating and deflating times in this experiment are considered as 2s and 5s respectively. So, the PID controller has much less time to adapt the signals up to 35000 Pa. The experimental result for the simulation of *fast mode* is shown in figure 6.25.

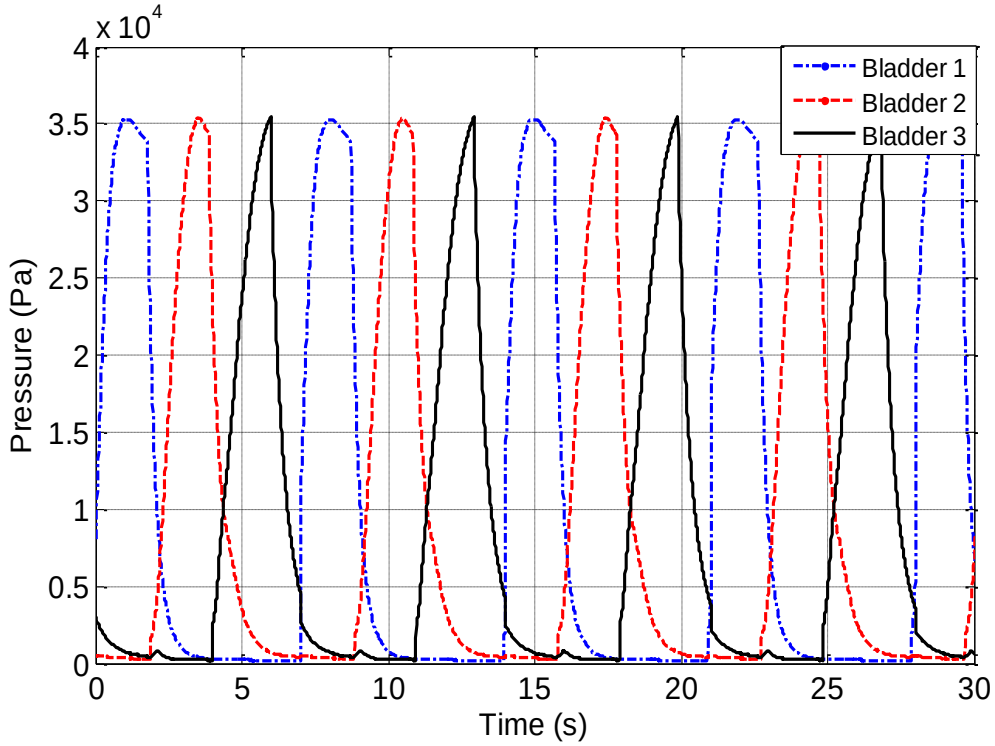

Figure 6.25. The experimental inner pressure Pi for the three bladders in presence of the PD controller for *Fast mode*

According to the figure 6.25, in the fast mode, the dynamic behaviour of the bladders are almost similar to the normal mode (4s deflating time) and PD controller tries to reach the inner pressure to the reference one as soon as possible. The result shows that the controller works well in the fast mode and the system is stable in this condition.

7. CONCLUSION

Goal of the project is the realisation and control of a biomechanical robotized Intermittent Pneumatic Compression (IPC) device to accomplish a therapeutic methodology for the recovery of cardio circulatory function in paraplegic patients. This impairment causes by the reduction of Venus return to the heart due to the absence of leg muscle contraction. The most advanced of the IPC device can produce defined compression/relaxation patterns on limb surfaces, improving the peripheral venous flow even in immobilized patients.

Despite there are many researchers investigating on IPC effects, the lack of a general methodology to study and develop an IPC device with physical and dynamical characteristics suitable for the intended application, is evident. In particular, the dynamic behaviour of the device in response of the control command is practically ignored.

The research activities and the accomplishments of this thesis can be categorized in the following three sections:

1. ***Designing and realization of the IPC device.*** Two prototypes of the IPC device were made in the laboratory of the Polytechnic University of Turin, which have been included 6 inflated bladders, shell to support the bladders and control system. The control system consists the 6 micro-electro valves, a programmable logic controller (PLC) and the pressure sensors for dynamic monitoring of air pressure inside bladders. The first one was with rigid body shell to support the bladder and it causes some problems to fit and adaptability of the device to the shape and dimension of the limb. Therefore, to eliminate the problems, in the second prototype, instead of the rigid body, the flexible and inextensible tissue is used to support the bladders. The prototype was tested experimentally on the 19 voluntary subjects and by the Echocardiography device the important parameters of the

cardiovascular system were recorded. The results of the experimental tests showed that the IPC device can improve the stroke volume (SV) +16% , the cardiac output (CO) +9.4%, and the end diastolic volume of left ventricle (LVEDV) +10%.

2. ***Mechanical characteristic and mathematical model of the IPC device.*** After validating the effectiveness of the IPC device on the cardiovascular system, we decided to model the device mathematically, to understand the dynamic behaviour of the IPC device and its interaction with the human, what it has been not considered in the literature. The obtained mathematical model considered all physiological and mechanical principles. To characterize the pneumatic circuit and device-limb interaction, we calculated all the parameters like transversal muscle stiffness and bladder stiffness experimentally. The transversal muscle stiffness is the most critical parameter, because its value depends on the muscle conditions. For example, there is different muscle stiffness between patients, normal persons and athletes. In this study, we have proposed the new method to estimate experimentally the value of the transversal muscle stiffness.

   The mathematical model has been implemented in Matlab-Simulink®, and simulations have been compared to experimental tests carried out on the prototype of IPC device, for validation. The results have shown that in both dynamic behaviour and maximum level of internal bladder pressure, the simulation has been verified by experimental one. So, the mathematical model can be used as a tool to simulate the real dynamic behavior of the IPC device and predict the effect produced on the limb, mainly the contact pressure and to define its control logic.

   The model is sensitive to the variation of the parameters and highlights the way this latter influence the action on the human. Thus, it is possible to obtain important indications on the values that must be respected in the design phase of the device.

3. ***Control of the IPC device***. In this section, the main issue is to individuate a proper control strategy able to create a desired pressure pattern on the limb surface, corresponding to a peristaltic and centripetal pressure wave. So, two control strategies was implemented in this research.

   - ***Control of the bladder pressure by regulating the inflating time of the bladder***. The value of inflating time is an important parameter in the IPC device. The experimental tests showed that differences 1 second in inflating time causes about 5000 *Pa* differences in the bladder pressure. So, the device

was controlled by regulating the inflating time by using two methods: Online and Offline, and the results showed about 37% improving in working the system on the desired value of the pressure bladder for inflating time equal to *4 s*.

- ***Control of the bladder pressure by applying a PID control*** properly tuned and to use proportional components for regulation of the pneumatic quantities of the system, i.e. the supply pressure and the air flow to the bladders. The results produced by this controller showed that the bladder can exert to the limb the exact value of the reference pressure for about the 60% of the desired active time (*4 s*). This is an excellent result, taking into consideration the natural low dynamics of such pneumatic systems. On the contrary, in absence of PID control the bladder pressure evolves only reaching a peak value, whose value is determined by the various parameters of the pneumatic circuit and is practically impossible to foresee.

  In addition, to verify the results of the control on the mathematical model, the device was controlled experimentally. The experimental tests were done by using the proportional components and engineering software LabView. The records showed a good corresponding between simulation and experimental results in both the dynamic behaviour of the device and stability of the pressure value in the desired one.

FUTURE WORK

Future work will concern more accurate modeling of the physiological system, including also damping characteristic of the soft tissues and a complete model of the cardio-circulatory system. This will allow to estimate the effect of the IPC device on the dynamic performance of the CCS, which is the final goal of the research. On this base, it will be possible to define also more precise patterns for the pressing action, which will constitute the reference for the study of more performing control algorithms.

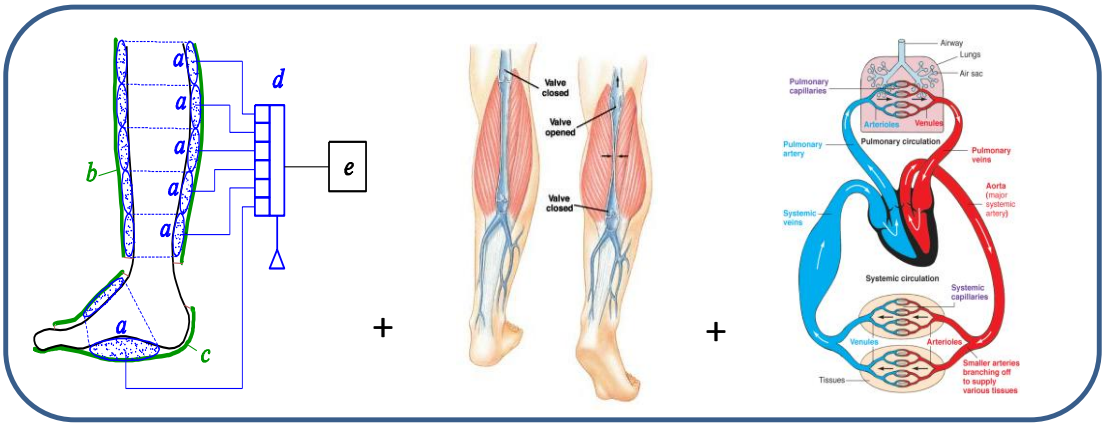

In addition, the device with controller which has been studied in this study can be test clinically in both healthy and impaired people to verify the effectiveness of the IPC device.

REFERENCES

[1] Herrmann LG, Reid MR.*the conservative treatment of arteriosclerotic peripheral vascular disease*, Ann Surg (1934),100:750-760.

[2] Landis EM, Gibbon JH, *the effect of alternative suction and pressure on blood flow to the lower extremities*, Ann Intern Med (1934);8:282-295.

[3] Clagett GP , Reisch JS, *prevention of venus thromboembolism in general surgical patients*, Results of meta-analysis, Ann Surgery 208 (1988), 227-240.

[4] Westrich GH, Haas SB, Mosca P and Peterson M, *Meta-analysis of thromboembolic prophylaxis after total knee arthroplasty*, Journal of Bone and Joint Surgery, British 82 (2000), 795-800.

[5] Flam E, Berry S, Coyle A, Dardik H and Raab L. *Blood-flow augmentation of intermittent pneumatic compression systems used for the prevention of deep vein thrombosis prior to surgery*, The American journal of surgery, vol. 171 (1996), pp. 312-315.

[6] Christen Y, Wutscher R, Weimer D, de Moerloose P, Kruithof E K O and Bounameaux H. *Effects of intermittent pneumatic compression on venous hemodynamics and fibrinolytic activity*, Blood coagulation and fibrinolysis, vol. 8, (1997), pp. 185-190.

[7] Froimson M I, Murray T G and Fazekas A F. *Venous Thromboemolic Disease Reduction with a Portable Pneumatic Compression Device*, The journal of Arthroplasty, vol. 24, n. 2, (2009), pp. 310-316.

[8] Louridas G, Saadia R, Spelay J, Abdoh A, Weighell W, Arneja AS, Tanner J and Guzman R. *The ArtAssist Device in chronic lower limb ischemia*, A pilot study, Int Angiol 21 (2002); pp 28-35.

[9] Delis KT, Nicolaides AN, Wolfe JH and Stansby G, *Improving walking ability and ankle brachial pressure indices in symptomatic peripheral vascular disease with intermittent pneumatic foot compression: a prospective controlled study with one-year follow-up*, Journal of vascular Surgery, 31 (2000): pp650-661.

[10] Labropoulos N, Leon LR, Bhatti A, Melton S, Kang SS, Mansour AM and Borge M, *Hemodynamic effect of intermittent pneumatic compression in patients with critical limb ischema*, journal of vascular surgery, vol 42, 4 (2005): pp 710-716.

[11] Nose Y, Murata K, Wada Yasuaki, Tanaka T, Fukagawa Y, Yoshino H,Susa T, Kihara C and Matsuzaki M, *The impact of intermittent pneumatic compression device on deep venus flow velocity in patients with congestive heart failure*, Journal of Cardiology, Vol 55:3 (2010) pp384-390.

[12] Johansson K, Lie E, Ekdahl C and Lindfelt J, *A randomized study comparing manual lymph drainage with sequential pneumatic compression for treatment of postoperative arm lymphedema*, Journal of Lymphology, 31 (1998), pp 56-64.

[13] Wiener A, Mizrahi J and Verbitsky O. *Enhancement of Tibialis Anterior Recovery by Intermittent Sequential Pneumatic Compression of the Legs*, Basic Appl Myol , vol .11, n.2 (2001), pp. 87-90.

[14] Waller T, Caine M and Morris R. *Intermittent Pneumatic Compression Technology for Sports Recovery*, The Engineering of Sport 6 Volume 3: Developments for Innovation, (2006), Springer. ISBN: 978-0-387-34680-9 (Print) 978-0-387-45951-6 (Online).

[15] Unger RJ, Feiner JR, *Hemodynamic effects of intermittent pneumatic compression of the legs*, Anesthesiology 67 (1987), pp266-268.

[16] Morgan RH, Carolan G, Psaila JV, Gardner AMN, Fox RH, and Woodcock JP, *Arterial flow enhancement by impulse compression*, Journal of Vascular Surgery 25 (1991), pp 8-15.

[17] Lurie F, Awaya DJ, Kinster RL, and Eklof B, *Hemodynamic effect of intermittent pneumatic compression and the position of the body*, Journal of Vascular Surgery, Vol 37, 1 (2003), pp 137-142, 2003.

[18] A. Porta, M. D. Rienzo, N. Wessel and J. Kurths, "Addressing the complexity of cardiovascular regulation A", Philosophical Transactions of the Royal Society, vol. 367, pp. 1215–1218, 2009.

[19] L. Opie, "The cardiac cycle", in Heart Disease: A Textbook of Cardiovascular Medicine, E. Braunwald, 6th pp. 462-475, 2001.

[20] Vander, A. J., J. H. Sherman, et al. (2001). Human physiology : the mechanisms of body function. Boston, McGraw-Hill.

[21] AHA. (2004). Heart Disease and Stroke Statistics--2004 Update. Texas: American Heart Association.

[22] Bittner, V. (2002). Women and coronary heart disease risk factors. Journal of Cardiovascular Risk, 9(6), 315-322.

[23] Charney, P. (2002). Presenting symptoms and diagnosis of coronary heart disease in women. Journal of Cardiovascular Risk, 9(6), 303-307.

[24] WHO. (2002a, 2004). Cardiovascular disease: reducing the risk. Retrieved July 23, 2003, 2004, from http://www.who.int/dg/speeches/2002/inbv/en/print.html

[25] K. Thygesen, J. S. Alpert and H. D. White, "Universal definition of myocardial infarction", European Heart Journal, vol. 28, pp. 2525–2538, 2007.

[26] Thes Colorado.

[27] J.J.F, Belch et al. Critical Issues in Peripheral arterial Disease: Detection and Management. A Call to Action. Archives of Internal Medicine 2003;163: 884-892.

[28] Cicala, R. (1997). The heart disease sourcebook. Los Angeles, Chicago, Lowell House; Contemporary Books.

[29] Steegers-Theunissen RP, Steegers EA. Nutrient-gene interactions in early pregnancy: a vascular hypothesis. Eur J Obstet Gynecol Reprod Biol 2003;106:115-7.

[30] Armstrong EJ, Bischoff J. Heart valve development: endothelial cell signalling and differentiation. Circ Res 2004;95:459-70.

[31] Roybal CN, Yang S, Sun CW, et al. Homocysteine increases the expression of vascular endothelial growth factor by a mechanism involving endoplasmic reticulum stress and transcription factor ATF4. J Biol Chem 2004;279:14844-52.

[32] Coleridge Smith, P.D. et al (1991) Deep vein thrombosis: effect of graduated compression stockings on distension of the deep veins of the calf. British Journal of Surgery; 78: 6, 724–726.

[33] Arcelus, J.I. et al (1995) Modifications of plasma levels of tissue factor pathway inhibitor and endothelial-1 induced by a reverse Trendelenburg position: influence of elastic compression – preliminary results. Journal of Vascular Surgery; 22: 5, 568–572.

[34] Morris R. J. Intermittent pneumatic compression – systems and applications. Journal of Medical Engineering and Technology, vol. 32, n. 3, 2008, pp. 179-188.

[35] Johansson K, Lie E, Ekdahl C and Lindfeldt J. A randomized study comparing manual lymph drainage with sequential pneumatic compression for treatment of postoperative arm lymphedema. Journal of Lymphology, 31, 1998, pp. 56-64.

[36] Partsch H. Intermittent pneumatic compression in immobile patients. International Wound Journal, vol.5, n.3, 2008, pp. 389-397.

[37] Wiener A, Mizrahi J and Verbitsky O. Enhancement of Tibialis Anterior Recovery by Intermittent Sequential Pneumatic Compression of the Legs. Basic Appl Myol , vol .11, n.2, 2001, pp. 87-90.

[38] Waller T, Caine M and Morris R. Intermittent Pneumatic Compression Technology for Sports Recovery. The Engineering of Sport 6 Volume 3: Developments for Innovation, 2006, Springer. ISBN: 978-0-387-34680-9 (Print) 978-0-387-45951-6 (Online).

[39] Comerota A J. Intermittent pneumatic compression: Physiologic and clinical basis to improve management of venous leg ulcers. Journal of vascular surgery, vol. 53, n.4, 2011, pp. 1121-1129.

[40] Nelson E A, Mani R, Thomas K and Vowden K. Intermittent pneumatic compression for treating venous leg ulcers (review). The Cochrane Collaboration, J. Wiley and sons, Ldt, 2011.

[41] Flam E, Berry S, Coyle A, Dardik H and Raab L. Blood-flow augmentation of intermittent pneumatic compression systems used for the prevention of deep vein thrombosis prior to surgery. The American journal of surgery, vol. 171, 1996, pp. 312-315.

[42] Christen Y, Wutscher R, Weimer D, de Moerloose P, Kruithof E K O and Bounameaux H. Effects of intermittent pneumatic compression on venous hemodynamics and fibrinolytic activity. Blood coagulation and fibrinolysis, vol. 8, 1997, pp. 185-190.

[43] Froimson M I, Murray T G and Fazekas A F. Venous Thromboemolic Disease Reduction with a Portable Pneumatic Compression Device. The journal of Arthroplasty, vol. 24, n. 2, 2009, pp. 310-316.

[44] Morris R J and Woodcock J P. Evidence-based Compression: Prevention of stasis and deep vein thrombosis. Ann Surg 239(2), 2004, pp. 162-171.

[45] Dai G, Gertler J P and Kamm R D. The effects of external compression on venous blood flow and tissue deformation in the lower leg. Journal of biomechanical engineering, vol.121, 1999, pp. 557-564.

[46] Malone M D, Cisek P L, Comerota A J Jr, Holland B, Eid I G and Comerota A J. High-pressure, rapid inflation pneumatic compression improves venous hemodynamics in healthy volunteers and patients who are post-thrombotic. Journal of vascular surgery, vol.29, n.4, 1999, pp.593-599.

[47] Lurie F, Scott V, Yoon H-C and Kitsner R L. On the mechanism of action of pneumatic compression devices: combined magnetic resonance imaging and duplex ultrasound investigation. Journal of vascular surgery, vol. 48, n. 4, 2008, pp. 1000-1006.

[48] LymphPro, http://www.lymphpro.com/

[49] Bio - Arterial Plus, http://www.biocompression.com/Products/Pumps/BioArterial-Plus.aspx

[50] Zrunek M, Bigenzahn W, Mayr W, Unger E, Feldner-Busztin H. A laryngeal pacemaker for inspiration controlled direct electrical stimulation of denervated posterior cricoarytaenoid muscle in sheep. Eur Arch Otorhinolaryngol 1991, 248(8):445-448.

[51] Wilburn O, Wilburn P, Rockson SG. A pilot, prospective evaluation of a novel alternative for maintenance therapy of breast cancer–associated lymphedema. BMC Cancer. March 2006, Volume 6, Number 84.

[52] Ridner S, McMahon E, Dietrich MS, Hoy S. Home–based lymphedema treatment in patients with and without cancer–related lymphedema. Oncology Nursing Forum. July 2008, Volume 35, Number 4.

[53] *LymphPro, http://www.lymphpro.com/*

[54] Ridner S, McMahon E, Dietrich MS, Hoy S. Home–based lymphedema treatment in patients with and without cancer–related lymphedema. Oncology Nursing Forum. July 2008, Volume 35, Number 4.

[55] http://www.dispositivimedici.biz/dispositivo_medicale/scheda/lympha-press-ballancer-303-et/93033

[56] http://medical.ausilium.it/p-16992-lympha-wavetm.htm

[57] Offer Galili, Dalit Mannheim, Sigalit Rapaport, Ron Karmeli, A novel intermittent mechanical compression device for stasis prevention in the lower limbs during limited mobility situations; Department of Vascular Surgery, Carmel Medical Center, Haifa, 34362, Israel; Thrombosis Research (2007) 121, 37–41.

[58] Davies LC, Francis DP, Crisafulli A, Concu A, Piepoli M, Coats AJS (2000) Oscillations in stroke volume and cardiac output arising from oscillatory ventilation. Exper Physiol 85:857-862.

[59] Crisafulli A, Salis E, Pittau G, Lorrai L, Tocco F, Melis F, Pagliaro P, Concu A (2006) Modulation of cardiac contractility by muscle metaboreflex following efforts of different intensities in humans. Am . Physiol (Heart Circ Physiol) 291:H3035-H3042.

[60] Crisafulli A, Salis E, Tocco F, Melis F, Milia R, Pittau G, Caria MA, Solinas R, Meloni L, Pagliaro P, Concu A (2007) Impaired central hemodynamic response and exaggerated vasoconstriction during muscle metaboreflex activation in heart failure patients. Am J Physiol (Heart Circ Physiol) 292: 2988-2996.

[61] Concu A, Marcello C (1993) Stroke volume response to progressive exercise in athletes engaged in different training modes. Eur J Appl Physiol 66:11-17.

[62] Luepker RV, Michael JR, Warbasse JR (1973) Transthoracic electrical impedance: quantitative evaluation of a non ivasive measure of thoracic fluid volume. Am Herart J 85:83-93

[63] Okutani H, Fujinami T, Nakamura K (1981) Studies on mean thoracic impedance (Zo). Proceedings of the 5th International Conference on Electrical Bioimpedance, Tokyo. Japan, pp 31-34

[64] Crisafulli A, Carta C, Melis F, Tocco F, Frongia F, Santoboni UM, Pagliaro P, Concu A (2004) Haemodynamic responses following intermittent supramaximal exercise in athletes. Exp Physiol 89(6):665-74.

[65] Crisafulli A, Melis F, Orrù V, Lener R, Lai C, Concu A (1999) Hemodynamic during a postexertional asystolia in a healthy athlete: a case study. Med Sci Sport Exer 32:4-9.

[66] Concu A, Marcello C, Esposito A, Ciuti C, Rocchitta A, Montaldo PL (1992) Thoracic fluid volume measured by electrical bioimpedance: a simple method for non-invasive assessment of preload changes during exercise. Proceedings of the VI^ Mediterranean Conference on Medical and Biological Engineering, Capri, Italy, 5/10 July, pp. 1261-1264.

[67] Schairer JR, Stein PD, Keteyian S, Fedel F, Ehrman J, Alam M, Henry JW, Shaw T (1992) Left ventricular response to submaximal exercise in endurance-trained athletes and sedentary adults. Am J Cardiol 70(9):930-933.

[68] Rerych SK, Scholz PM, Newman EG, Sabiston DC and Jones HR, (1978), Cardiac Function at Rest and During Exercise in Normals and in Patients with Coronary Heart Disease: Evaluation by Radionuclide Angiocardiography, journal of Annals of Surgery, 187(5): 449-463.

[69] L R Poliner, G J Dehmer, S E Lewis, R W Parkey, C G Blomqvist and J T Willerson, (1980) Left ventricular performance in normal subjects: a comparison of the responses to exercise in the upright and supine positions, Circulation, 62: 528-534.

[70] International Standard ISO6358. Pneumatic Fluid Power - Components using Compressible Fluids - Determination of Flow-rate Characteristics. 1989, 15p.

[71] Tzafestas S, and Papanikolopoulos NP (1990). Incremental Fuzzy expert PID control. IEEE transaction on industrial electronics, Vol. 37 (5), pp. 365-371.

[72] Bennet S (1996). A brief history of automatic control. IEEE Control Systems, Vol. 16 (3), pp.17-25.

[73] Ziegler JG and Nichols NB (1942). Optimum settings for automatic controllers. Trans. ASME, Vol. 64, pp. 759–768.

[74] Kiam Heong Ang, Chong G, and Yun li (2005). PID control system analysis, design, and technology. IEEE transaction on control systems technology, Vol. 13 (4), pp. 559-576.

[75] Astrom KJ and Haggund T (1988). Automatic tuning of PID controller. Research triangle park, NC.

[76] Franklin GF, Powell JD, and Naeini AE (1986). Feedback control of dynamic systems, Addison-Wesley.

[77] Cohen GH, and Coon GA (1953). Theoretical consideration of retarded control. Trans ASME, Vol. 75, pp. 827-834.

[78] Seborg DE, Edgar TF, and Mellichamp DA (1989). Process dynamics and control. New York: Wiley.

[79] Ferraresi C and Sorli M (1994). Modelling and analysis of systems for control of the pressure. (In Italian), Fluid, No 357, pp. 58-65.

[80] Ferraresi C and Velardocchia M (1990). Pneumatic proportional valve with internal feedback. Proceeding of the 9th international symposium on Fluid power, Oxford UK, pp. 125-136.

APPENDIX

In this part, the three published papers based on the thesis in full format are presented.

I. C. Ferraresi, D. Maffiodo, **H. Hajimirzaalian**, "*A model-based method for the design of Intermittent Pneumatic Compression Systems acting on humans"*, published in the Journal of Engineering in Medicine, Vol. 228 (2), pp. 118-126, 2014.

URL: http://pih.sagepub.com/content/228/2/118

Original Article

Institution of MECHANICAL ENGINEERS
Journal of ENGINEERING IN MEDICINE

Proc IMechE Part H:
J Engineering in Medicine
2014, Vol. 228(2) 118–126

DOI: 10.1177/0954411913516307
pih.sagepub.com
SAGE

A model-based method for the design of intermittent pneumatic compression systems acting on humans

Carlo Ferraresi, Daniela Maffiodo and Hamidreza Hajimirzaalian

Abstract

Intermittent pneumatic compression is a well-known technique, which can be used for several therapeutic treatments like sports recovery, lymphoedema drainage, deep vein thrombosis prevention or others, which may require very different operating characteristics as regards the desired pressure values and the operating velocity. The performance and the effectiveness of the device are often difficult to predict and must be usually optimized through empirical adjustments. This article presents a general method based on the mathematical modelling of a generic IPC system, aimed at studying and developing such a device with physical and dynamical characteristics suitable for the intended application.

Keywords

Intermittent pneumatic compression system, human–machine interface, muscular pump

Date received: 18 April 2013; accepted: 4 November 2013

Introduction

During any physical activity, the intermittent contraction of the limb muscles exerts important pumping actions on physiological systems such as the muscular, cardiovascular or lymphatic system. When the muscular efficiency is compromised for some reason, its function can be mimicked by a mechanical device properly conceived.

Although the various forms of mechanical intermittent compression of limbs have a 70-year history of published clinical effectiveness, a complete knowledge of the cause and effect process is not yet fully reached.

One of the first significant commercial devices based on real physiological evidence was the ColWil pump developed in the 1960s. Many other devices were developed since that early system, with different characteristics and to accommodate different medical applications.[1]

Today, in various therapeutic situations, the use of an intermittent pneumatic compression (IPC) system may be recommended: lymphoedema treatment, deep vein thrombosis prevention, management of venous leg ulcers (VLU), sport recovery, critical limb ischaemia and improving of walking distance in patients with intermittent claudication.

Johansson et al.[2] effected a lymphoedema treatment by an IPC device for the arm (Lympa-Press, Liljenberg Medical AB, Malmo, Sweden) employing nine compression cells, 40–60 mmHg for 2 h/day for 2 weeks 5 days/week, and made a comparison with a corresponding manual treatment. They refer no significant difference between the two methods, thus demonstrating the possibility to substitute the manual operation with an automatic mechanical system.

Partsch[3] focuses on the importance of using IPC devices in immobile patients because their active venous calf muscle pump does not work. He stresses a lack of specific references in literature and lists many parameters being influenced by an IPC (venous pressure and velocity, foot/calf venous volume, skin blood flux and many others). He highlights the need to understand which IPC system is most suitable for which application.

Another field of use is sports recovery: Wiener et al.[4] examined the effect of IPC on the legs for the recovery of fatigued tibial anterior muscles. After an

Department of Mechanical and Aerospace Engineering, Politecnico di Torino, Torino, Italy

Corresponding author:
Daniela Maffiodo, Department of Mechanical and Aerospace Engineering, Politecnico di Torino, Corso Duca degli Abruzzi 24, 10129 Torino, Italy.
Email: daniela.maffiodo@polito.it

IPC treatment, the muscle fatigue was monitored by surface electromyography (EMG), showing significant improvement with respect to manual passive treatment. For this experience, a Lympha Wave (model 301 ET, Mego Afek, Israel) system was used, provided with seven bladders and operated at maximum pressure of 80 mmHg, used for 3 min after a training, performing 2 cycles/min with 21 s inflation and 9 s deflation.

Similarly, Waller et al.[5] made a pilot study aiming to demonstrate that IPC devices may be beneficial to the warm-down activities of athletes. They compared two different treatments with low pressure (20:15:10 mmHg) and high pressure (70:65:60 mmHg) and concluded that 'athletes undertaking IPC as part of their training regime should be able to increase their training volume with a reduced risk of discomfort and injury'.

A pair of recent review articles, Comerota[6] and Nelson et al.,[7] underlines that in various researches, an IPC device can be used for the management of advanced chronic venous disease, specifically VLU. They underline that different devices with different pressure levels, duration per day and duration of treatment have been performed. Comerota suggests that use of IPC as an adjunct to sustained compression may be the optimal choice for treating patients with VLUs; however, a number of questions remain, for example, the type of compression. Nelson et al. conclude that there is no robust evidence that IPC improves ulcer healing when compared with continuous compression alone or when added to a standard regimen of compression bandages. There is only some generic indication that 'fast' IPC therapy has more effectiveness than 'slow' therapy.

Various researchers (Flam et al.,[8] Christen et al.[9] and Froimson et al.[10]) investigated the effectiveness of several commercial IPC devices for the prevention of deep vein thrombosis. In general, they observed positive results, although each device was used with very different settings, as concerns pressure values and cycle times, thus indicating a poor knowledge of the relationship between the characteristic and setting of the device and the effect on the human.

Morris and Woodcock[11] tried to evaluate the variety of available systems, with different compression techniques and sequences, in order to individuate appropriate choice criteria for each patient. They conclude that rapid inflation, high pressure and graded sequential IPC show particular augmentation profiles, but there is no evidence that such features improve the prophylactic ability of the device. According to them, the most important parameters are the patient compliance and the appropriateness of the site of compression. In particular, as regards to the extent of the bladders, they prefer the asymmetric solution, with smaller bladder placed only at the back of the limb, rather than bladders extended circumferentially around the whole limb. This is because smaller bladders require limited size pumps and allow higher operating frequencies.

A research by Dai et al.,[12] oriented to a more quantitative study, defines a method to model the deformation of a limb under different cuffs (circumferentially symmetric and asymmetric) and to examine the stress distribution within the tissues and the corresponding venous blood flow. With a two-dimensional (2D) finite element method (FEM) model, they found that asymmetric compression would generate larger blood flow velocities and shear stresses than circumferentially symmetric compression. However, no consideration is made on dynamic effects.

Malone et al.[13] made a comparison between five IPC devices, two of standard type (low pressure: ranging from 40 to 50 mmHg, slow dynamics: 1 min cycle, inflation 11–12 s) and three high pressure (160, 160, 120 mmHg), rapid (22, 22, 30 s cycle, inflation 2 s) compression systems. They evaluated the maximal venous velocities at the common femoral vein and at the popliteal vein and observed an increase for all devices. The comparison between the two kinds of devices showed an increased velocity response to the high-pressure, rapid inflation device. Thus, this research raises a question about the need to understand the dynamic behaviour of the device, considering the effect of two parameters: pressure level and inflation/deflation time. Actually, these parameters are correlated: if inflating time is very short, the contact pressure between leg and device could not reach the supply pressure value.

The need to relate the supply pressure with the real operation pressure (i.e. the contact pressure between leg and bladder) as a function of the device characteristics and the work cycle timing is an important topic, poorly investigated.

This crucial point was caught by Lurie et al.[14] Their study attempted to investigate the relationships between the interface pressure produced by IPC devices, the deformation of extremity tissues produced by this pressure and changes in venous blood flow, by use of magnetic resonance imaging and duplex ultrasound scans in addition to pressure measurement. They used Venaflow® (Aircast, Inc., Summit, NJ) (6 s inflating with 0.3 s delay between the two chambers, rapid deflating, at 52 (distal), 45 (proximal) mmHg and WizAir® (MCS Medical Compression Systems Ltd, Or Akiva, Israel) (slow inflation and slow deflation at 80 mmHg). They concluded that while in the past the difference between haemodynamic effects produced by various IPC devices has been attributed only to the different levels of the air supply pressure, the patterns of pressure actually applied to the extremity might be different due to different materials and construction of the garments. They also conclude that 'further investigation of biomechanical mechanisms of IPC is needed to guide the development of better engineering solutions …'

Summarizing, this review highlights the lack of a general methodology to study and develop an IPC device with physical and dynamical characteristics suitable for the intended application. In particular, the

dynamic behaviour of the device in response of the control command is practically ignored.

The goal of the present research is to realize such a methodology, aimed at supporting the design and realization of an IPC system, once a given pattern of human–device contact pressure has been defined. This latter can be very different depending on the required therapy, as regards pressure levels and timings necessary to optimize clinical results, since treatments like sports recovery, lymphoedema drainage, deep vein thrombosis prevention or others may require very different operating characteristics.

The methodology is based on the realization of a mathematical model able to represent the dynamic behaviour of the device and its interaction with the human.

The IPC device

This work is focused on a device aimed at exerting an intermittent pressing action on foot and calf, to the aim of improving the venous return in impaired people, like paraplegics. However, the same concept could concern any device aimed at exerting a compressing action, like a massage for lymphoedema treatment or sports recovery.

A typical structure of such a device could be the one depicted in Figure 1. In this case, it is provided with a given number of inflatable bladders (*a*), included into shells (*b, c*), and acting on the skin of the calf and foot. The shells could be rigid or, more conveniently, a sort of sleeves, flexible but inextensible, so self-adapting to the shape and size of the limb but also avoiding stretching and therefore directing all the pneumatic energy towards the limb.

The control system can be arranged with several levels of complexity; basically, it must include a group of valves (*d*) and a programmable logic controller, that is a PLC (*e*); for given applications, it may be convenient to include also some sensors, for dynamic monitoring of air pressure inside bladders or contact pressure to the skin.

The operating principle is simple since it consists in inflating and deflating the bladders with given values of pressure and defined timing, but it may be very demanding in terms of the dynamic evolution of the air pressure, according to the intended application. The effectiveness of the device is based on several factors, which are discussed below.

The mechanical action is provided by pneumatic energy, through sealed cells (bladders), which are a very strategic element of the system. Figure 2 shows one single bladder and a group of five that could be used for such an application. In order to optimize the performance, it is convenient that the air energy is directed as much as possible towards the biological tissues of the limb, rather than used to deform the materials of the device structure. To this aim, the bladders should be able to expand with limited or null stretching of the wall and this can be achieved both by proper shaping of the cell and adopting a material which should be compliant but, of course, airtight.

Another key element of the device is the shell to which the bladders are attached. Its shape should be adaptable as much as possible to the anatomy of the limb, in order to minimize dead volumes that would affect the dynamic performance. On the other side, the expansion of the bladders must occur only on the limb side, with no stretching of the supporting shell. In order to meet these demands, the shell may be realized with some material which should be as much as possible flexible and inextensible.

Finally, the pneumatic circuit is important since it must provide the supplying of the bladders with given dynamic performance; this could be very demanding for certain applications and will require an accurate definition of the general layout and a proper choice of the components. To realize a mathematical model of the device, a complete knowledge of all the physical and functional characteristics of the components will be required.

The action of the device on the limb depends also on the physiological characteristic of the latter; this will

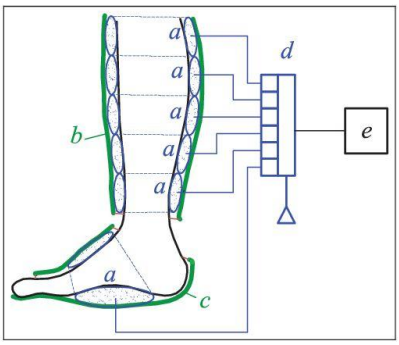

Figure 1. Typical configuration of an IPC device.

Figure 2. The bladders of the IPC device.

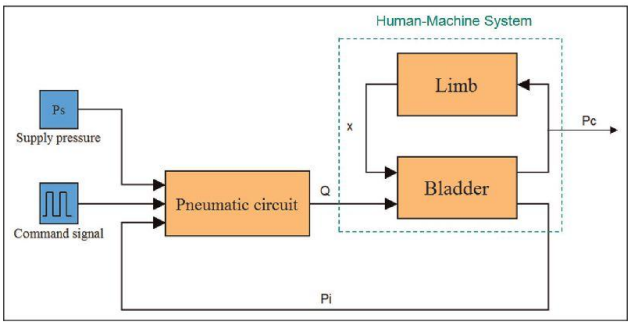

Figure 3. Conceptual block diagram of the system.

require the knowledge of the mechanical characteristic of the limb biological tissues.

Mathematical model of the IPC device

An accurate mathematical model of the device is a fundamental tool for understanding the physical behaviour and setting all structural and functional parameters. The model must consider all physiological and mechanical principles which have to be harmonized for the expected therapeutic methodology.

It is supposed that the basic requirement for a given therapeutic protocol is the application of a rhythmic pressure to a limb; the pressure must be automatically controlled as regards in particular the frequency and the maximum/minimum levels.

A conceptual block diagram of the system may consider a single module with one bladder supplied by one pneumatic valve, as depicted in Figure 3. The bladder and the limb together form the so-called human–machine system.

The valve is supplied by a given pressure source p_S and is commanded by a digital on–off signal; the air flow Q from the valve inflates the bladder, producing a variation of the internal air pressure p_i and of the contact pressure p_C on the limb; this latter is then deformed by an amount x which in turn affects the volume of the bladder. The bladder pressure p_i also influences the mass flow rate Q. The contact pressure p_C is the physical quantity which must be controlled.

To model the whole of the system, it is required to characterize all subsystems and determine their parameters. In the following, the modelling procedure is described.

Modelling of the human–machine subsystem

The human–machine system represents the interaction between the bladder and the limb. A possible schematization of the system is shown in Figure 4. The bladder is considered as a compliant closed volume supported

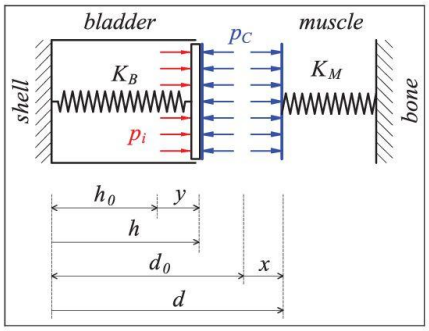

Figure 4. Scheme of the human–machine system.

by the device shell; the limb is schematized as a compliant body (the muscle) supported by the bone.

The main mechanical characteristics are the transversal muscular stiffness K_M and the bladder wall stiffness K_B. p_i is the pressure inside the bladder; p_C is the contact pressure between bladder and limb. x and y represent, respectively, the deformation of limb and bladder under the effect of the pressure. The actual height of the bladder is indicated as h, whose initial value (no pressure in bladder) is h_0; d represents the actual distance (gap) between the shell and the limb, with initial value d_0; in case of skin–bladder contact, $h = d$. The initial values h_0 and d_0 represent the 'rest condition' of bladder and limb, respectively, that is, when a null pressure is acting on the system.

The physical behaviour of the bladder can be described by the scheme of Figure 5. The internal pressure p_i depends on the mass flow rate Q coming from the valve and on the deformation y of the bladder; the contact pressure p_C on the limb depends on the inner pressure p_i and on the deformation y. The relationship between the bladder deformation y and the limb deformation x can be determined by a discussion of the contact condition.

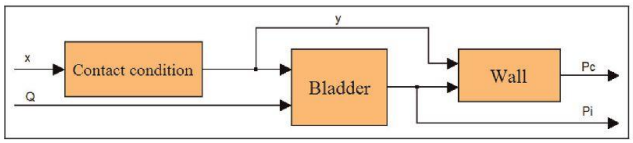

Figure 5. Scheme of physical behaviour of the bladder.

The flow continuity equation for the bladder can be written as

$$Q = \frac{W}{RT}\frac{dP_i}{dt} + \frac{P_i A}{RT}\frac{dy}{dt} \tag{1}$$

where Q is the air mass flow rate entering the bladder, P_i is the absolute internal air pressure, W is the actual volume of the bladder, R is the air constant, T is the absolute temperature and A is the bladder-limb contact area.

The volume of the bladder can be expressed as

$$W = A(h_0 + y) \tag{2}$$

Equation (1) is nonlinear; its integration allows the calculation of the absolute bladder pressure P_i but requires the knowledge of the bladder deformation y.

In the article, all symbols with capital P indicate absolute air pressure, while symbols with lowercase p indicate pressure relative to ambient. The difference between p_i and p_C depends on the stiffness of the bladder wall and is a function of its expansion, as expressed by the following equation

$$p_C = p_i - K_B y \tag{3}$$

To evaluate the bladder stiffness K_B, it is worth mentioning that because of the bladder material, the elastic term $K_B y$ exists only when the bladder wall is stretched. The variation of the bladder elastic force with respect to the bladder height can be experimentally valued by inflating the bladder in no-constraint condition, as represented in Figure 6.

In this way, a variation in the inner pressure determines variation of the height, according to a given trend; this function can be approximated by two straight lines, so individuating a 'height at rest' h_0, reached at an almost null inner pressure, and an 'elastic range' in which the bladder wall is stretched and the height increases with the pressure. Therefore, equation (3) can be split to consider the full range of the bladder expansion

$$\begin{aligned} p_C &= p_i \quad for\ h \leqslant h_0 \\ p_C &= p_i - K_B(h - h_0) \quad for\ h > h_0 \end{aligned} \tag{4}$$

The actual value of K_B depends on the wall material and also on the shape and dimension of the bladder. By way of example, a rectangular bladder of 5 × 30 cm sides, made of Medical Windtex® (Windtex Vagotex S.p.A., Italy), presents an average $K_B = \Delta p/\Delta h$ of about 5×10^5 Pa/m.

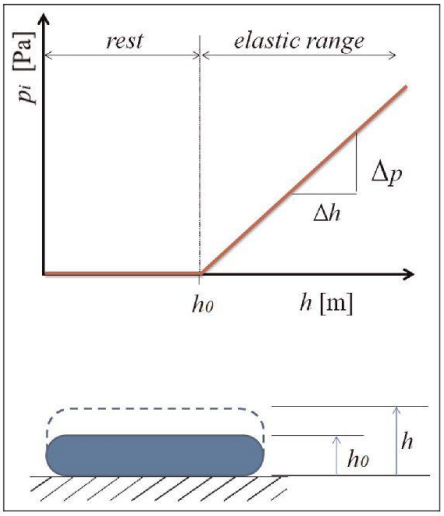

Figure 6. Evaluation of the bladder elastic stiffness. The diagram reports an approximated relationship between the internal pressure pi and the bladder height h.

From the muscle side, it is possible to write

$$p_C = K_M x \tag{5}$$

The determination of the transversal muscular stiffness K_M is a very crucial point. The value of this parameter is subjective and depends on the muscular condition of the limb. No information about that is available in the literature and very few researchers, like Dai et al.,[12] tried to experimentally measure this characteristic. A possible way to determine it is described by the scheme of Figure 7.

In such a device, a tension T is applied to a strip 3 wrapped around the limb; the tension is regulated by a screw device 1 and measured by a load cell 2.

When the tension T is applied, the limb deforms by a given amount, depending on its muscular stiffness. The applied contact pressure can be calculated considering the muscular tissue 4 as a fluid mass, as depicted in Figure 8, by the following equation

$$p_C = \frac{T}{r \cdot l} \tag{6}$$

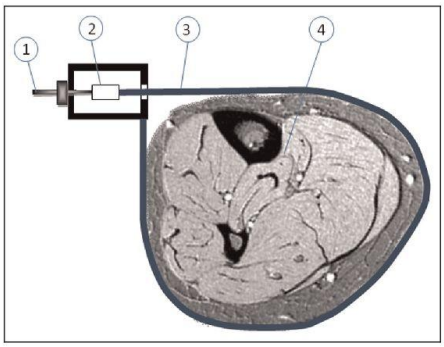

Figure 7. Scheme of experimental set-up to evaluate the transversal muscular stiffness.

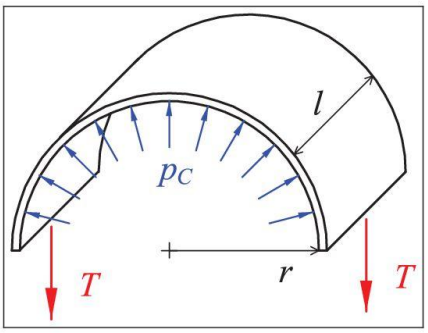

Figure 8. Calculation of the transversal muscular stiffness.

where r is the radius of the limb and l is the height of the strip. The muscular stiffness is measured and expressed as

$$K_M = \frac{\Delta p_C}{\Delta r} \tag{7}$$

Experimental tests on three different subjects provided values of muscular stiffness ranging from 3×10^6 to 7×10^6 Pa/m.

The integration of equation (1) requires to express the bladder deformation y as a function of pressure P_i. To do that, it is necessary to detect if there is contact between bladder and limb.

The existence of the contact can be determined by calculating and comparing the values of the bladder height $h = h_0 + y$ and the total gap $d = d_0 + x$ (with reference to Figure 4).

In case of no contact ($h < d$) one has

$$x = 0 \tag{8}$$

$$y = \frac{p_i}{K_B} \tag{9}$$

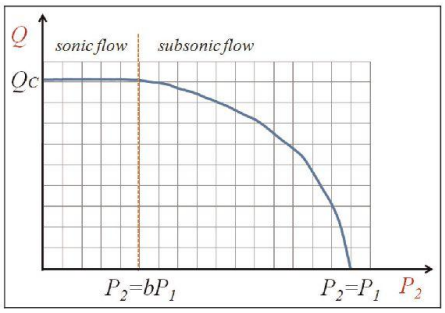

Figure 9. The flow curve of a pneumatic valve.

while in case of contact, it will be

$$x = \frac{p_C}{K_M} \tag{10}$$

$$y = \frac{p_C}{K_M} + (h_0 - d_0) \tag{11}$$

with p_C expressed as per equation (4).

Modelling of the pneumatic subsystem

The pneumatic subsystem for one bladder comprises a three-port electro-pneumatic mini-valve connected to a supply source on one side and to the bladder on the other side. The switching of the valve between its two operating conditions connects in turn the bladder either to the supply source or to the exhaust.

To model the pneumatic system, it is necessary to express the air mass flow rate through the valve as a function of the supply and bladder pressures and of the operating conditions. This can be done by using the formulation defined by the ISO 6358 Standard,[15] which considers the two possible conditions of sonic and subsonic flow. Figure 9 shows the typical shape of a valve flow curve for fixed upstream pressure P_1 and variable downstream pressure P_2. The symbol Q_C indicates the critical flow rate. One must consider that depending on the valve condition, the bladder inner pressure P_i can correspond either to the downstream pressure P_2 (when the bladder is inflated and the upstream pressure is the supply pressure P_S) or to the upstream pressure (when the bladder is deflated and the downstream pressure is the ambient pressure P_A).

According to the above Standard, the valve mass flow rate can be analytically expressed by interpolating functions

$$\begin{aligned} Q &= C \cdot P_1 \cdot K_T \sqrt{1 - \left(\frac{r-b}{1-b}\right)^2} \quad \text{for subsonic flow} \\ Q &= C \cdot P_1 \cdot K_T \quad \text{for sonic flow} \end{aligned} \tag{14}$$

Table 1. Experimental and simulated conditions.

Parameter	Symbol	Value	Unit
Absolute supply pressure	P_S	1.5×10^5	Pa
Absolute ambient pressure	P_A	1×10^5	Pa
Contact area of the bladder	A	0.015	m^2
Pneumatic conductance	C	3×10^{-10}	$m^3/(s\ Pa)$
Critical pressure ratio	b	0.02 (inflating); 0.2 (deflating)	
Temperature	T	293	K
Temperature coefficient	K_T	1	
Bladder height at rest	h_0	0.006	m
Initial shell-limb gap	d_0	0.01	m
Bladder stiffness	K_B	5×10^5	Pa/m
Muscle stiffness	K_M	7×10^6	Pa/m
Inflating time	t_I	4	s
Total cycle time	t_C	13	s

where C is the valve conductance; K_T is a corrective factor depending on the inlet air temperature ($K_T = 1$ at standard conditions, with $P_1 = 1.013$ bar and $T = 273$ K); $r = P_2/P_1$ is the actual pressure ratio; and b is the critical pressure ratio (when P_2 reaches the critical value $P_{2CR} = b \cdot P_1$).

The valve coefficients C and b can be evaluated by the experimental curve of Figure 9. Since the valve is connected to the supply source and to the bladder by means of tubes and fittings, the experimental characterization must consider also these elements.

Validation and use of the IPC mathematical model

In order to verify the effectiveness of the mathematical model here proposed, it has been numerically implemented in MATLAB–Simulink ambient. A validation of the numerical model has been made by comparing the simulation with the experimental registration of the dynamic bladder pressure during the operation of a prototype. The physical and operating conditions for the system are shown in Table 1.

The bladder is made of Medical Windtex® (Windtex Vagotex S.p.A., Italy), a compliant but airtight tissue; the shell supporting the bladder is made of a flexible inextensible tissue (Aqualight 160D®, D&D SNC, Italy); the device was applied to the leg, to exert its action mainly on the gastrocnemius.

Figure 10 shows the experimental registration of the relative internal bladder pressure in comparison with the one simulated by the numerical model in the same condition. The figure reports also the contact pressure calculated by the model. The following remarks may be done:

- The inflating condition is well simulated: the model reaches the same value of the bladder pressure with quite a similar dynamic behaviour.

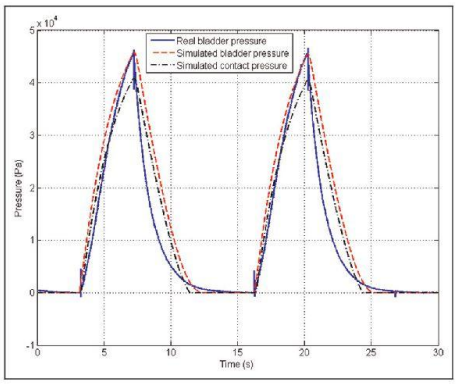

Figure 10. Comparison between the real and simulated relative bladder pressures.

- The simulation of the deflating phase shows some difference from reality: this could mainly be due to the identification of the bladder stiffness, which is considered constant in the model but should be more likely defined as increasing with the pressure.
- In general, the model is able to simulate the main dynamic behaviour of the bladder, thus providing a tool useful to foresee the dynamic evolution of the internal pressure and the contact pressure on the limb, as a function of the main physical characteristics of the device and the control conditions.

The model has then been used to simulate the sensitivity of the device to the variation of several parameters. All simulations have been made by varying one parameter at a time starting from the 'nominal condition' reported in Table 1.

Figure 11 reports the maximum values of the relative bladder pressure and the contact pressure, as a function of the initial shell-limb gap d_0, the bladder height at rest h_0, the bladder inflating time t_I and the relative air supply pressure p_S.

Moreover, the model has been used to simulate the dynamic evolution of bladder pressure and contact pressure supposing a very fast command cycle, with 1 s inflating time and 1 s deflating time. The result is reported in Figure 12 and shows a behaviour of the device similar to the *tetanus* phenomenon in skeletal muscles.

Discussion of simulation results

The mathematical model can be used as a tool to simulate the real dynamic behaviour of the IPC device and predict the effect produced on the limb, mainly the contact pressure. In this way, it is possible to choose proper values of the main physical characteristics or to

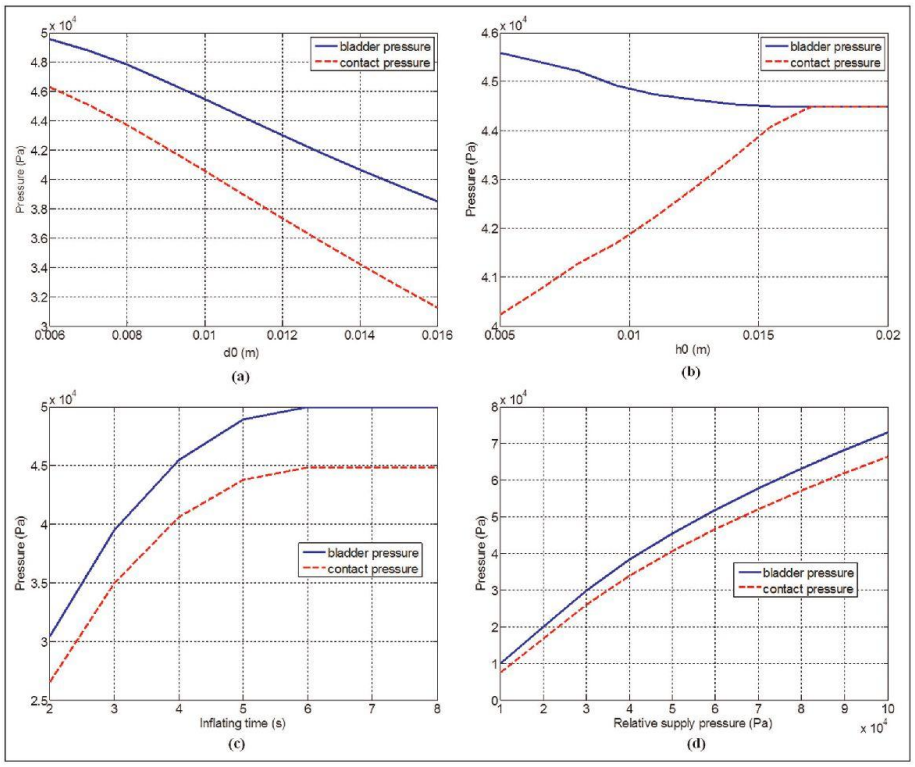

Figure 11. Maximum values of bladder pressure and contact pressure as a function of (a) initial shell-limb gap d_0, (b) bladder height at rest h_0, (c) inflating time t_1 and (d) relative air supply pressure p_S.

individuate the most appropriate control command to realize the desired effect from the therapeutic point of view.

The model is sensitive to the variation of the parameters and highlights the way these latter influence the action on the human. Thus, it is possible to obtain important indications on the values that must be respected in the design phase of the device.

For instance, Figure 11(a) shows the influence of the initial gap on the device performance, this demonstrates the importance of considering the anatomical aspects in the development of the device.

Figure 11(b) gives indications on the shape and material of the bladder: a high value of the parameter h_0, convenient for the performance, can be achieved both using a soft material and choosing a shape allowing high dilatation with no stretching of the wall.

From Figures 11(c) and 12, it is possible to get indications on the relationship between the control command and the characteristics of the pneumatic circuit, including the bladder volume, the air supply pressure and all the pneumatic components. From such

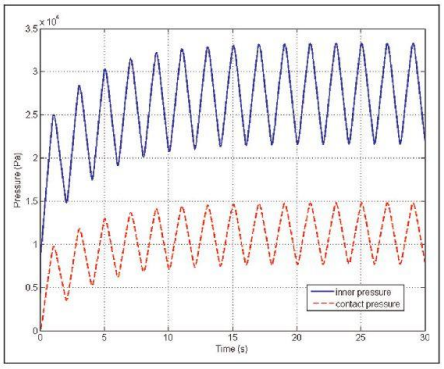

Figure 12. Bladder pressure and contact pressure for a fast command cycle.

simulations, it is possible to foresee the dynamic performance of the device and recognize the maximum operating velocity that can be reached by the device.

Figure 11(d) shows how the device performance may be influenced by the value of the air supply pressure, for a given configuration of the physical parameters and the control law.

Conclusion

The methodology described in this article is aimed at analysing and defining the characteristics and performance of a generic IPC system. The method is based on the mathematical model of the system, which has been implemented and simulated by means of a numerical code.

The validation of the model demonstrated that it can simulate with good correlation the dynamic behaviour of the IPC system, thus representing an useful tool to choose the parametric values of the device or to define its control logic. The model is able to highlight the influence of the device physical characteristics on its performance and efficiency. The effectiveness of the model is strictly and critically related to the experimental identification of such characteristics. In particular, a significant improvement would be obtained by a more accurate identification of the elements involved in the human–machine interaction, that is, the mechanical characteristics of the bladders and of the limb biological tissues.

Acknowledgements

We thank the Vagotex Company for the valuable support to the research.

Declaration of conflicting interests

The authors declare that there is no conflict of interest.

Funding

This work was partially supported by the Italian Ministry of University and Research (MIUR) through the PRIN'08 project (grant number 2008ZRLPWS).

References

1. Morris RJ. Intermittent pneumatic compression – systems and applications. *J Med Eng Technol* 2008; 32(3): 179–188.
2. Johansson K, Lie E, Ekdahl C, et al. A randomized study comparing manual lymph drainage with sequential pneumatic compression for treatment of postoperative arm lymphedema. *Lymphology* 1998; 31: 56–64.
3. Partsch H. Intermittent pneumatic compression in immobile patients. *Int Wound J* 2008; 5(3): 389–397.
4. Wiener A, Mizrahi J and Verbitsky O. Enhancement of tibialis anterior recovery by intermittent sequential pneumatic compression of the legs. *Basic Appl Myol* 2001; 11(2): 87–90.
5. Waller T, Caine M and Morris R. Intermittent pneumatic compression technology for sports recovery. In: Moritz EF and Haake S (eds) *The engineering of sport 6. Volume 3: developments for innovation*. New York: Springer, 2006, pp.391–396.
6. Comerota AJ. Intermittent pneumatic compression: physiologic and clinical basis to improve management of venous leg ulcers. *J Vasc Surg* 2011; 53(4): 1121–1129.
7. Nelson EA, Mani R, Thomas K, et al. *Intermittent pneumatic compression for treating venous leg ulcers (review). The Cochrane Collaboration*. Bognor Regis: John Wiley & Sons Ltd, 2011.
8. Flam E, Berry S, Coyle A, et al. Blood-flow augmentation of intermittent pneumatic compression systems used for the prevention of deep vein thrombosis prior to surgery. *Am J Surg* 1996; 171: 312–315.
9. Christen Y, Wutscher R, Weimer D, et al. Effects of intermittent pneumatic compression on venous haemodynamics and fibrinolytic activity. *Blood Coagul Fibrinolysis* 1997; 8: 185–190.
10. Froimson MI, Murray TG and Fazekas AF. Venous thromboembolic disease reduction with a portable pneumatic compression device. *J Arthroplasty* 2009; 24(2): 310–316.
11. Morris RJ and Woodcock JP. Evidence-based Compression: prevention of stasis and deep vein thrombosis. *Ann Surg* 2004; 239(2): 162–171.
12. Dai G, Gertler JP and Kamm RD. The effects of external compression on venous blood flow and tissue deformation in the lower leg. *J Biomech Eng* 1999; 121: 557–564.
13. Malone MD, Cisek PL, Comerota AJ Jr, et al. High-pressure, rapid inflation pneumatic compression improves venous hemodynamics in healthy volunteers and patients who are post-thrombotic. *J Vasc Surg* 1999; 29(4): 593–599.
14. Lurie F, Scott V, Yoon H-C, et al. On the mechanism of action of pneumatic compression devices: combined magnetic resonance imaging and duplex ultrasound investigation. *J Vasc Surg* 2008; 48(4): 1000–1006.
15. ISO 6358:1989. Pneumatic fluid power – components using compressible fluids – determination of flow-rate characteristics, 15 pp.

II. C. Ferraresi, **H. Hajimirzaalian** and D. Maffiodo, *"Identification of physical parameters in a robotized IPC device interacting with human"* , published in Journal of Applied Mechanics and Material, Vol 490-491, pp. 1729-1733, 2014.

URL: http://www.scientific.net/AMM.490-491.1729

Applied Mechanics and Materials Vols. 490-491 (2014) pp 1729-1733
© (2014) Trans Tech Publications, Switzerland
doi: 10.4028/www.scientific.net/AMM.490-491.1729

Identification of Physical Parameters in a Robotized IPC Device Interacting with Human

Carlo Ferraresi[1,a], Hamidreza Hajimirzaalian[1,b] and Daniela Maffiodo[1,c]

[1]Department of Mechanical and Aerospace Engineering, Technical University Politecnico di Torino
Corso Duca degli Abruzzi 24, 10129 Torino, Italy

[a]carlo.ferraresi@polito.it, [b]hamidreza.hajimirzaalian@polito.it, [c]daniela.maffiodo@polito.it

Keywords: Intermittent pneumatic compression, human-machine interaction, IPC device.

Abstract. Intermittent Pneumatic Compression devices are widely used for various therapies concerning the cardio-circulatory or lymphatic system, and also for performance recovery in sports activity. The development and setup of such devices are mainly based on empirical procedures, while few researches adopt an engineering approach based on mathematical modeling and identification. In this approach, the most critical point is the definition of parameters concerning the human-machine interaction. This paper proposes an original and simple method to identify such parameters, which allows to describe in effective way the main dynamic characteristics, fundamental for a correct design and control of the device.

Introduction

Since 1930s Intermittent Pneumatic Compression (IPC) has been widely used to exert a mechanical action on limbs, for a number of applications like improving blood circulation in lower limbs [1], preventing deep vein thrombosis [2-4], treatment of lymphedema [5], and sports recovery [6], [7].

The Fig. 1 shows the typical scheme of an IPC device, which consists on a number of inflatable bladders (a) supported by rigid or flexible shells (b, c). The device is controlled by a group of electro-pneumatic valves, which connect the bladders to an air pressure source or to the exhaust, and by a programmable logic controller (PLC), which sends an on-off command signal to the valves. The adoption of a PLC allows to choose a proper control logic of the device, to generate for example a peristaltic centripetal pressure wave aimed at increasing the venous blood return.

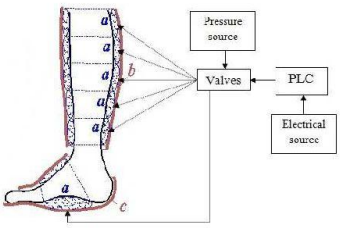

Figure 1. Typical scheme of an IPC device

Despite many works concern the use of IPC for various applications, few studies consider the mechanical and control aspect of IPC devices. However, the determination of the mechanical and physiological parameters of a biomedical device is the initial and crucial step to control its performance. In this study, mechanical characteristic and mathematical model of the IPC device are expressed to represent the dynamic behavior of the device and interaction with human. Moreover, an original method is proposed to determine the exact value of the transversal muscle stiffness and the shell-skin gap, which are very critical parameters in the mathematical model.

Mathematical Model of the IPC Device

To understand the physical behavior of the device while acting on the human, an accurate mathematical model is required, which must consider all physiological and mechanical principles. In particular, the model must consider the way all mechanical and pneumatic parts of the device interact with the limb. A general scheme of the model is described in Fig. 2.

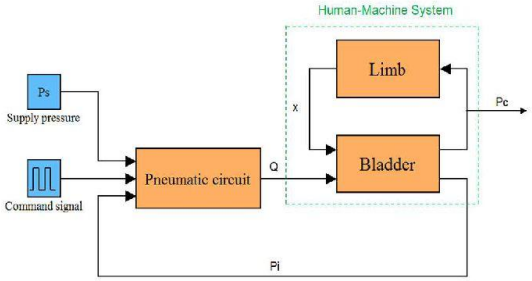

Figure 2. Block scheme of the IPC mathematical model

The model consists of two subsystems: the *Pneumatic circuit* and the *Human-Machine system*; both subsystems must be characterized and all their mechanical and physiological parameters must be identified. The PLC command signal determines connection of the bladder to the supply pressure source or to the exhaust, by means of the *Pneumatic circuit*, which is provided with a three-way valve for each bladder. The output of each valve is the air mass flow rate Q, which can be modeled in several ways; in our application we adopted the indication of the ISO 6358 Standard, which expresses the flow rate as a function of the pressure drop and the valve pneumatic conductance C. The PLC command signal determines positive or negative sign of the conductance C, thus causing inflating or deflating of the bladder and a resulting variation of the inner pressure P_i. This lattes is converted in part into the contact pressure P_c on the limb, which deforms in the radial direction as x. In all model equations, the pressures may be expressed as absolute (indicated by a capital P) or relative to the ambient (lowercase p).

To characterize the Human-machine subsystem, the scheme in 3 can be considered. The two main elements are the limb muscular tissue and the bladder, whose mechanical characteristics are the transversal muscular stiffness K_M and the bladder wall stiffness K_B. P_i is the pressure inside the bladder; P_C is the contact pressure between bladder and limb. x and y represent respectively the deformation of limb and bladder under the effect of the pressure. The actual height (or thickness) of the bladder is indicated as h, whose initial value (no pressure in bladder) is h_0; d represents the actual distance (gap) between the shell and the limb, with initial value d_0; in case of skin-bladder contact, $h=d$. The initial values h_0 and d_0 represent the "rest condition" of bladder and limb respectively, i.e. when a null pressure is acting on the system.

The internal bladder pressure P_i can be calculated by integrating the continuity equation:

$$Q = \frac{W}{RT}\frac{dP_i}{dt} + \frac{P_i A}{RT}\frac{dy}{dt} \tag{1}$$

Where R is the air constant, T is the absolute temperature, A is the bladder-limb contact area, $W = A(h_0 + y)$ is the actual volume of the bladder.

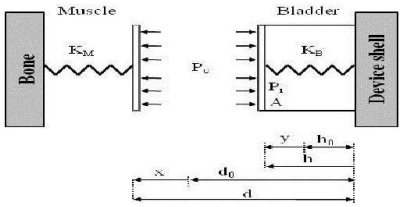

Figure 3. Scheme of the human-machine system

According to Fig. 3 and assuming constant values for muscle and bladder stiffness, the following equations express the bladder-limb interaction:

$$Pc = P_i - K_B y \tag{2}$$

$$Pc = K_M{}^x \tag{3}$$

$$y = \frac{Pc}{K_M} + (d_o - h_o) \tag{4}$$

Transversal muscle stiffness K_M and bladder stiffness K_B are two important parameters that are required to characterize the system.

To evaluate the bladder stiffness, it is possible to measure statically the variation of bladder height as a function of the internal pressure. Of course, this characteristic has to be considered only from the "rest condition" on, indicated by the h_0 value. The actual value of K_B depends on the wall material, shape and dimension of the bladder. By way of example, a rectangular bladder of *5* by *30 cm* sides, made of Windtex®, presents an average $K_B = \Delta p_i / \Delta h$ of about $5 \cdot 10^5$ *Pa/m*.

The transversal muscle stiffness K_M can be defined as ratio between the contact pressure and the radial deformation of the limb ($K_M = \Delta p_C / \Delta r$) and is the most critical parameter to be measured experimentally. Its value depends on the muscle condition: for example, there is different muscle stiffness between patients, normal persons and athletes. Moreover, on the same subject this parameter can be different in different areas of the limb. Experimental tests on three different subjects' legs provided values of muscular stiffness ranging from $3 \cdot 10^6$ to $7 \cdot 10^6$ *Pa/m*.

The mathematical model here described has been implemented in Matlab-Simulink, and simulations have been compared to experimental tests carried out on a corresponding prototype of IPC device, for validation. The Fig. 4 shows an example of such a comparison, which demonstrates good correspondence with the simulated ones in both dynamic behavior and maximum level of internal bladder pressure.

The reliability of the model allows to foresee the dynamic value of the contact pressure, which is the most important and effective variable of the device. In this way, by means of the model simulation, it will be possible to determine the most effective control protocol, in agreement with the intended application. However, this can be achieved only by an accurate identification of all physical parameters. In this regard, when an IPC device is applied to a subject during a normal therapy session, it is almost impossible to measure the actual muscle stiffness K_M and the initial limb-device gap d_0. The value of d_0 depends on how the device has been adapted and fastened to the limb. On the other hand, the value of K_M, as mentioned before, depends on the condition of the muscle and the region of the leg. In next section an original method is proposed to identify such parameters.

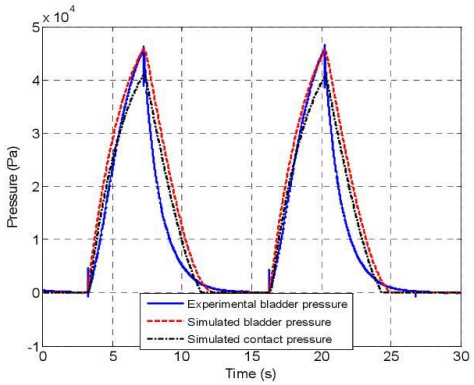

Figure 4. Comparison between the real behavior and the simulation of an IPC device.

Identification of Initial Gap d0 and Transversal Muscle Stiffness KM for the Model

The following steps can describe the proposed method in this study to estimate the values of K_M and d_0 for using in the model of the IPC device:

1. Simulation of the model for different combinations of K_M and d_0 values, to generate a table reporting the corresponding maximum value of p_i;
2. Record the experimental value of p_i by applying the device to the person for a given number of cycles;
3. Find the experimental maximum value of p_i in the table of step 1, and individuate a corresponding combination of K_M and d_0 for the model.

This procedure should be repeated for each bladder of the device and requires a pressure transducer to be placed in each bladder.

TABLE I. The Maximum Inner Bladder Pressure (Pascal) For Given Combinations of D_0 and K_M

K_M (Pa/m) / d_0 (m)	$3.0 \cdot 10^6$	$3.5 \cdot 10^6$	$4.0 \cdot 10^6$	$4.5 \cdot 10^6$	$5.0 \cdot 10^6$	$5.5 \cdot 10^6$	$6.0 \cdot 10^6$	$6.5 \cdot 10^6$	$7.0 \cdot 10^6$	$7.5 \cdot 10^6$	$8.0 \cdot 10^6$
0.005	46011	47133	47998	48658	49153	49511	49757	49909	49985	50000	50000
0.006	45009	46124	47012	47720	48285	48734	49087	49364	49575	49732	49849
0.007	43939	45029	45914	46641	47241	47738	48152	48498	48787	49028	49229
0.008	42982	44024	44879	45591	46189	46693	47125	47494	47812	48087	48326
0.009	41985	42971	43787	44471	45050	45546	45974	46346	46672	46958	47212
0.010	41008	41933	42701	43347	43898	44372	44785	45146	45464	45747	45999

The Table I reports the maximum values of bladder pressure p_i calculated by the model for given combinations of K_M and d_0. The Fig. 5 shows the experimental recording of the air pressure in the corresponding bladder; the maximum pressure value is around 45300 Pa. It is then possible to find in Table 1 a cell indicating a similar value: all cells grouped in the green field could be selected.

How to choose the right combination could be entrusted to the therapist's experience: for example, if the bladder is acting on a thick muscle zone (e.g. on the gastrocnemious), a lower value of K_M should be selected; on the contrary, zones near the ankle have higher K_M. The selection could consider also the type of person: obviously the muscle stiffness will be different for patients, normal people or athletes. Once K_M has been chosen, the right value of d_0 is the one corresponding to the selected cell in the table. For the example analyzed here, values of $K_M=7*10^6$ Pa/m and $d_0=0.01$ m represent a solution providing optimum correspondence between simulation and reality.

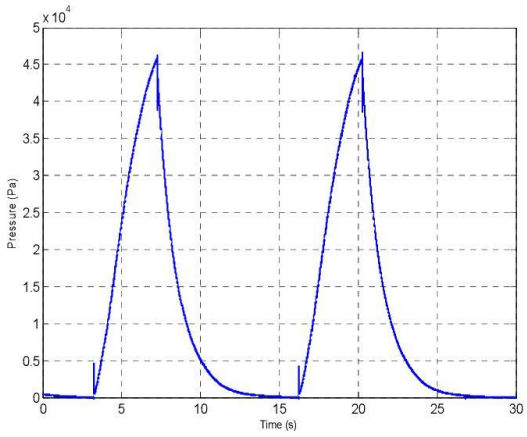

Figure 5. The experimental record of the bladder inner pressure p_i

Conclusion

In this study, a mechanical and physiological characterization of an IPC device is presented and the device is modeled mathematically. The model is validated by experimental records, and the results show the model is so accurate and can predict the dynamic behavior of the device and the maximum level of pressure. Moreover, the values of the important parameters, transversal muscle stiffness and sell-skin gap, depending on specific characteristics of the tested subject and on the way the device has been applied to the limb, are obtained and optimized with a method based on an initial setup procedure of the device. This allows a complete identification of the general dynamic characteristic of the system, which is fundamental for an effective use of the device.

References

[1] Y. Christen, R. Wutscher, D. Weimer, P. de Moerloose, E. K. O. Kruithof and H. Bounameaux: Effects of Intermittent Pneumatic Compression on Venous Hemodynamics and Fibrinolytic Activity. Blood coagulation and fibrinolysis, vol. 8, (1997), pp. 185-190.

[2] E. Flam, S. Berry, A. Coyle, H. Dardik and L. Raab: Blood-flow augmentation of intermittent pneumatic compression systems used for the prevention of deep vein thrombosis prior to surgery. The American journal of surgery, vol. 171, (1996), pp. 312-315.

[3] G. Westrich, S. Haas, P. Mosca and M. Peterson: Meta-analysis of thromboembolic prophylaxis after total knee arthroplasty. Journal of Bone and Joint Surgery, British, 82, (2000), pp. 795-800.

[4] M. Froimson, T. Murray and A. Fazekas: Venous Thromboemolic Disease Reduction with a Portable Pneumatic Compression Device, The journal of Arthroplasty, vol. 24, n. 2, (2009), pp. 310-316.

[5] K. Johansson, E. Lie, C. Ekdahl and J. Lindfelt: A Randomized Study Comparing Manual Lymph Drainage with Sequential Pneumatic Compression for Treatment of Postoperative Arm Lymphedema, Journal of Lymphology, 31, (1998), pp. 56-64.

[6] T. Waller, M. Caine and R. Morris: Intermittent Pneumatic Compression Technology for Sports Recovery, The Engineering of Sport 6 Volumes 3: Developments for Innovation, (2006), Springer. ISBN: 978-0-387-34680-9 (Print) 978-0-387-45951-6 (Online).

[7] A. Wiener, J. Mizrahi and O. Verbitsky: Enhancement of Tibialis Anterior Recovery by Intermittent Sequential Pneumatic Compression of the Legs, Basic Appl Myol, vol .11, n.2 (2001), pp. 87-90.

III. C. Ferraresi, **H. Hajimirzaalian**, D. Maffiodo, **"***Control strategies of an intermittent pneumatic compression device for cardio-circulatory rehabilitation***",** accepted in Robotica, January 2014.

Control strategies of an intermittent pneumatic compression device for cardio-circulatory rehabilitation

Carlo Ferraresi, Hamidreza Hajimirzaalian, Daniela Maffiodo
Department of Mechanical and Aerospace Engineering
Politecnico di Torino, Italy

Abstract

In immobilized people, like paraplegic subjects, due to absence of leg muscle contraction, venous return to the heart is reduced and this may induce important diseases like a reduction of cardiac output. The application to legs of a mechanical stimulation operated by an Intermittent Pneumatic Compression (IPC) device, in replacing striate muscle pump on limb veins, may recover in these patients venous return to the heart, thus restoring correct cardio-circulatory performance. This paper deals with the study of the effective way to control such a device. First a mathematical model of the whole human-machine system is realized and validated; then several control logics, based on the PID control of electro-pneumatic proportional components, are investigated; finally, an effective solution is defined to control a multi-bladder IPC device with adequate performance to the objective.

Keywords: cardio-circulatory rehabilitation, intermittent pneumatic compression, IPC mechatronic device, multi-bladder pneumatic device, PID control, Man-Machine Systems.

1. Introduction

Nowadays, the great majority of rehabilitation robotized devices is addressed to mobility [1, 2] however, a robotized rehabilitation can be adopted also to deal with diseases affecting other physiological compartments, like the cardio-circulatory system (CCS).

Actually, during any physical activity, the intermittent contraction of the limb muscles exerts important pumping action on physiological systems such as the muscular, cardiovascular or lymphatic system.

In immobilized people, e.g. paraplegic subjects, due to absence of leg muscle contraction, venous return to the heart is reduced and this may induce a reduction of cardiac output

(CO). As a matter of fact, according to the well-known Starling's law, "the output of the heart is equal to and determined by the amount of blood flowing into the heart, and may be increased or diminished within very wide limits according to the inflow". In other words, the cardiac output is directly influenced by the venous return, which is determined primarily by the mechanical properties of the systemic circulation.

Therefore it is reasonable to suppose that the application to legs of a mechanical stimulation operated by actuators, in replacing striate muscle pump on limbs veins, may recover in these patients venous return to the heart, thus restoring sufficient performance of the cardiovascular system.

Since 1930s, it was evaluated that intermittent pneumatic compression (IPC) has a positive effect on lower extremity blood flow of calf and foot [3, 4]. Starting from a first commercial device designed during the sixties, many IPC devices were developed to accommodate different medical applications: to prevent deep vein thrombosis [5, 6], for the treatment of critical limb ischemia [7-9], to compensate congestive heart failure [10] and it was recommended for lymphedema treatment [11] and sport recovery [12, 13]. Studies have shown that IPC application on legs changes central venous pressure, pulmonary artery pressure, and pulse pressure [14] and IPC application on foot increases popliteal artery blood flow [15]. Moreover various researches have suggested that this mechanical method effectively reduces the incidence of the diseases without any side effects, increasing volume flow and velocities in deep veins [8, 9, 16].

Various researchers [17, 18, 19] compared different commercial IPC devices and observed positive results, although devices were different and worked with different pressure values, cycle times and other parameters, thus indicating a poor knowledge of the relationship between the characteristics and settings of the device and the effects on the human

Although it is possible to find in the literature the need for a more quantitative study of these devices, for example trying to model the deformation of the limb [20], the need to understand the dynamic behavior of the device, relating the supply pressure with the real operation pressure on the limb as a function of the device characteristic and the dynamic control of the actual limb/device contact pressure, seems to be barely considered. Few researchers tried somehow to consider the effect of pressure level and inflation/deflation time [21]. Others [16], while comparing the behavior of two different commercial devices, conclude that not only the different levels of the air supply pressure have to be considered, but also the different behavior depends on the different patterns of pressure, garnments,

materials and design of the device. They also state that "further investigation of biomechanical mechanisms of IPC is needed to guide the development of better engineering solutions …".

Therefore, despite many researchers investigated on IPC effects, the lack of a general methodology to study and develop an IPC device with physical and dynamical characteristics suitable for the intended application is evident. In particular, the dynamic behavior of the device in response of the control command is practically ignored.

The subject of this paper is the study of an effective control strategy for the realization of an IPC device able to act at the level of the cardio-circulatory system, in order to recover normal performance in impaired people. An IPC device is mainly composed by pneumatic elements: compressed air source, valves, pipes and bladders. A first step towards quantitative understanding of its dynamic behavior is modeling and identification of this pneumatic part of the device, which has a preponderant influence on system dynamics. Also, the interaction between device and limb is an essential part to determine the actual contact pressure, and must be modeled.

The article starts with the description of an existing IPC prototype previously realized [22], then a simplified mathematical model of the system, considering limb/device interaction, is presented; based on the model, the definition and optimal tuning of a PID controller, considering only one bladder but for different system configurations, is proposed; finally the control of a multi-bladder system is discussed.

2. The IPC device

The present study is focused on a prototype device previously realized in our laboratory.

Figure 1 shows the prototype and its basic functional scheme. It includes inflatable bladders (*a*) supported by shells (*b, c*), a pneumatic circuit with on/off electro-pneumatic valves (*d*) and a programmable logic controller (*e*) which imposes a defined command sequence to the valves, according to a predetermined protocol.

The operating of the device is simple: by inflating the bladders with the compressed air, the pressure can be applied to the limb surface. The programmable logic controller (PLC) controls the valves with a defined time sequence, so as to arrange the sequential acting to the bladders and to generate a peristaltic and centripetal pressure wave on the limb. The design and realization of the prototype required several factors to be considered, aimed at achieving better performance. The main design criteria are described below.

Bladders are key elements of the system: in order to optimize the performance, the pneumatic energy should be directed as much as possible towards the limb soft tissues, rather than used to deform the materials of the device structure. To this aim, bladders should be free to expand with limited or null stretching of their wall, and this can be achieved both by proper shaping of the cells and adopting a material which is compliant but, of course, airtight. The number and dimension of bladders must allow to generate a pressure wave on the limb and at the same time to guarantee high response speed: it was assumed that one bladder acting on the foot sole and five acting on the calf were a good compromise. To realize the bladders, a special airtight and compliant tissue was selected: the Medical Windtex® (Windtex Vagotex S.p.A., Italy).

Also the shells are fundamental elements of the device: a key aspect is choice of rigid or flexible structure. After evaluating a first prototype with rigid shells, with the drawback of variable and large gap between device and limb, the shells were conceived as a sort of sleeves, flexible but inextensible, so self-adapting to the shape and size of the limb but also avoiding stretching and therefore directing all pneumatic energy to the limb. To realize the shells, a special inextensible and airtight trilaminate tissue (Aqualight 160D®, D&D SNC, Italy) was selected.

Also the pneumatic circuit was designed in order to favor high response speed: the six on/off electro-valves were placed onboard of the prototype, to shorten as much as possible the tubes for bladder supply, the choice of valves Festo type MHP1-M1H-3/2-M3 provided a good compromise between lightness and flow rate. The circuit is controlled by a Siemens Logo! PLC, which imposes a defined opening/closing sequence to the valves.

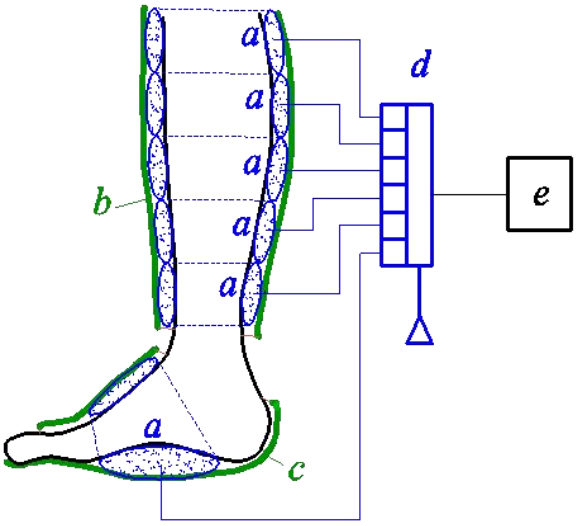

Figure 1. Prototype of IPC device and its basic functional scheme: inflatable bladders (a), shell (b, c), electro-pneumatic valves (d), programmable logic controller (e)

The main shortcoming of this system is the lack of direct control of the action actually produced on the limb. The dynamic evolution of the pressure in the bladders is due not only to the time sequence imposed by the PLC, but also to the characteristic of the pneumatic circuit, to physiological parameters of the subject and to the way the device is coupled with the limb.

The work described in this article was devoted to the search of a more effective control technique, based on a Proportional-Integral-Derivative (PID) feedback controller and the use of electro-pneumatic proportional components for regulation of the pneumatic power.

3. Mathematical model of the IPC device

To understand the physical behavior of the device while acting on the human, an overall mathematical model is required, which must consider all physiological and mechanical principles, including all properties of the pneumatic circuit. The conceptual block diagram of the model can be described as in figure 2.

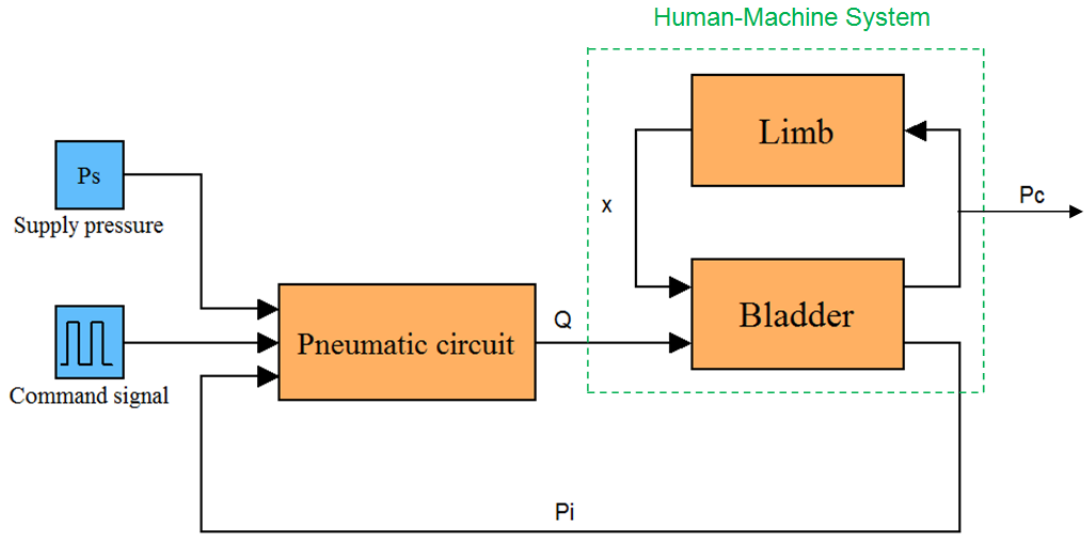

Figure 2. Conceptual block diagram of the model

The model is considered for a single module with one bladder supplied by one electro-pneumatic digital valve. In the model, the supply pressure and the command signal of a PLC apply to the pneumatic circuit which is provided with a three-way valve for each bladder. The output of each valve is the air mass flow rate Q that can inflate (positive Q) or deflate (negative Q) any single bladder. By inflating the bladder, the inner pressure P_i increases and exerts the contact pressure P_c on the limb. Therefore, the limb deforms in the radial direction as x. The interaction between bladder and limb is named as human-machine system. To model the system, it is required to characterize both subsystems

(pneumatic circuit and human-machine) and determine all mechanical and physiological parameters. As concerns notation, an uppercase *P* indicates absolute pressure, a lowercase *p* indicates relative to ambient pressure.
To express the air mass flow rate through the valve, from upstream section (pressure P_1) to downstream (P_2) the following formula, according to the ISO 6358 standard [23], can be adopted:

$$Q = \rho \cdot C \cdot P_1 \cdot K_T \sqrt{1 - \left(\frac{r-b}{1-b}\right)^2} \quad \text{for subsonic flow} \qquad (1)$$

$$Q = \rho \cdot C \cdot P_1 \cdot K_T \quad \text{for sonic flow}$$

Where: ρ is the air density, C is the valve conductance, K_T is a corrective factor depending on the inlet air temperature; $r=P_2/P_1$ is the actual pressure ratio; b is the critical pressure ratio at which the flow switches from subsonic to sonic condition. The conductance C can be considered positive or negative, thus determining inflating or deflating effect on the bladder.
To characterize the human-machine subsystem, the scheme in figure 3 can be considered.

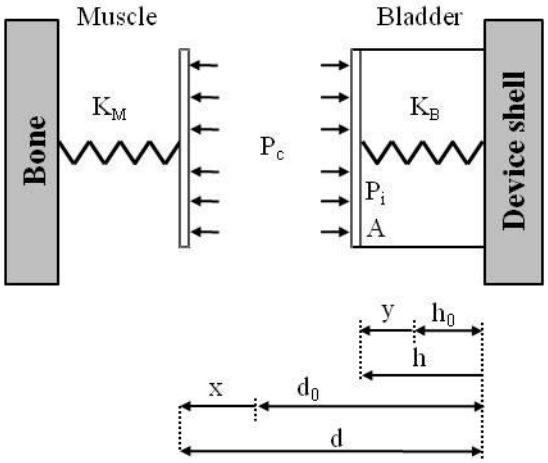

Figure 3. Scheme of the human-machine system

Where the main mechanical characteristics are the transversal stiffness K_M of the soft tissues and the bladder wall stiffness K_B. P_i is the pressure inside of the bladder; P_C is the contact pressure between bladder and limb. x and y represent respectively the deformation of limb and bladder under the effect of the pressure. The actual height of the bladder is indicated as h, whose initial value (no pressure in bladder) is h_0; d represents the actual distance (gap) between the shell and the limb, with initial value d_0; in case of skin-bladder contact, it will be $h=d$. The initial values h_0 and d_0 represent the "rest condition" of bladder and limb respectively, i.e. when a null pressure is acting on the system.
The internal bladder pressure P_i , assuming isothermal condition, can be calculated by integrating the continuity equation:

$$Q = \frac{W}{RT}\frac{dP_i}{dt} + \frac{P_i A}{RT}\frac{dy}{dt} \tag{2}$$

Where R is the air constant, T is the absolute temperature, A is the bladder-limb contact area, $W = A(h_0 + y)$ is the actual volume of the bladder.
According to figure 3, the following equations express the bladder-limb interaction:

$$p_C = p_i - K_B y \tag{3}$$

$$p_C = K_M x \tag{4}$$

$$y = \frac{p_C}{K_M} + (d_0 - h_0) \tag{5}$$

Transversal stiffness K_M of soft tissues and bladder stiffness K_B are two important parameters that are required to characterize the system. In general, K_M should be considered as depending on limb deformation x and K_B as depending on bladder deformation y.
To evaluate the bladder stiffness, it is possible to measure statically the variation of bladder height as a function of the internal pressure. Of course, this characteristic has to be considered only from the "rest condition" on, indicated by the h_0 value. As an example, figure 4 shows the result of the linearized characteristic of a tested bladder.

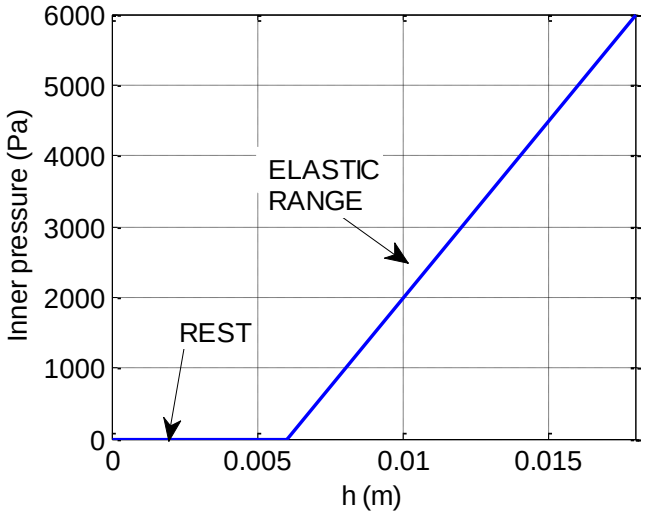

Figure 4. Example of stiffness characteristic of a bladder

The actual value of K_B depends on the wall material, shape and dimension of the bladder. By way of example, a rectangular bladder of *5 by 30 cm* sides, made of Windtex®, presents an average $K_B = \Delta p_i / \Delta h$ of about $5 \cdot 10^5$ *Pa/m*, with a rest thickness of *6 mm*.
According to the characteristic of figure 4, the equation (3) can be split to consider the full range of the bladder expansion:

$$\begin{aligned} p_C &= p_i && for\ h \le h_0 \\ p_C &= p_i - K_B(h - h_0) && for\ h > h_0 \end{aligned} \tag{6}$$

The soft tissue stiffness K_M is the most critical parameter to be measured experimentally. Its value depends on the muscle condition: for example, there is different muscle stiffness between patients, normal persons and athletes. Moreover, on the same subject this parameter can be different in different areas of the limb. In addition, there is no information in literature and very few researchers like Dai et al. [20] tried to experimentally measure this characteristic. A possible way is to deform the limb by means of a band wrapped around it and correlate the reduction of the circumferential contact line with the tension applied to the band: it will be simple to derive the ratio between the pressure exerted on the limb and the radial deformation, which expresses the muscle stiffness $K_M = \Delta p_C / \Delta r$. Adopting this methodology, the test was performed on three healthy subjects (two females and one male), placing the test band on the belly of gastrocnemius muscle, asking the subjects to keep the muscle as relaxed as possible. For each subject the test was repeated three times, applying a contact pressure up to *45 kPa*. The results showed in general a slightly "hardening" trend, but with considerable data dispersion. Therefore we decided to assume constant mean values as representative of the stiffness. The three average measured values were respectively of *2.9 MPa/m*, *5.2 MPa/m* and 7.1 *MPa/m*.

Such a static identification does not take into account other effects like the typical damping of soft tissues, which would have been much more difficult to estimate. Future work is planned for more accurate identification of soft tissue characteristic, however considerable damping effect of the pneumatic system (circuit plus bladder) is taken into account in the mathematical model equations.

The mathematical model here described has been implemented in Matlab-Simulink®, and simulations have been compared to experimental tests carried out on a corresponding prototype of IPC device, for validation. The prototype was applied to the leg of a healthy male subject and the internal pressure of the bladder located on the gastrocnemius belly was acquired.

The physical and operating conditions for the system are reported in table 1.

Figure 5 shows the result of the comparison. It emerges a good correspondence as regards the maximum value of the internal pressure and also the time occurring to reach it; while there is a certain difference in the dynamic behavior of the discharging phase. In the complex, the model shows a sufficient ability to represent the prototype dynamics.

The model is also able to calculate the contact pressure p_C, which is traced in figure 5 as well. The difference between bladder and contact pressure can be evaluated by means of the bladder stiffness considered in the model equations.

Table 1. Experimental and simulated conditions.

Parameter	***Symbol***	***Value***	***Unit***

Relative supply pressure	p_S	$5 \cdot 10^4$	Pa
Absolute ambient pressure	P_A	$1 \cdot 10^5$	Pa
Contact area of the bladder	A	0.015	m^2
Pneumatic conductance	C	$3 \cdot 10^{-10}$	$m^3/(s \cdot Pa)$
Critical pressure ratio	b	0.02 (inflating) 0.2 (deflating)	
Temperature	T	293	K
Temperature coefficient	K_T	1	
Bladder height at rest	h_0	0.006	M
Initial shell-limb gap	d_0	0.01	M
Bladder stiffness	K_B	$5 \cdot 10^5$	Pa/m
Soft tissue stiffness	K_M	$7 \cdot 10^6$	Pa/m
Inflating time	t_1	4	S
Total cycle time	t_C	13	S

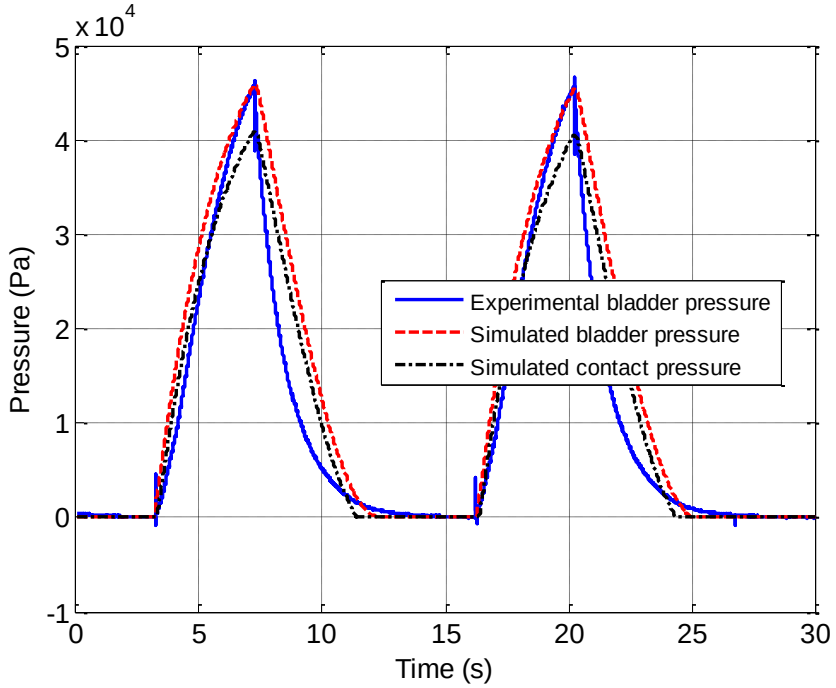

Figure 5. Comparison between experimental and simulated relative bladder pressures. Contact pressure between bladder and limb is also calculated and traced.

4. PID control of the device

As concerns control of the IPC device, it must be considered that the final goal is not a precise tracking of the bladder pressure or the contact pressure, but the control of effects produced by the device on the cardio-circulatory system (CCS) performance. Such performance can be described by certain heart functional parameters like Heart Rate (HR), Stroke Volume (SV), Cardiac Output (CO), Ejection Fraction (EF), which can be monitored in real time during the device operation, or evaluated off-line after a training period.

Currently poor knowledge exists on a direct correlation between a pressing action on the leg and corresponding effect on the CCS, therefore it is impossible to define an “optimal” reference function as regards the pattern of the applied pressure.

IPC devices currently used for several applications are usually developed and employed on the base of empirical methods. The application protocol is almost always defined by the value of supply pressure to the on/off valves and their activation/deactivation times, but no knowledge exists about the actual pressure exerted in real time on the limb by the bladders. The major weakness is that the dynamics of the pneumatic section is not taken into account.

At this stage of the research the goal was to realize a prototype allowing to perform sufficiently significant clinical tests, deferring to a later stage further improvement actions, which will include of course control algorithms for bladder pressure tracking.

For these reasons the main requirement for device control was not absolute dynamic accuracy, but simplicity and low cost of implementation, while ensuring sufficient performance in response time and ability to maintain an actual value of the desired pressure for a given time.

In this context, a PID controller has been considered adequate, due to its simplicity from both the design and the parameter-tuning point of view [24]. Also implementation in the device is little demanding as concerns pneumatic hardware and instrumentation.

To tune the PID controller, the mix method of Ziegler-Nichols [25] and manual tuning has been used. Since the whole system is represented by a highly non-linear and stiff mathematical model, the first step, consisting on the determination of PID coefficients (K_P, K_I, K_D) by means of Ziegler-Nichols methods, was not sufficient to produce satisfactory results. Thus the first attempt values were changed by further manual fine-tuning, for an optimal result.

4.1 Application of PID controller to the model

The scheme of the system in presence of the PID controller can be described as shown in figure 6:

In the IPC device, the contact pressure p_c is considered as output controlled value, while for the regulated value, there are two distinct possibilities. Supply pressure p_S and mass flow rate Q are two different quantities that can be regulated by PID controller to track the reference p_C. In the following, both methods to control p_C based on regulating p_S and Q are described.

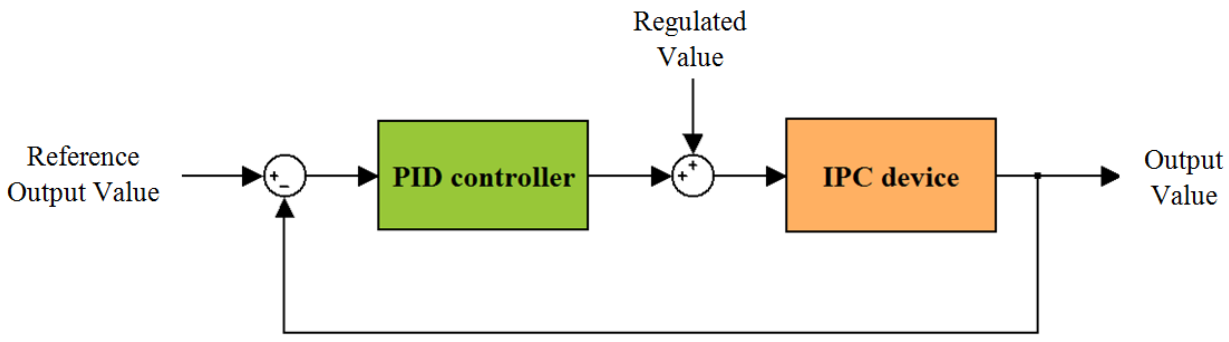

Figure 6. Scheme of the system with PID controller

4.1.1 System control based on regulating p_S

In the simulation and experimental validation shown in figure 5, the supply pressure to the system was kept constant and equal to $5 \cdot 10^4$ *Pa* relative. The value of the internal bladder pressure and the contact pressure was then determined by the natural dynamic characteristic of the pneumatic circuit and by the inflating/deflating times commanded by the PLC. If a feedback was available (e.g. the contact pressure or the inner bladder pressure), the supply pressure to the system could be regulated by a PID closed loop controller for optimal tracking of the desired value. This can be done by proper integration of an electro-pneumatic pressure proportional valve (PPV) into the system. Such component will transform the electrical input signal sent by the controller into the supply pressure to the IPC device.

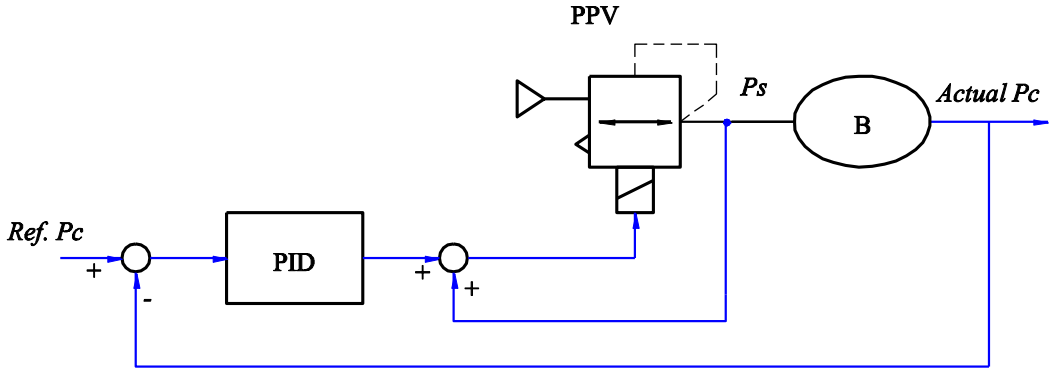

Figure 7. Block scheme of the system with supply pressure (*Ps*) controlled by pressure proportional valve (PPV); contact pressure (*Pc*) is the outlet from bladder (B)

Figure 7 shows the block scheme of the single-bladder system with supply pressure controlled by pressure proportional valve (PPV).

To design the PID control, the mathematical model of the PPV has been integrated in the model. The parameters of the device were maintained as reported in table 1. The model of the PPV can be represented by the block diagram shown in figure 8 [26], where *Kv* is the flow coefficient, *Tv* is the time constant and *Cv* is the interior capacity of the proportional valve. P_{in} and P_{out} are the input and the output pressure of the proportional valve respectively. For a commercial proportional valve type Festo MPPE-3-1/4, which has been considered in simulations, the parameter values are $Kv=5 \cdot 10^{-7}$ $m^3/Pa/s$, $Tv=0.01$ *s* and $Cv=1.43 \cdot 10^{-8}$ m^3/Pa.

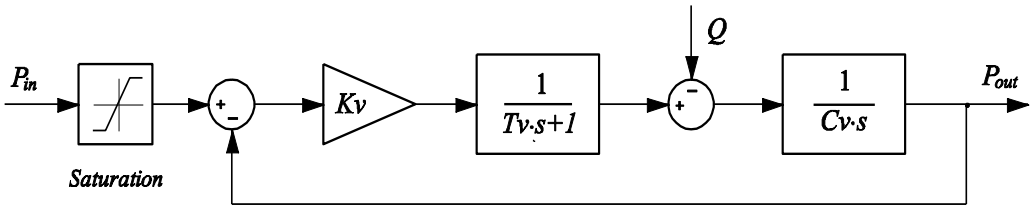

Figure 8. Block diagram of a pressure proportional valve

With a reference contact pressure of $3.5 \cdot 10^4$ *Pa* relative to the ambient in inflating and zero in the deflating state, the best tuning was found with the coefficients: $K_P = 0.03$, $K_I = 0$, $K_D = 0.0044$, i.e. in this case the best solution corresponds to a PD controller.

The solution was both simulated and experimentally tested. The PID control was implemented on the system by means of a NI PCI 6036E board and the above cited Festo proportional valve. A single bladder was placed in a test bench reproducing all conditions of table 1, including soft tissue stiffness K_M. Figure 9 reports the reference pressure, the simulated contact pressure and the bladder actual internal pressure.

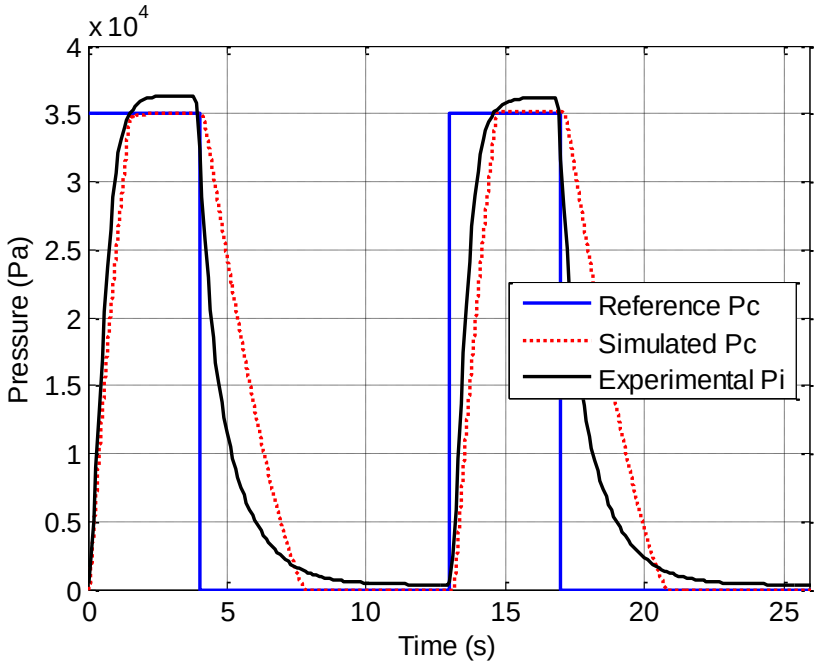

Figure 9. Reference and simulated contact pressure with PD control of the bladder supply, compared with the experimental internal bladder pressure

Result of figure 9 shows the effectiveness of the control: both the simulated contact pressure and the actual air pressure inside the bladder reach the desired value in less than 2 seconds and they are maintained until the end of the inflating phase. It is interesting to

note that the controller regulates the bladder air pressure at a slightly greater value than the desired contact pressure, taking into account the bladder stiffness.

To obtain this result, the controller must command in a proper way the proportional valve: this is testified by figure 10, which shows the variation of the absolute supply pressure P_S, operated by the pressure proportional valve. At the beginning of the inflating phase, the supply pressure reaches the saturation level (2 bar absolute), so speeding up as much as possible the rising of the bladder and contact pressures.

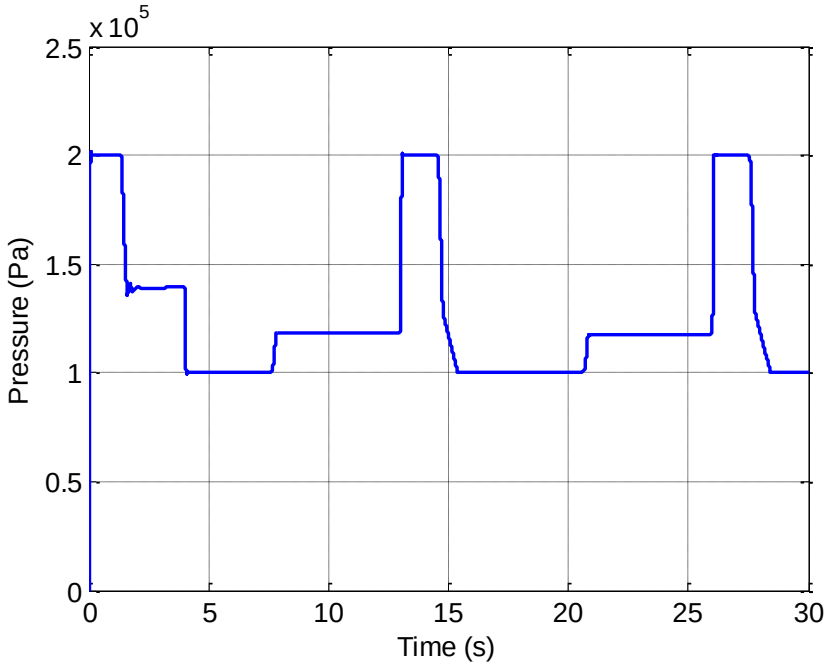

Figure 10. Supply pressure controlled by the proportional valve

The saturation level of the supply pressure, which can be set by the controller, determines the response speed of the system, in particular the rising time of the bladder pressure. Defining the rising time as the time required for actual bladder pressure to rise from 10% to 90% of the reference value, figure 11 shows the variation of the rising time versus the saturation level of the supply pressure, as calculated by the mathematical model. Therefore the curve of figure 11 can be used to choose the most convenient value for the saturation level of the pressure proportional valve.

A further sensitivity analysis was performed to investigate the influence on system performance of the soft tissue stiffness K_M, which was recognized as a very critical parameter to be identified. Like in the previous case, the rising time of bladder pressure in inflating phase was considered to represent the IPC dynamic performance.

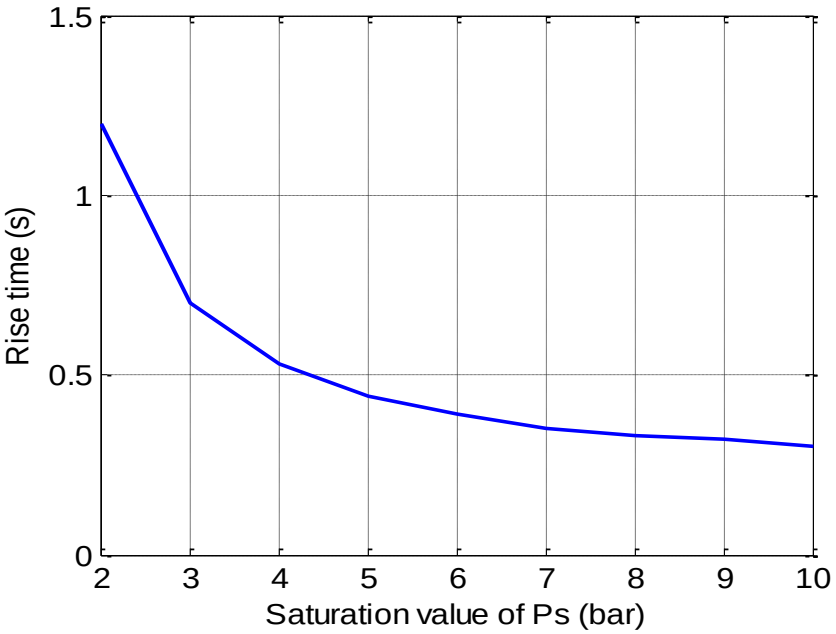

Figure 11. Rising time versus saturation value of P_s

Figure 12 shows the result of the analysis: for K_M varying from 7 to 3 MPa/m, the rising time increases of about 38%. This is certainly a noteworthy indication, that suggests the search for more effective control solutions in the continuation of research.

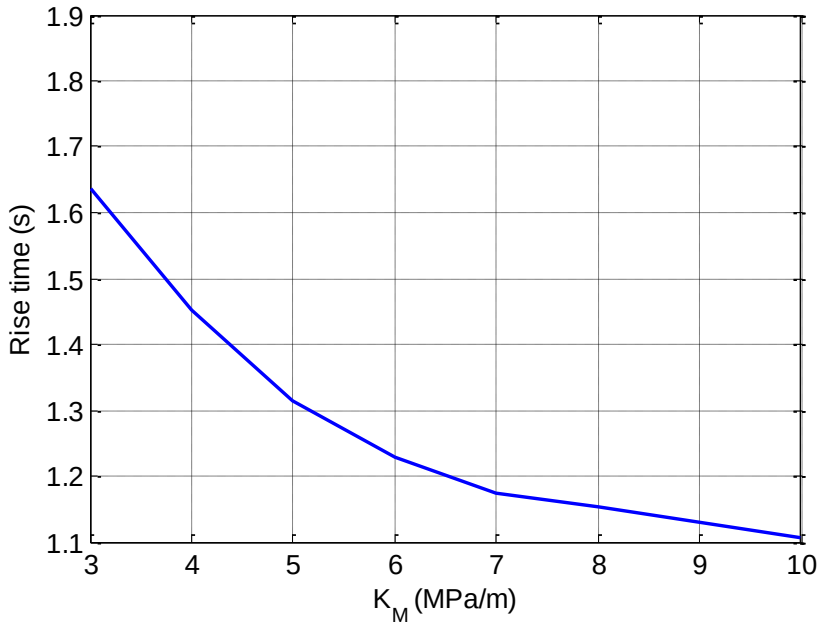

Figure 12. Rising time versus soft tissue stiffness K_M

4.1.2 Control of the system based on regulating Q

The air pressure inside the bladder can be controlled directly by regulating the air flow rate. In this case, the supply to the bladder must be controlled by an electro-pneumatic flow-proportional valve (FPV), commanded by the PID control. In fact, referring to equation (2), the mass flow rate *Q* entering the bladder is directly related to the derivative of the pressure; therefore, to control the pressure it will be necessary to act on the valve conductance *C*, as defined in equation (1).

Figure 13 shows the scheme of such a system. In particular, FPV is a 3-way flow proportional valve, whose conductance *C* can be regulated in analogical way by the controller.

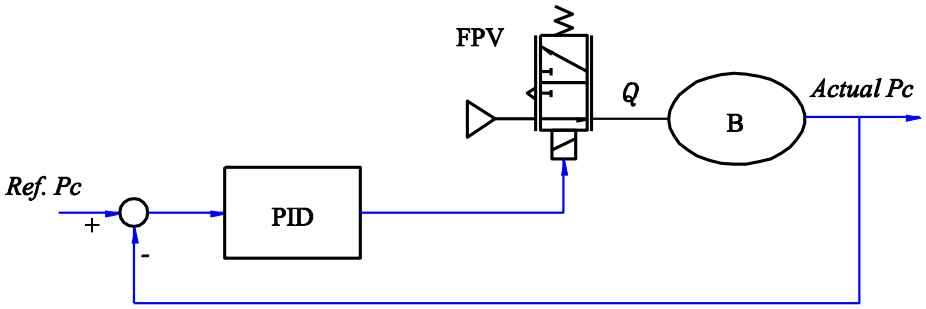

Figure 13. Scheme of the single-bladder system with PID controller and flow proportional valve (FPV)

Figure 14 shows a block scheme of an electro-pneumatic flow-proportional valve [27], where *K* is the electro-pneumatic gain and *Tv* is the time constant of the valve. Referring to a commercial proportional valve type Martonair SPGB 18913, the characteristic values are: $K=1\cdot10^{-9}\ m^3/Pa/s/A$ *and* $Tv=0.1\ s$.

Applying to the system the mixed Ziegler-Nichols plus manual tuning method previously described, the PID coefficients have been calculated. The optimal result has been obtained with $K_P=0.005$, $K_I=0$ and $K_D=0.001$. Also in this case the best configuration corresponds to a Proportional-Derivative PD controller.

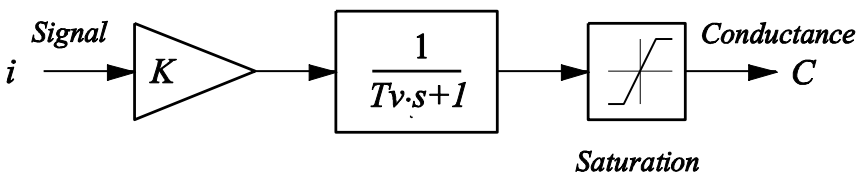

Figure 14. Block diagram of a flow proportional valve

The mathematical model including the optimized PID controller and the flow-proportional valve has then been simulated. Figure 15 reports the result of the simulation, showing a comparison between the actual and reference contact pressure.The result is very similar to the one produced by the control with regulation of the supply pressure: this confirms that also the solution with flow regulation is theoretically able to control the device in an effective manner.

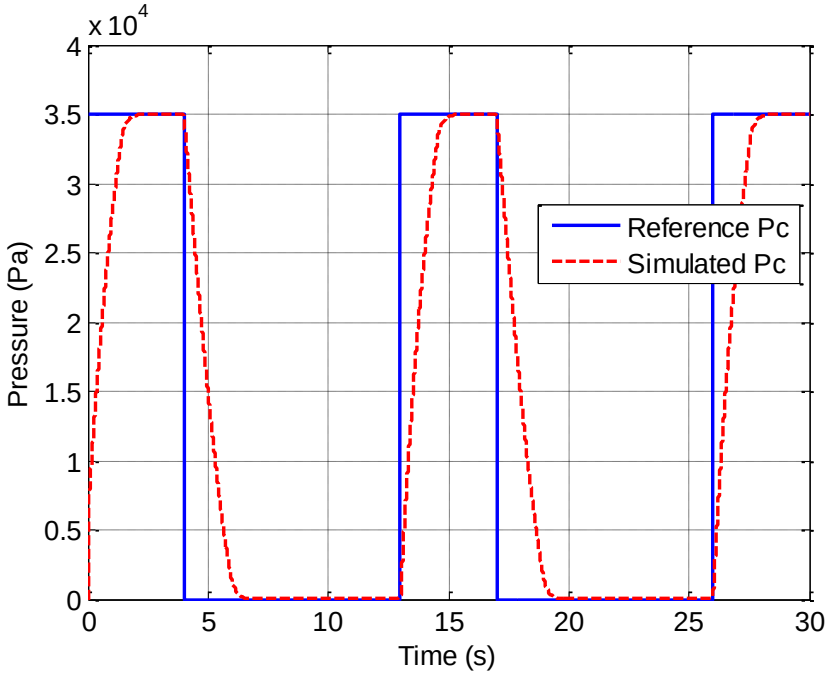

Figure 15. Reference and actual contact pressure of the bladder with PID control and the flow rate regulated by a proportional valve

Figure 16 shows the variation of the valve conductance, under the regulation of the PID controller. A positive value corresponds to inflating condition, and vice-versa.

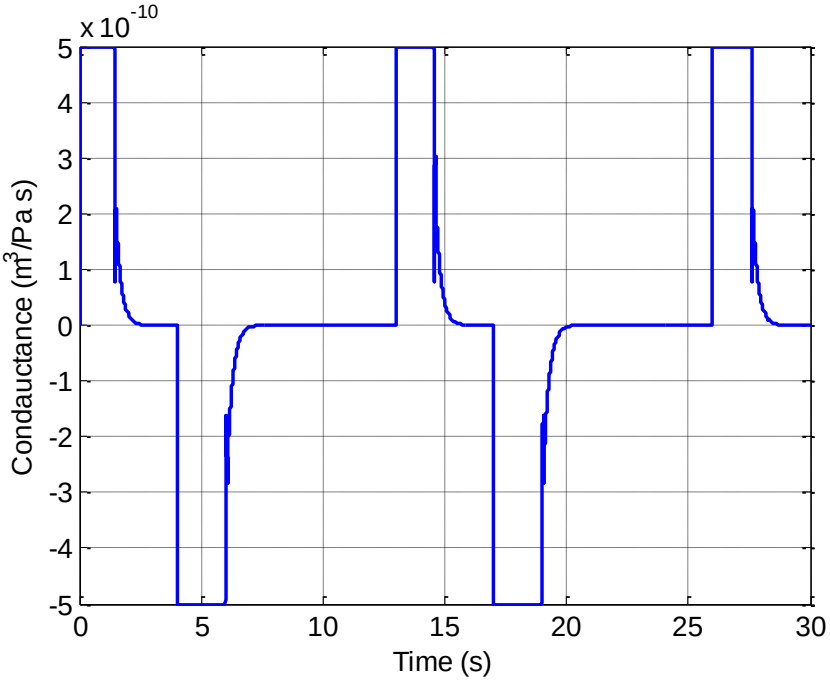

Figure 16. Valve conductance variation versus time.

4.1.3 Parallel control of 3 bladders by one pressure proportional valve

In section 4.1.1 the way to control a single bladder with one pressure proportional valve and a PID controller was described. Actually, an IPC device includes a given number of bladders, which must be controlled in a coordinated way, in order to generate a definite pressure pattern on the limb surface. It is supposed that the device should generate a peristaltic and centripetal pressure wave, i.e. proceeding from distal to proximal position, in order to facilitate the venous blood return to the heart. To this aim, the activation sequence of the bladders must follow the same logic. Thus a definite reference pressure must be tracked in any bladder. In addition, for cost and complexity reasons, it would not be permissible to have a proportional valve for each bladder. Therefore, a system of three bladders controlled by one PID controller and one pressure proportional valve has been studied and simulated.

For such a multi-bladder system the controller, acting as a PLC, must switch among the bladders, commanding the proper on-off control valve, selecting the proper contact pressure feedback and sending the proper pressure reference to the PID controller. A possible scheme of the system is presented in figure 17, where, posing n=1,2,3, *Bn* are the bladders, *Vn* are the corresponding on-off control valves, *Pn* are the bladder-limb actual contact pressures, *PPV* is the pressure-proportional electro-valve.

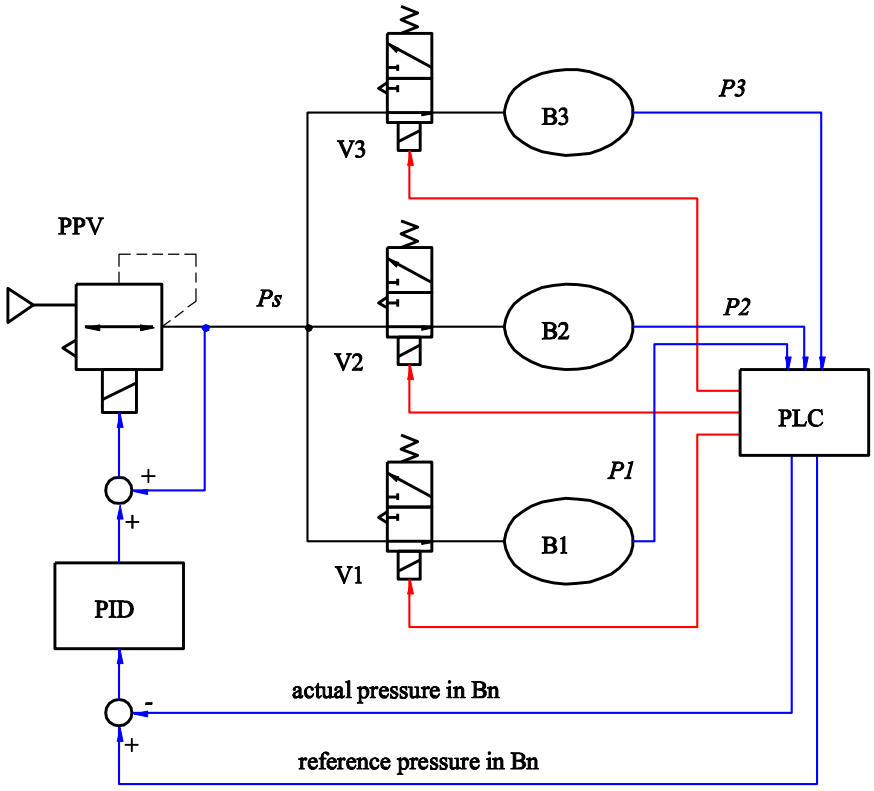

Figure 17. Three-bladder system with one pressure-proportional valve (PPV) controlled by PID

In the model the three bladders were configured with different parameters, including the contact area A, the soft tissue stiffness K_M of the leg region where the bladder acts on, and the gap between the bladder and leg d_0. The values of such parameters, which are shown in table 3, were selected in such a way as to represent possible variations due to muscular condition, location of the bladder on the limb and different device dressing that may occur using the actual prototype. In particular, with parameter values of table 3, the system is configured in such a way as to present increasing response time from bladder 1 to bladder 3.

Table 3. Parameters of the 3 bladders

	Contact area A (m^2)	Soft tissue stiffness K_M (Pa/m)	Gap d_0 (m)
Bladder 1	0.014	7.10^6	0.006
Bladder 2	0.017	6.10^6	0.009

Bladder 3	0.02	5.10^6	0.012

The inflating and deflating times, imposed by the PLC for each bladder, were 4 s and 9 s respectively, and the three cycles were shifted to produce a peristaltic effect, as it is shown in the command sequence of figure 18. When command is OFF the reference pressure is *0*, when command is ON the reference pressure is set at a defined value for all bladders.

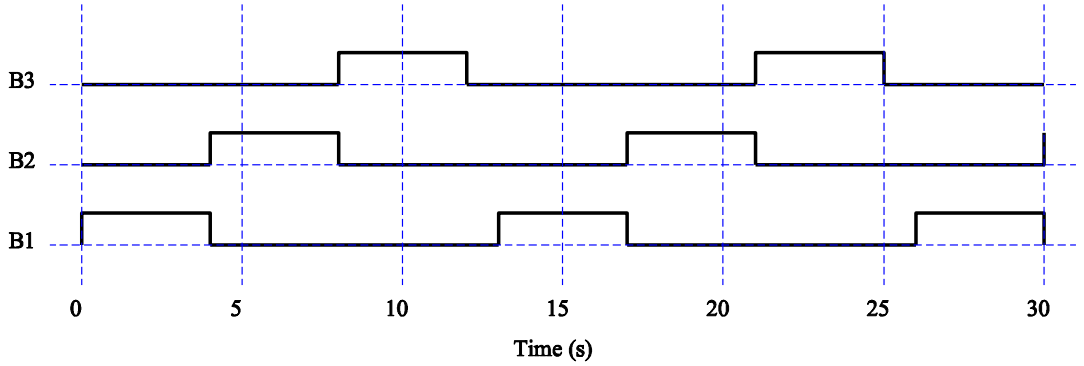

Figure 18. Command sequence of the three bladders

The system was simulated in two conditions:

c) Without proportional valve and PID control: each control valve *Vn* is supplied at $5{\cdot}10^4$ *Pa* relative pressure
d) With proportional valve and PID control: the absolute supply pressure to the valves *Vn* is regulated by the proportional valve and is saturated at $2{\cdot}10^5$ *Pa*; the relative reference pressure to the PID is set to $3.5{\cdot}10^4$ *Pa* in inflating state and *0* in deflating state, for all bladders.

Figure 19 shows the simulation results without PID controller (a) and with PID controller (b).

The simulation shows that an effective control of the bladder actions is almost impossible without a feedback control system, since the dynamic behavior and the maximum level of the pressures are affected by a number of randomness that are difficult to evaluate properly. As it can be observed in figure 19(a), the dynamic behavior and the maximum level of the contact pressure are very different among the bladders, due to the differences imposed to the bladder parameters. On the contrary, when the PID controller acts on the system (figure 19 (b)), the contact pressure tracks much better the reference one, which is set at $3.5{\cdot}10^4$ *Pa*, in each bladder. Obviously the feedback controller gives better result, and simply including feedback in the control of on/off valves would guarantee achieving of the desired pressure, but the use of a pressure proportional valve provides advantage

also for the system dynamics and general tracking: in this case the bladders can be supplied with pressure much higher than the desired internal value, thus reducing the rising time and allowing to maintain the desired value for a defined period, as highlighted by figures 10 and 11.

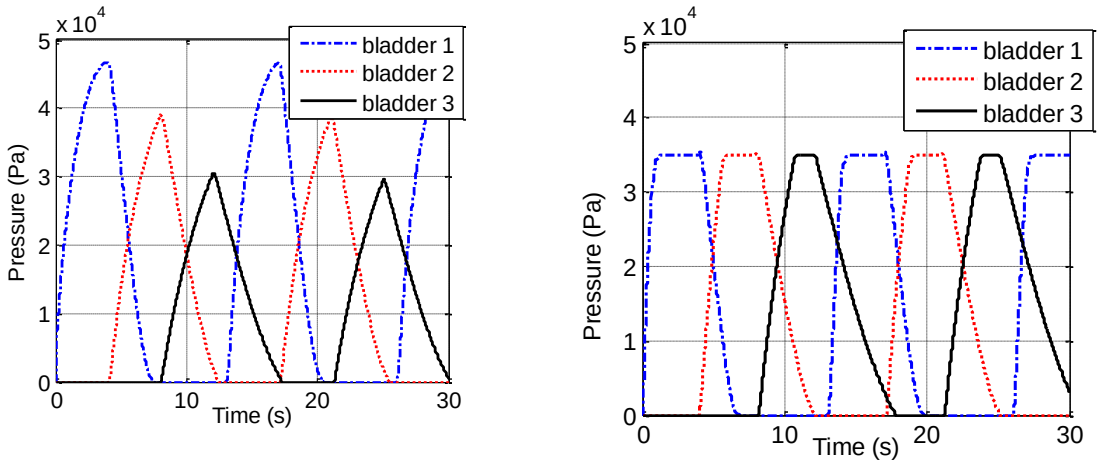

Figure 19. Simulation of the multi-bladder system in absence (a) and in presence (b) of the PID controller

Due to the difference in the bladder parameters, the dynamic behaviors of the three bladders are still different, as highlighted by the rise and fall times, but each bladder can reach the reference contact pressure and maintains it for a significant time: totally, in a cycle of 13 s, the bladders 1, 2 and 3 can stay about 8 s in the reference contact pressure, that is equal to 62% of the whole time. You should also consider that the tuning of the PID coefficients has been made for only one bladder, but gives acceptable results for the whole system, thus testifying the ability to compensate in some extent also uncertainties like the actual value of the soft tissue stiffness and the limb/device gap.

Conclusion

This study concerned the effective control of an IPC device, conceived as a multi-bladder system able to realize important rehabilitation action on the cardio-circulatory system of people with very serious mobility problems. The main issue was to individuate a proper control strategy able to create a defined pressure pattern on the limb surface, corresponding to a peristaltic and centripetal pressure wave. To solve this problem we

decided to apply a PID control properly tuned and to use proportional components for regulation of the pneumatic quantities of the system.

First a mathematical model of one bladder and its interaction with the human has been realized and experimentally validated. The comparison has shown good correspondence between experiment and simulation, in both dynamic behavior and maximum level of internal bladder pressure. The model is also able to calculate the contact pressure P_C between bladder and limb.

Then two different strategies to control the bladder pressure have been studied, considering the use of proportional electro-pneumatic components for regulation of the two basic quantities acting in the system: i.e. the supply pressure and the air flow to the bladders.

The first method is based on the use of an electro-pneumatic pressure-proportional valve, the second involves the use of a flow-proportional valve. In both solutions the PID control must track a desired trend of the pressure, trying to reach and maintain a defined value for a given time.

The results produced by the two different controls are similar, as reported in figures 9 and 15. In both methods the bladder exerts to the limb the exact value of the reference pressure for about the 60% of the desired active time (4 s). This is an excellent result, taking into consideration the natural low dynamics of such pneumatic systems. On the contrary, in absence of PID control the bladder pressure evolves only reaching a peak value, whose value is determined by the various parameters of the pneumatic circuit and is practically impossible to foresee.

The choice between the two methods must then consider the general cost and complexity of the device, since it is made up of a given number of bladders intended to generate a proper pressure wave on the limb surface. In this regard, while the adoption of the flow-proportional method would require one proportional valve for each bladder, the method based on the pressure-proportional valve can allow to realize the whole control system with only one proportional valve, thus limiting the cost and complexity of the device. The simulation of a system with three bladders fed by one pressure-proportional valve demonstrated the feasibility and effectiveness of such a system.

In conclusion, the study permitted to individuate an effective way to control such a multi-bladder pneumatic system, capable of providing adequate performance for a positive effect on the cardiovascular system. The optimal solution, based on PID control of one pressure-proportional electro-pneumatic valve, presents adequate for the realization of a quite inexpensive device, suitable for simple and comfortable use.

Future work will concern more accurate modeling of the physiological system, including also damping characteristic of the soft tissues and a complete model of the cardio-circulatory system. This will allow to estimate the effect of the IPC device on the dynamic performance of the CCS, which is the final goal of the research. On this base, it will be possible to define also more precise patterns for the pressing action, that will constitute the reference for the study of more performing control algorithms.

The effectiveness of the IPC device will be verified by means of clinical testing both on healthy and impaired people.

References

[1] Mahoney RM, Van der Loos HFM, Lum PS, and Burger C (2003). Robotic stroke therapy assistant. Robotica, Vol. 21, pp. 33-44.

[2] Diaz I, Gil J J, and Sanchez E (2011). Lower-limb robotic rehabilitation: Literature review and challenges. Journal of Robotics, Vol. 2011, DOI:10.1155/2011/759764.

[3] Herrmann LG, Reid MR (1934). The conservative treatment of arteriosclerotic peripheral vascular disease. Annuals of Surgery, Vol. 100, pp.750-760.

[4] Landis EM, and Gibbon JH (1933). The effect of alternative suction and pressure on blood flow to the lower extremities. The Journal of Clinical Investigation, Vol. 12 (5), pp. 925-961.

[5] Clagett GP, Reisch JS (1988). Prevention of Venus thromboembolism in general surgical patients. Results of meta-analysis, Ann Surgery, Vol. 208, pp. 227-240.

[6] Westrich GH, Haas SB, Mosca P and Peterson M (2000). Meta-analysis of thromboembolic prophylaxis after total knee arthroplasty. Journal of Bone and Joint Surgery, British 82, pp. 795-800. Louridas G, Saadia R, Spelay J, Abdoh A, Weighell W, Arneja AS, Tanner J and Guzman R (2002). The ArtAssist Device in chronic lower limb ischemia. A pilot study, Int Angiol Vol. 21, pp. 28-35.

[7] Delis KT, Nicolaides AN, Wolfe JH and Stansby G (2000). Improving walking ability and ankle brachial pressure indices in symptomatic peripheral vascular disease with intermittent pneumatic foot compression: a prospective controlled study with one-year follow-up. Journal of vascular Surgery, Vol. 31, pp. 650-661.

[8] Labropoulos N, Leon LR, Bhatti A, Melton S, Kang SS, Mansour AM and Borge M (2005). Hemodynamic effect of intermittent pneumatic compression in patients with critical limb ischemia. Journal of vascular surgery, Vol. 42 (4), pp. 710-716.

[9] Nose Y, Murata K, Wada Yasuaki, Tanaka T, Fukagawa Y, Yoshino H,Susa T, Kihara C and Matsuzaki M (2010). The impact of intermittent pneumatic compression device on deep Venus flow velocity in patients with congestive heart failure. Journal of Cardiology, Vol. 55 (3), pp. 384-390.

[10] Johansson K, Lie E, Ekdahl C and Lindfelt J (1998). A randomized study comparing manual lymph drainage with sequential pneumatic compression for treatment of postoperative arm lymphedema. Journal of Lymphology, Vol. 31, pp. 56-64.

[11] Wiener A, Mizrahi J and Verbitsky O (2001). Enhancement of Tibialis Anterior Recovery by Intermittent Sequential Pneumatic Compression of the Legs. Basic Appl Myol, Vol. 11 (2), pp. 87-90.

[12] Waller T, Caine M and Morris R (2006). Intermittent Pneumatic Compression Technology for Sports Recovery. The Engineering of Sport, Vol. 3. ISBN: 978-0-387-34680-9 (Print) 978-0-387-45951-6 (Online).

[13] Unger RJ, Feiner JR (1987). Hemodynamic effects of intermittent pneumatic compression of the legs. Anesthesiology, Vol. 67, pp. 266-268.

[14] Morgan RH, Carolan G, Psaila JV, Gardner AMN, Fox RH, and Woodcock JP (1991). Arterial flow enhancement by impulse compression. Journal of Vascular Surgery, Vol. 25, 8-15.

[15] Lurie F, Awaya DJ, Kinster RL, and Eklof B (2003). Hemodynamic effect of intermittent pneumatic compression and the position of the body. Journal of Vascular Surgery, Vol. 37, pp. 137-142.

[16] Flam E, Berry S, Coyle A, Dardik H and Raab L (1996). Blood-flow augmentation of intermittent pneumatic compression systems used for the prevention of deep vein thrombosis prior to surgery. The American journal of surgery, Vol. 171, pp. 312-315.

[17] Christen Y, Wutscher R, Weimer D, de Moerloose P, Kruithof EKO and Bounameaux H (1997). Effects of intermittent pneumatic compression on venous hemodynamics and fibrinolytic activity. Blood coagulation and fibrinolysis, vol. 8, pp. 185-190.

[18] Froimson MI, Murray TG and Fazekas AF (2009). Venous Thromboemolic Disease Reduction with a Portable Pneumatic Compression Device. The journal of Arthroplasty, Vol. 24 (2), pp. 310-316.

[19] Dai G, Gertler J P and Kamm R D (1999). The effects of external compression on venous blood flow and tissue deformation in the lower leg. Journal of biomechanical engineering, Vol.121, pp. 557-564.

[20] Malone M D, Cisek P L, Comerota A J Jr, Holland B, Eid I G and Comerota A J. High-pressure, rapid inflation pneumatic compression improves venous hemodynamics in healthy volunteers and patients who are post-thrombotic. Journal of vascular surgery, vol.29, n.4, 1999, pp.593-599.

[21] Ferraresi C, Hajimirzaalin H, Maffiodo D. A model-based method for the design of intermittent pneumatic compression systems acting on humans. Proceedings of the Institution of Mechanical Engineers. Part H, Journal of engineering in medicine 12/2013; DOI:10.1177/0954411913516307

[22] International Standard ISO6358 (1989). Pneumatic Fluid Power - Components using Compressible Fluids - Determination of Flow-rate Characteristics.

[23] Tzafestas S, and Papanikolopoulos NP (1990). Incremental Fuzzy expert PID control. IEEE transaction on industrial electronics, Vol. 37 (5), pp. 365-371.

[24] Ziegler JG and Nichols NB (1942). Optimum settings for automatic controllers. Trans. ASME, Vol. 64, pp. 759–768.

[25] Ferraresi C and Sorli M (1994). Modelling and analysis of systems for control of the pressure. (In Italian), Fluid, No 357, pp. 58-65.

[26] Ferraresi C and Velardocchia M (1990). Pneumatic proportional valve with internal feedback. Proceeding of the 9th international symposium on Fluid power, Oxford UK, pp. 125-136.